Understanding Non-viral Nucleic Acid Delivery Vehicles with Different Charge Centers and Degradation Profiles

Hao Lu

Virginia Polytechnic Institute and State University

Master of Science in Chemistry

Theresa M. Reineke

T. Daniel Crawford

Webster L. Santos

May 10, 2010

Blacksburg, Virginia

Keywords: Non-viral Nucleic Acid Delivery, Biodegradable Polymer, Guanidine, Self-degradable Polymer, Amide Hydrolysis, Poly(glycoamidoamine), Gene Expression

Understanding Non-viral Nucleic Acid Delivery Vehicles with Different Charge Centers and Degradation Profiles

Abstract

Different structures of non-viral cationic polymer delivery vehicles, including charge center type, molecular weight and degradability, could significantly affect toxicity, release of nucleic acid and transfection efficiency.

Poly(glycoamidoamine)s (PGAAs) contained different carbohydrate and secondary amine moieties and showed high transfection efficiency to different cell lines in a nontoxic manner. The “proton sponge hypothesis” has attempted to relate the buffering capacity to endosomal release of polyethylenimine (PEI) based polyplexes, which could contribute to high transfection efficiency. Secondary amine structures rendered PGAAs buffering capacity around physiological pH. To test the feasibility of the mechanism for PGAAs, new no buffering capacity guanidine or methylguanidine containing poly(glycoamidoguanidine)s (PGAGs) were synthesized. PGAGs formed stable polyplexes with pDNA from *N/P* (# secondary amine or guanidine group on polymer backbone / # phosphate group on pDNA backbone) ratio 3. PGAG based polyplexes expressed low cytotoxicity and were internalized by 90% of cells at *N/P* 25. Furthermore, two PGAG based polyplexes showed higher transfection efficiency from *N/P* 5 to 30 than their PGAA based analogs. These data suggested the low transfection could be due to the difficulties to release pDNA from polyplexes; also, the “proton sponge theory” could not explain the higher transfection efficiency by some PGAGs.

Degradation of delivery vehicles could potentially release pDNA in cells and increase transfection efficiency. PGAAs degraded rapidly at physiological conditions and the proposed mechanism was amide hydrolysis. Typically, amide groups are stable and hydrolyze slowly in absence of enzyme. Different models mimicking PGAAs were synthesized to study the fast hydrolysis. Amide groups showed asymmetric hydrolysis. Different hydrolysis behaviors suggested neighboring group participation of two terminal groups to induce rapid amide hydrolysis. These new models could potentially be used to design new polymer delivery vehicles with various degradation profiles.

Acknowledgements

Firstly, I would like to thank Dr. Theresa M. Reineke for her instruction, care and encouragement during my research. She shows me how to use time more efficiently. She also establishes a warm and cooperative environment in the lab. Discussion with Dr. Reineke helps me to think more independently and generate new ideas. Secondly, I would like to thank Dr. T. Daniel Crawford for all the computational work on the amide hydrolysis project. I also would like to thank Dr. Webster L. Santos for all the organic guidance during my class and research.

Special thanks are to Dr. Vijay P. Taori for his guidance and encouragement when collaborating on the two projects. I am grateful to Dr. Patrick McLendon and Giovanna Grandinetti for their help in biological experiments. I also want to thank Antons Sizovs for his insightful discussion. I am also thankful to all members in Dr. Reineke's group for all their support and collaboration.

Finally, I would like to thank my family for all their support and care in my life and career. Special thanks go to my father (Baoguang), mother (Zhen), grandpa (Shangpin) and grandma (Shujiu) for all their encouragement when I was depressed and all sacrifices in my life.

Table of Contents

List of Tables

List of Figures

List of Schemes

Chapter 1

Novel Cationic Polymers for Nucleic Acids Delivery

Nucleic acid therapy has gained much attention over last two decades as a potential treatment of cancer and other genetic disorder diseases.[1] However, as negatively charged molecules, nucleic acids are not easy to pass through the negatively charged cell membrane due to charge repulsion. Also, nucleic acids are easy to degrade under the environment of DNAse and RNAse.[2] Therefore, many types of vehicles have been developed to protect and deliver nucleic acids into the cells. This process may require delivery vehicles to have the ability to form nanoparticles with nucleic acids and transfect cells, as well as the property to lower binding ability and release nucleic acids after that.[3] Also, the delivery vehicles should be non-toxic enough as not to affect healthy cells.

Tremendous research has been completed on viral carriers due to their high efficiency at delivering DNA and RNA to different cell lines. However, the high toxicity and immunogenicity issues have limited their clinical use.[4] Non-viral vehicle systems are being developed rapidly to offer potential routes for nucleic acid delivery. These vehicles include cationic lipids and cationic polymers. They both show low immunogenicity, good ability to bind nucleic acids and low production cost. However, low transfection efficiency and high cytotoxicity are also observed.[5] Currently, research is mainly focusing on modifying non-viral vehicle structures to increase transfection efficiency and reduce toxicity profiles. In the Reineke group, we are focusing on polymer vehicles to deliver plasmid DNA and small interfering RNA.

Another property of a good delivery vehicle should have is to release nucleic acids after cellular uptake via endocytosis. This requires polymers to be cleavable or degradable to reduce the binding properties with the nucleic acid.[6] These polymers usually have photo-, pH- or redox-sensitive cleavable linkers, hydrolysable moieties and enzymatically degradable groups in their structures.[7-11] Biodegradable polymers include polyesters, disulfides and acetals.[12-17]

The research in our group mainly focuses on synthesizing novel poly(glycoamidoamine)s (PGAAs) and examining these polymers for pDNA transfection.[18-20] PGAAs have secondary amine moieties that can bind pDNA and form polymer-pDNA complexes (polyplexes). These polyplexes have transfection efficiency as high as jet-PEI in different cell lines such as HeLa, BHK-21 and HepG2 cells while maintaining low cytotoxicity.[19] PGAAs can also degrade under mild pH condition mimicking physiological conditions.[21] This property could render PGAAs abilities to release pDNAs inside cells.

My work mainly focuses on figuring out the roles different charge centers could play when polymers are binding pDNAs, and the mechanism of how PGAAs degrade under mild pH conditions to help develop new polymers with desired degradation profiles.

The thesis will follow the sequence mentioned above. Chapter 2 discusses novel polymer transfection agents with guanidine groups as charge centers. Binding and other biological experiments were conducted to examine and identify the difference both colloidally and biologically caused by new charge centers. Chapter 3 discusses the degradation mechanism of poly(L-tartramidopentaethylenetetramine) (**T4**). Different small molecule models mimicking **T4** structures are studied to elucidate a possible mechanism for rapid and tunable amide hydrolysis.

1.1 Polymer Vehicles for Nucleic Acid Delivery

As mentioned above, many difficulties are encountered during the delivery of nucleic acids that are not bound to a carrier such as, 1) electric charge repulsion, 2) fragility to enzymes in physiological conditions, and 3) their large size. Therefore, different cationic polymers were developed to condense and protect DNA via electrostatic interactions and hydrogen bonding.[5,19,22] Cationic polymers have several advantages over viral delivery vehicles. First, the positive charges on polymer backbone make them highly soluble in water. This property enable polymers to condense DNA more efficiently to form smaller and more stable polyplexes.[15] Second, the size and surface charge of the polyplexes are greatly dependent on the formulation conditions of the colloidal complexes, such as positive charge (from polymer) to negative charge (from DNA backbone) ratios. Higher positive to negative charge ratios usually give smaller polyplex size and higher surface charge.[5] Herein, several polymer vehicles are outlined and discussed including chitosan, polyethylenimine (PEI), poly(amido-amine) (PAA) and some biodegradable polymers.[23-26]

Chitosan

Chitosan is biocompatible, biodegradable and a naturally occuring polysaccharide. Its structure makes it one of the dominant non-viral vehicles of study. Chitosan is commercially available and made from by the deacetylation of chitin. Therefore, the product contains randomly distributed N-acetyl-D-glucosamine (acetylated unit) and D-glucosamine (deacetylated unit) (**Scheme 1.1**). The amines from D-glucosamine have pKa of about 6.5 at 25 ^{o}C and most of them can be protonated to form cationic chitosan under acidic pH conditions (lower than pKa).[27] Cationic chitosan can assemble with nucleic acids and form polyplexes spontaneously for nucleic

acid delivery. However, chitosan itself is not a promising delivery vehicle due to its low charge density at physiological pH. Therefore, poor solubility will lead to aggregation and poor stability of polyplexes.[27] Previous studies also showed that chitosan that has a high degree of deacetylation and degree of polymerization (>50) promoted cellular internalization.[24] However, highest molecular weight chitosan typically does not give highest gene transfection efficiency which may be caused by the difficulties to release DNA.[5] Charge ratio and DNA concentration influences the size of resulting polyplexes. Higher *N/P* charge ratios (# deacetylated amines on chitosan / # phosphates on DNA ratio) and lower DNA concentration generally give smaller polyplexes. Typically, the particles around 100 nm can be endocytosed by cells. However, for different cell lines, the optimum polyplexes sizes are different.[28]

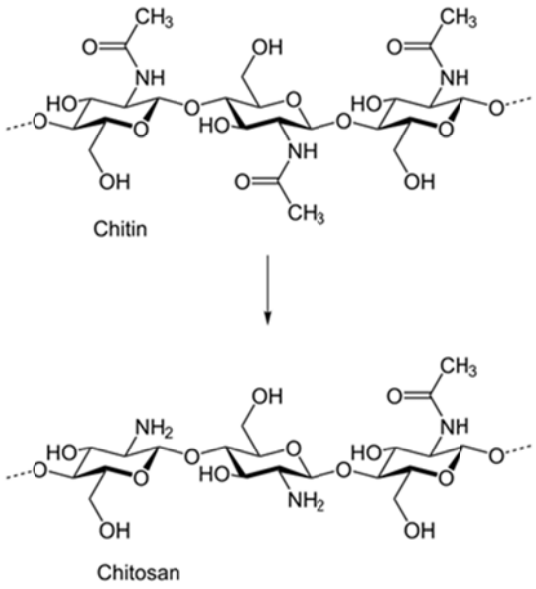

Scheme 1.1, Deacetylation of chitin to chitosan

Because the high hydrophobicity and high acidic pH requirement to protonate amines hinder the nucleic acid transfection for chitosan, numerous derivatives were developed to

improve the bioactivity. Trimethyl chitosans, which can be protonated more easily at physiological pH were developed to overcome the hydrophobicity of regular chitosan. Gene transfection results for the 40% and 50% quaternized trimethyl chitosans were 10 to 100 fold to regular chitosan with similar molecular weight, while maintaining low toxicity.[24,29] Polyethylene glycol-conjugated chitosan DNA complexes were used to improve stability from aggregation and were for as long as one month.[29,30] Transferrin modified chitosan DNA nanoparticles were introduced to increase transfection efficiency through a receptor-mediated endocytosis mechanism as transferrin receptor is found on many mammalian cells and transferrin is able to transfer non-bioactive molecules efficiently.[30]

Polyethylenimine (PEI)

PEI is considered one of the most widely-studied gene delivery agents. Commercially available PEIs such as jetPEI are used as positive controls in many transfection studies. There exist two types of PEI structures: linear PEI and branched PEI. Linear PEI is synthesized through ring opening polymerization of 2-ethyl-2-oxazoline followed by hydrolysis of propionamide groups,[31] while branched PEI is synthesized through acid catalyzed ring opening polymerization of aziridine.[5] (**Scheme 1.2**) Linear PEI only contains only secondary amines excluding the terminal primary amines; while branched PEI has primary, secondary and tertiary amines. Typically, the ratio of primary/secondary/tertiary amines is 1:2:1 based on theoretical calculation.[5] Now that every three atoms of its chain is nitrogen, PEI has high cationic charge if amine groups are protonated. At physiological pH, around 20% of amines are protonated examined by pH titration.[32]

Similar to chitosan, different factors could affect bioactivities of PEI, including molecular weight and polymer structure. Higher molecular weight usually gave a decrease in polyplex size and higher gene transfection efficiency, however, higher cytotoxicity was observed as well.[32,33] The optimal molecular weight for PEI is from 5 to 25 kDa.[32] Different PEI structures can also affect transfection efficiency. Generally, branched PEI is more effective at binding and condensing DNA than linear PEI with similar molecular weight.[5] This effect could be caused by the low entanglement interaction between linear PEI and DNA chain. Also, primary amines are better to condense DNA than other amines due to their ability to be protonated more easily.[32] However, compared to branched PEI, linear PEI showed lower cytotoxicity.

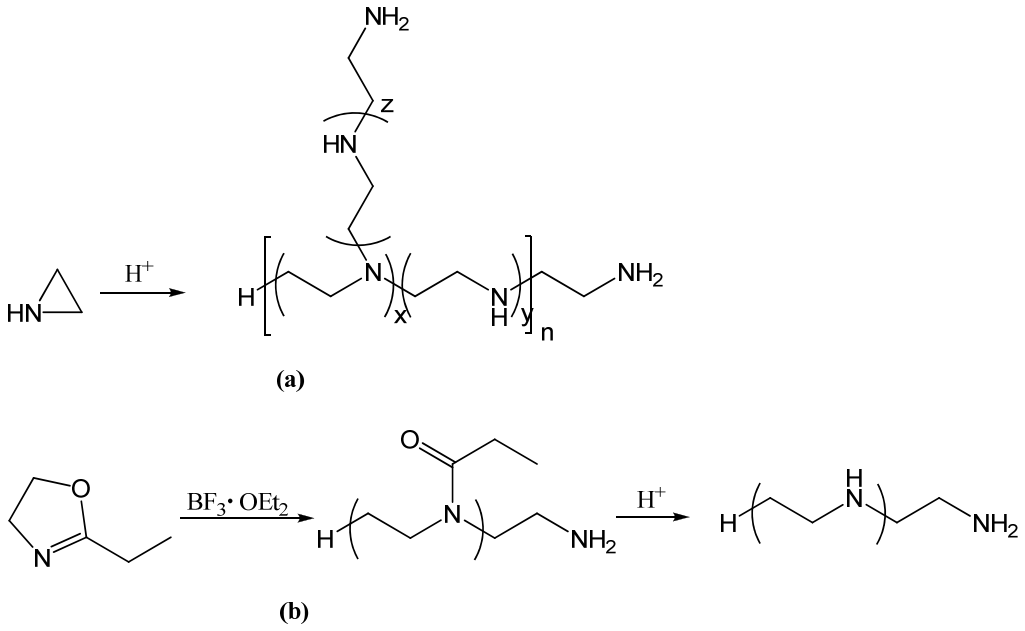

Scheme 1.2, **(a)** Synthesis of branched PEI, **(b)** Synthesis of linear PEI

Different theories were developed to explain the endosomal release of PEI polyplexes which lead to high transfection efficiency, including pore formation,[34,35] fusion and flip-flop

mechanism.[36,37] The "proton sponge hypothesis" was recognized to well explain why PEI based polyplexes have the ability to induce endosomal release.[38] When pH decreases from 7.4 to 5, PEI becomes more protonated in endosomes. This process induces an influx of Cl^- ions with H^+ followed by the influx of water to balance osmotic pressure, which finally causes the swelling and rupture of endosomes.[39,40] The high buffering capacity around physiological pH could lead to the higher transfection efficiency. However, this hypothesis is still under controversy.

Studies showed that branched PEI has higher transfection efficiency with higher cytotoxicity and linear PEI has lower transfection efficiency with lower cytotoxicity. However, this trend is not always true in different cells. Also, neither of these two types of PEIs is biocompatible or biodegradable. Therefore, different modified PEIs were developed to overcome these drawbacks. The common way is to copolymerize PEI with other biocompatible or biodegradable polymers such as PEG and disulfide linkages.[5,41,42] Moreover, PEI conjugated with different receptors has been tested for targeting different cell lines.

PEI-g-PEG copolymers are more hydrophilic and more soluble in water. Therefore, the resulting polyplexes are more stable and do not aggregate.[32,41] PEG has low toxicity and it is a biocompatible compound, which can lower cytotoxicity compared with PEI itself at similar molecular weight. However, PEGylated PEI usually gave lower transfection efficiency. The length and density of PEG group can significantly affect transfection efficiency. Too many neutral PEG groups can shield the surface charges of polyplexes and hinder the interaction between polyplexes and cell membrane.[5] Davis, M. E. showed that around 10% cyclodextrin grafted linear or branched PEI had reduced cytotoxicity, higher stability and competitive transfection efficiency compared to PEI itself.[43]

PEI conjugated with different targeting groups were also used to increase specific transfection to different cell lines. G. H. Hsiue, *et al*, showed that folate-polyethylenimine-block-poly(L-lactide) (folate-PEI-PLLA) polyplexes were stable in water solution, less toxic, and they targeted folate receptor overexpressed tumor cells followed by receptor-mediated endocytosis.[44] E. Wagner, *et al*, showed that transferrin conjugated low molecular PEI polyplexes improved transfection efficiency to tumor cells. Also, transferrin could shield the positive surface charge of polyplexes, increase body circulation time and reduce nonspecific interactions *in vivo*.[45]

Poly(amidoamine)

Poly(amidoamine)s include linear poly(amidoamine)s (PAA) and poly(amidoamine) dendrimers (PAMAM). PAA is made by Michael addition of primary monoamines or bis(secondary amines) and bisacrylamides.[46] (**Scheme 1.3**)

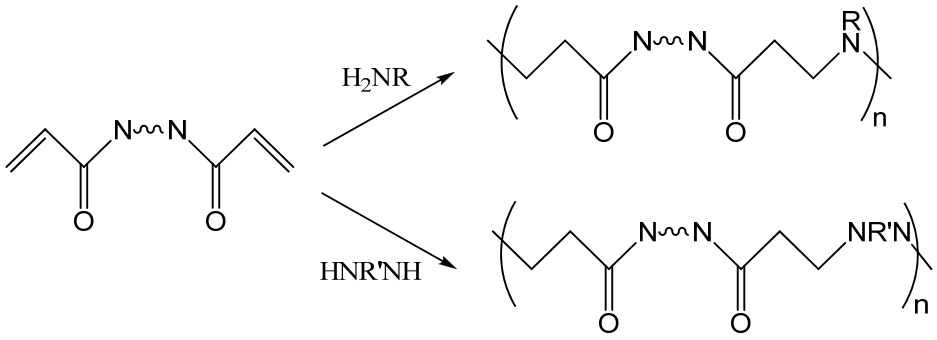

Scheme 1.3, Synthesis of linear poly(amidoamine)s (PAA)s

Protonation of PAAs under low pH will lead to a more rigid backbone structure instead of a random coil structure, which could be caused by hydrogen bonding with carbonyl groups and electrostatic repulsion.[47] *In vitro* studies, compared to PEI, amphoteric PAAs show lower

cytotoxicity with a comparable transfection efficiency.[48] The possible endosomolytic properties of this polymer likely contribute to high transfection efficiency by inducing endosomal release of polyplexes.[49] However, higher cytotoxicity is also observed which could be due to the presence of secondary amines in the structures.[48]

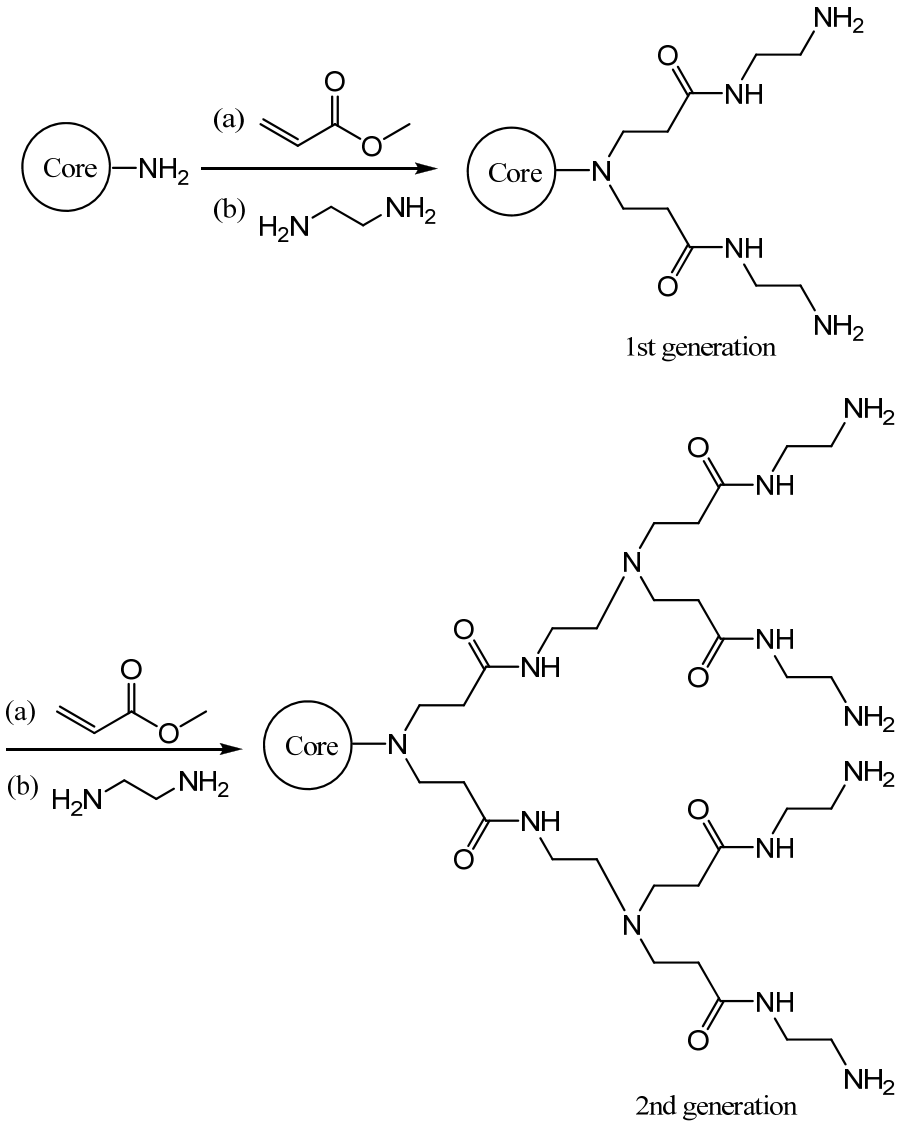

Scheme 1.4, Synthesis of PAMAM, **(a)** Michael addition of a nucleophilic core to methyl acrylate, **(b)** amidation of the dendrimer ester with a diamine

Poly(amidoamine) dendrimers (PAMAM) are branched poly(amidoamine)s. The synthesis undergoes a repetitive sequence of (1) Michael addition of a nucleophilic core to methyl acrylate, (2) amidation of the dendrimer ester with a diamine.[50] (**Scheme 1.4**) The number of generation and surface charges significantly affect the binding with DNA. Higher *N/P* ratios yield stable and water soluble polyplexes.[51] Furthermore, PAMAM with higher generation had higher transfection efficiency. This could be due to its hydrophobic structure increasing cellular penetration and its higher buffer capacity induced endosomal release explained by "proton sponge theory".[52]

1.2 Poly(glycoamidoamine)s (PGAA)

Because chitosan based delivery vehicles showed low cytotoxicity with low transfection efficiency, PEI based delivery vehicles showed high transfection efficiency and high cytotoxicity, the Reineke group has developed a series of new delivery vehicles by combing the carbohydrate structures mimicking chitosan moiety and the oligoamine structures mimicking PEI moiety. Also, inspired by the linkages from poly(amidoamine)s, the new series of delivery vehicles were linked by amido groups and called poly(glycoamidoamine)s (PGAAs).

Dr. Yemin Liu synthesized PGAAs with four different types of carbohydrates and four types of amines through a step-growth polymerization reaction.[18,19,53] (**Scheme 1.5**) The four types of carbohydrate monomers include difunctional D-glucarate, *meso*-galactarate, D-mannarate and L-tartrate. The four different amines are diethylenetriamine, triethylenetetramine, tetraethylenepentamine and pentaethylenehexamine. All these amines have primary amines at the ends and differ in number of secondary amines in the structures. The resulting polymers were named poly(D-glucaramidoamine)s (**D1-D4**), poly(galactaramidoamine)s (**G1-G4**), poly(D-

mannaramidoamine)s (**M1-M4**) and poly(L-tartaramidoamine)s (**T1-T4**). The "**G**, **D**, **M**, **T**" in the symbol represents the monomer type, and the "**1-4**" denotes the number of secondary amines in the repeat unit. Secondary amines in these polymers can be charged at physiological pH. Dr. Lisa E. Prevette, *et al*, showed that PGAAs bond pDNA and formed polyplexes via electrostatic, van der Waals and hydrogen bonding forces. The hydroxyl groups can enhance the binding with pDNA.[54]

All these polymers have degrees of polymerization (DP) from 11 to 14. The similar DP ensured that the transfection efficiency and cytotoxicity are not affected by molecular weight.[19] Gel binding studies showed that **D2-D4**, **G1-G4** and **T1-T4** bond pDNA between *N/P* (N = number of secondary amine groups, P = number of phosphate groups on DNA backbones) ratio 1 and 3 compared to linear PEI at 2 and chitosan at 1. **M1-M4** showed polymers bond pDNA at higher *N/P* ratios between 3 and 5.[19,55] As the only difference among all these types of polymers are the stereochemistry and number of hydroxyl groups on carbohydrates, these hydroxyl groups could contribute to the binding with pDNA.[19] Heparin competitive assay was used to test how stable the polyplexes were by competitively binding pDNA. A higher concentration used to release pDNA from polyplexes represents a more stable polyplex. Results showed that **G4** and **T4** polyplexes were more stable than **D4** and **M4** polyplexes at same *N/P* ratios.[19,53]

The polyplexes sizes were measured by dynamic light scattering (DLS) and ranged from 50 to 500 nm for *N/P* ratio 20. Polymers with less secondary amines (1 or 2) in each repeating unit usually had larger polyplexes sizes. Also, with same number of secondary amines, **T** and **G** polymers had smaller polyplexes. *N/P* ratio is an important factor to size. Higher *N/P* ratio always gave smaller polyplexes.[19,55] TEM studies showed that the shape of polyplexes is spherical. The sizes or radiuses measured by TEM were consistent with DLS results.[18,19,55]

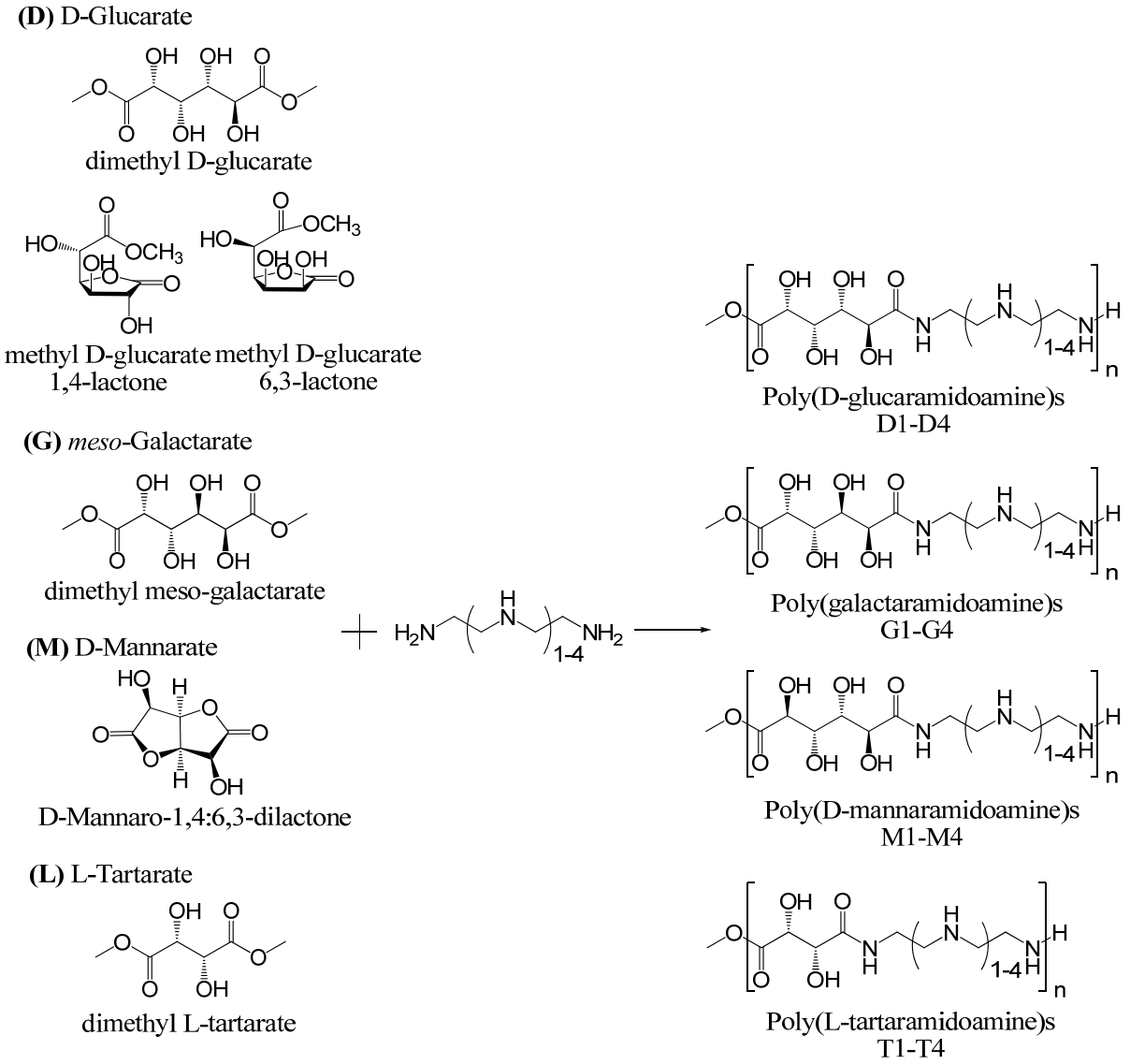

Scheme 1.5, Syntheses of PGAAs

Biological studies included toxicity assay and transfection efficiency assay. Hamster kidney fibroblast cell line (BHK-21), human cervical cancer epithelial cell line (HeLa) and human liver carcinoma cell line (HepG2) were used for **G**, **D** and **M** polymers, while **T** polymers were tested with HeLa only.

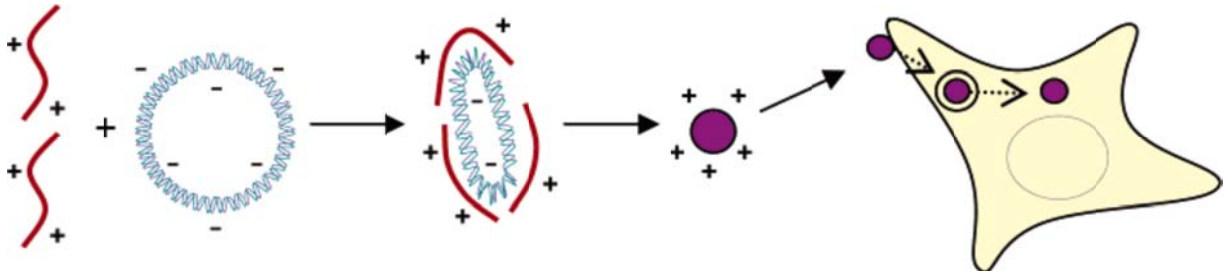

Figure 1.1, Formation of polyplexes followed by cellular uptake. Figure is from Ref. [19]

Toxicity assays showed that all PGAAs were non-toxic to different cell lines, even at the *N/P* ratios higher than 20. Furthermore, the toxicity still was found to be at a low level as the secondary amine density increased in the polymer backbone. The toxicity of the PGAAs was found to be as low as that of chitosan.

Reporter gene expression assays were used to examine the ability to deliver pDNA and gene transfection efficiency by PGAAs. Luciferase reporter gene (pCMV-*luc*) was used to produce luciferase in cells. The protein will catalyze oxidation of luciferin in the assay substrate and generate luminescence. By measuring the intensity of luminescence, we can determine which polymer delivers pDNA better. Results showed that transfection efficiency increased as amine density increased. Also, **T** and **G** based polymers functioned better than **D** and **M** based polymers at same amine density and *N/P* ratios.[19,53,55] However, the trend was not always consistent with different cell lines.[19]

Previous work has found that secondary amine density plays an important role in delivering pDNA. Dr. Chen-Chang Lee, *et al*, extended secondary amine number to 5 and 6 per repeating unit. Also, regular PGAAs are likely not completely linear due to the possible reaction with the secondary amines, as well as branched PEI and linear PEI showed different ability to deliver pDNA, branched and linear PGAAs were also synthesized to examine whether the

topology of PGAAs can affect biological activities.[20] Biological studies showed that transfection efficiency by the polymers with 5 or 6 protonatable amines in each repeating unit remained similar to the structures with 4 protonatable amines in the repeating unit, however, toxicity started to increase. Studies also showed that linear **M** and **D** based polymers gave higher transfection efficiency than the branched systems, but this trend was not obvious for **G** and **T** based polymers. Moreover, linear PGAAs were a little more toxic than the branched analogs.[20]

Because previous studies showed that the release of DNA promoted transfection efficiency,[14,56-59] Dr Yemin Liu, *et al*, studied the fast degradation of PGAAs. PGAAs had a faster degradation rate at pH 7.4 than pH 5. These properties could contribute to the high transfection efficiency by PGAAs.[21]

1.3 Biodegradable Polymers

As the polymers with high molecular weight cause higher cytotoxicity, people are trying to use low molecular weight polymers for nucleic acid delivery. However, the polymers with lower molecular weight usually generated less stable polyplexes and lower transfection efficiency. Therefore, biodegradable polymer vehicles are highly focused to be applied in nucleic acid delivery to avoid the accumulations of polymer and the induced cytotoxicity.[6] Furthermore, the release of nucleic acid by biodegradable polymers could potentially release drugs and increase transfection efficiency. Currently, several biodegradable polymers have been tested for nucleic acid delivery, including esters,[13,59] acetals,[12,60] and disulfides[17,57,61].

Water-soluble polyesters can be modified to contain polyamines that could be potentially used to form polyplexes with nucleic acid for delivery. These polymers can degrade rapidly at physiological conditions. Poly(γ-(4-aminobutyl)-L-glycolic acid) (PAGA) (**Figure 1.2**) showed a

rapid degradation which yielded one-third of the starting molecular weight after 100 min at 37 ^{o}C.[14,62] Polyplexes formulated with these polymers were stable under physiological conditions for 8 hours measured by gel binding assay, indicating polymers in the polyplexes likely degraded less rapidly than free polymers. Compared to poly(L-lysine) (PLL), PAGA was non-toxic, while the transfection efficiency to 293 cells was twice as high as that by PLL from β-galactosidase enzyme activity assay.[14] *In vivo* studies carried out with 3-week-old NOD mice and PAGA/pCAGGS mouse IL-10 complexes showed the resulting protein can be detected for more than 9 weeks.[16] Poly(aminoester)s were developed to attain slower degradation rate with half-lives from days to months.[63-65] The cross-linked poly(β-aminoester)s showed good ability to complex DNA. The polymers were non-toxic to 293 cells compared with PEI controls, and transfection efficiency was comparable to PEI.

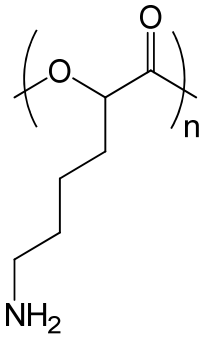

Figure 1.2, Poly(γ-(4-aminobutyl)-L-glycolic acid) (PAGA)[14,62]

Acetal groups are acid sensitive. When these groups are introduced into polymers, polymers tend to have tunable degradation rates based on different pH. Frechet, *et al*, modified dextran by reaction with 2-methoxypropene.[12] Degradation studies with the resulting acetalated dextran degraded faster at pH 5.0 (half-life 10 h) than at pH 7.4 (half-life 15 days). Frechet, *et al*,

also synthesized PEO based drug molecules which can form linkages with drugs.[66] These polymers can be applied to release drugs at mildly acidic endosomes.

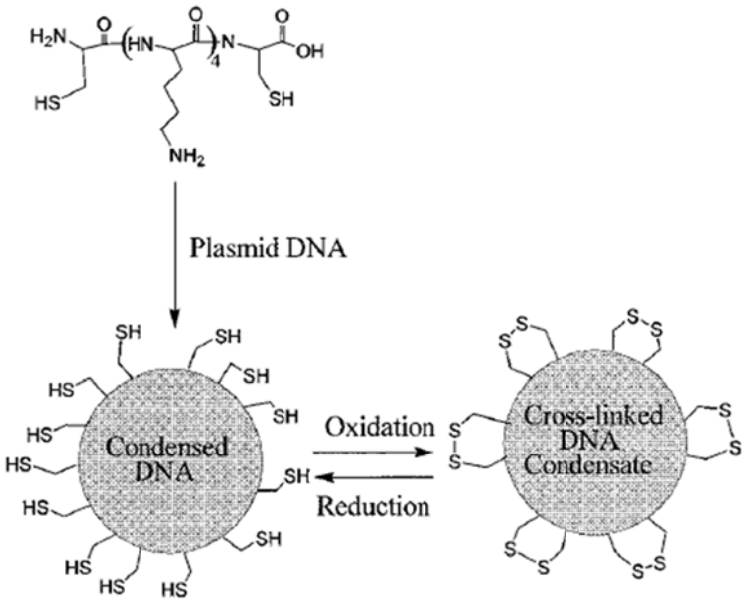

Figure 1.3, Formation of peptide DNA polyplexes. Figure is from Ref. [67]

Disulfide groups are also widely used to link polymers and drugs due to their cleavable properties under reducing environment via thiol-disulfide exchange reactions. Rice, *et al*, synthesized low molecular weight disulfide cross-linking peptides for DNA delivery.[67] Peptides containing hydrosulfide groups (from cysteine) were used to complex DNA followed by formation of disulfide bonds and cross-linking. (**Figure 1.3**) The resulting polyplexes showed significantly higher stability as well as higher *in vitro* gene transfection efficiency.

1.4 Conclusions

My research is to examine whether the "proton sponge theory" could potentially explain the high transfection efficiency by replacing secondary amines with guanidine or

methylguanidine groups. Also, to understand the degradation mechanism of different PGAAs, further hydrolysis studies with small model compounds are conducted. Moreover, the difference in hydrolysis could potentially lead to novel delivery vehicles with tunable degradation rate for desired nucleic acid release.

Chapter 2

Structure-Activity Examination of Poly(glycoamidoguanidine)s: Glycopolycations Containing Guanidine Units for Nucleic Acid Delivery

Adapted from

Taori, V. P.; Lu, H.; Reineke, T. M. *Biomacromolecules* XXXX, XX, XXX

All synthetic and polymer characterization studies were done by Dr. Vijay P. Taori, and all biological studies were done by me.

Key words:

Guanidine, buffering capacity, proton sponge hypothesis, pDNA delivery, low cytotoxicity

2.1 Introduction

The cellular delivery of nucleic acids has been the focus of increasing attention due to the incredible promise of this new therapeutic modality.[68] Many polycation macromolecules are under investigation as non-viral polynucleotide delivery vehicles as they have the ability to bind and compact nucleic acids into nanoparticle complexes termed polyplexes.[19,69,70] In addition, many studies have shown that the polymeric vehicles can facilitate the cellular uptake and transport of polynucleotides into various regions of the cell, such as the cytoplasm and nucleus.[71,72] Non-viral delivery vehicles are advantageous as they are easy to synthesize, can carry a high therapeutic payload, and can be easily tailored to display stabilizing and targeting groups to increase circulation time and tissue specific delivery.[18,72-75]

Our group has focused on the design and development of a novel class of polymers that we have termed poly(glycoamidoamine)s (PGAAs).[18,19,22,53,73,76,77] These structures were strategically designed and synthesized to incorporate both oligoethyleneamine and carbohydrate moieties in the repeat units.[18,19,75,78] Numerous analogous structures have been created and examined;[53,54,76,78] several comprehensive studies using a variety of mammalian cell lines have shown that PGAAs exhibit similar high transfection efficiency when compared to the positive control that contains repeated ethylenimines, polyethylenimine (PEI), but with significantly reduced toxicity, similar to chitosan, which consists of repeated carbohydrates. Moreover, earlier studies have shown that the carbohydrate groups in our PGAA structures provide a biologically-benign attribute, contributes to polyplex stability via hydrogen-bonding to the nucleic acids,[22] and when copolymerized with the amine structures, helps to facilitate rapid polymer degradation through hydrolysis of the amide bond.[21,79] Among the library of PGAAs we have created and studied, the compounds with four secondary amines in the oligoethyleneamine unit exhibited the

best biological delivery efficiency results. The interaction of the polyplexes with glycosaminoglycans (GAGs) on the cell surface has been shown to be essential for the internalization of these polyplexes.[80,81] We have also performed an extensive mechanistic studies to show that while PGAA polyplexes are internalized via clathrin and caveolae-mediated endocytosis, caveolae appear to be the major route leading to nuclear delivery of pDNA for subsequent expression.[82] Although PGAAs have revealed interesting biological behavior, it is essential to have a thorough understanding of the complex factors that dictate the cellular delivery of nucleic acids.[76] To this end, a systematic investigation of structure-bioactivity relationships is critical for the design of more efficient delivery vehicles for therapeutic compounds.

One of the critical biological barriers in non-viral polynucleotide delivery involves the transit of the polyplexes from endosomes to the final destination. While the mechanisms of polymer-mediated nucleic acid delivery are still under intense investigation, endosomal release of polyplexes into the cytoplasm is thought to be essential to facilitate high delivery efficiency, particularly in therapeutic modalities that function in the cytoplasm, such as siRNA. A number of theories have been proposed for this process, including pore formation,[34,35] the fusion and/or flip-flop[83] mechanism, and the proton sponge hypothesis,[84] which is associated with the endosomal release of the polyplexes due to their high buffering capacity. This theory states that during the acidification event of the early endosomes, the protonation of amines in the polymer backbone provide a buffering capacity, which causes the subsequent influx of H^+ ions to further reduce the pH of these vesicles (and in turn, it is thought that an influx of Cl^- ions also takes place as a charge neutralization event). As a result of this osmotic imbalance across the endosomal membrane, water rushes in and swells the endosomes, which eventually rupture and release their

cargo into the cytoplasm. Although this theory has been widely studied, the various mechanisms involved in this process are debated within this field as much evidence both for and against this theory have been published.[53,85-89]

In the current study, we synthesized a novel group of macromolecules that we have termed poly(glycoamidoguanine)s (PGAGs) that contain guanidine cationic groups copolymerized with a *meso*-galactarate or L-tartrate moiety. These structures were created as a series of oligomers analogous to original PGAAs structures;[18,19,21,22,53,73,76,77,79,82] however, we have replaced the "buffering" oligoethyleneamine groups with cationic charges that do not have a buffering capacity. These oligomers were developed to study and compare the structure-property relationships, in particular, the biological effect of changes in amine (PGAAs) versus guanidine (PGAGs) charge type present on the backbone. As discussed earlier, subtle changes in the chemical structure of a delivery vehicle can affect its complexation with DNA, and thus the biological activity of the complex. Although some polymer vehicles have been reported that contain guanidine functionalities, the cationic groups are typically grafted as a pendant on the polymer backbone (i.e. poly-L-arginine, PLA),[90] or grafted to the ends of the macromolecule vehicle.[91,92] While those polymers have shown to facilitate the cellular delivery of polynucleotides, they also have been shown to vary in their toxicity profile (typically between 60-80% cell survival at low N/P ratios) in vitro.[91,92]

The results of the current study revealed that the low molecular weight PGAG structures created from galatarate or tartrate are able to bind with pDNA and form stable complexes (polyplexes) in the range of 60 to 200 nm. Biological assays with HeLa cells revealed that the polyplexes formed with the PGAGs displayed higher cellular uptake over polyplexes formed their analogous PGAAs created by copolymerizing galactarate or tartrate with

diethylenetriamine. Despite the lack of buffering capacity of the guanidine group, our studies have revealed that the galactaramide and tartaramide-based PGAG polyplexes transfect HeLa cells and yield higher gene expression than their PGAA analogs. In addition, this study has found that the PGAG polyplexes exhibit non-toxic behavior at a variety of polymer-to-DNA ratios (*N/P* ratios), and it could be related to the presence of carbohydrates and/or the low molecular weight of these materials.

2.2 Experimental Procedures

***General*:** Unless specified otherwise, almost all of chemicals used in the monomer synthesis were purchased from Sigma Aldrich Chemical Co. and were used without any further purification. Di-tert-butyl dicarbonate was purchased from Alfa Aesar Chemical Co. Monomers dimethyl-meso-galactarate and dimethyl-L-tartrate and polymers G1 and T1 were synthesized as previously described.[19,73] *Glycofect Transfection Reagent*^{TM} was obtained as a gift from Techulon, Inc. (Blacksburg, VA). Poly-L-Arginine (PLA) (Mw = 5000 – 15000 Da) was purchased from Sigma Aldrich Chemical Co. NMR spectra were collected on an Inova MR-400MHz spectrometer and mass spectra were obtained on an IonSpec HiResESI mass spectrometer. Cell culture media and supplements were purchased from Gibco/Invitrogen (Carlsbad,CA). pCMV-lacZ was labeled with a *Cy5* nucleic acid labeling kit (Mirus, Madison, WI), and purified by a QIAquick PCR purification kit (QIAGEN, Valencia, CA). HeLa cells were purchased from ATCC (Rockville, MD). The luciferase assays were completed with a Promega Luciferase Assay Kit (Madison, WI). The toxicity assays were performed with a Bio-Rad DC Protein Assay Kit (Hercules, CA). (3-(4,5-Dimethylthiazol-2-yl)-2,5-diphenyltetrazolium bromide (MTT) was purchased from Invitrogen (Carlsbad, CA).

Monomer Synthesis:

***1,3-bis(2-((tert-butoxycarbonyl)amino)ethyl)thiourea (2)*:** Dry methylene chloride (200 mL) was added to a 3-neck flask and was brought to -78 ^{o}C. Thiophosgene (1.665 mL, 21.84 mmol) was added carefully to this flask under nitrogen. It should be noted that thiophosgene is a highly toxic liquid and this procedure should be completed only in a hood and with proper safety precautions. A mixture of mono-*N*-Boc-ethylenediamine (**1**) (7.00 g, 43.68 mmol) and diisopropylethylamine (DIPEA) (5.60 g, 43.68 mmol) in 200 mL of dry methylene chloride was added slowly and carefully to the dark orange thiophosgene in methylene chloride over a period of 2 h. This reaction was stirred for 2 h at -78 ^{o}C and then warmed to room temperature and stirred for an additional 2 h. After, the reaction mixture was refluxed for another 2 h, and then washed with ultrahigh purity water. The organic layer was dried over Na_2SO_4 and the methylene chloride was evaporated *en vacuo* yielding a sticky yellow solid. Ethyl acetate (100 mL) was added to this residue, which was then sonicated for 30 mins and the white precipitate was filtered and isolated, washed again with cold ethyl acetate and dried to yield 5.06 g (13.98 mmol, 64%). ^{1}H NMR (400 MHz, $CDCl_3$, TMS): δ = 1.44 (s, 18H, $C(CH_3)_3$), 3.33 (m, 4H, CH_2NHCO), 3.54 (m, 4H, CH_2NHCS), 5.14 (br, 2H, NHCO), 6.70-7.06 (br, 2H, NHCS). ^{13}C NMR ($CDCl_3$): δ = 28.26, 39.73, 44.78, 79.88, 157.18, 181.99. ESI-MS $[C_{15}H_{31}N_4O_4S]^+$: m/z observed 363.2065, calculated 363.2061.

1,3-bis(2-((tert-butoxycarbonyl)amino)ethyl)-2-methylisothiouronium iodide (3): Compound **2** (3.00 g, 8.28 mmol) was dissolved in 100 ml of acetonitrile in a round bottom flask and then a 10 fold molar excess of methyl iodide (11.76 g, 82.80 mmol) was added. This reaction mixture was then stirred at 40 ^{o}C for 8 h. Acetonitrile and excess methyl iodide were evaporated *en vacuo* and the resulting pure product was dried and characterized to yield 3.84 g (7.62 mmol,

92%) of the final product. ^{1}H NMR (400 MHz, $CDCl_3$, TMS): δ = 1.42 (s, 18H, $C(CH_3)_3$), 2.75 (s, 3H, CH_3S), 3.43-3.56 (m, 6H, CH_2CH_2NHCO), 3.54 (m, 2H, $CH_2{}^{+}NH{=}CS$), 5.58, 5.72 (2 x s, 2H, NHCO), 8.74, 8.98 (2 x s, 2H, $^{+}NH{=}CS(CH_3)NH$). ^{13}C NMR ($CDCl_3$): δ = 15.27, 28.33, 38.25, 39.30, 45.94, 79.74, 80.59, 156.65, 158.28, 168.28. ESI-MS $[C_{16}H_{34}N_5O_4 - I]^{+}$: m/z observed 377.2216, calculated 377.2222.

1,3-bis(2-(tert-butoxycarbonylamino)ethyl)-2-methylguanidinium iodide (4): Compound **3** (1.00 g, 1.98 mmol) was dissolved in 100 ml of chloroform and was stirred at 50 ^{o}C. To this mixture, 2 ml of 2 M methylamine in tetrahydrofuran (THF) was added every 1 h for the first 4 h After 20 h, the reaction mixture was filtered to remove the precipitated impurity, and then the low boiling compounds were evaporated under reduced pressure to leave a very viscous colorless oil. This oil was dried *en vacuo* and then weighed to recover 0.93 g (1.90 mmol, 96%) of compound 4 ^{1}H NMR (400 MHz, $CDCl_3$, TMS): δ = 1.43 (s, 18H, $C(CH_3)_3$), 2.99 (s, 3H, $CH_3{}^{+}NH{=}C$), 3.39 (q, 4H, CH_2NHCO), 3.51 (m, 4H, CH_2NHCS), 5.78 (t, 2H, NHCO), 7.30 (s, 2H, NHCS), 7.32 (s, 1H, $^{+}NH{=}CS$). ^{13}C NMR ($CDCl_3$): δ = 28.32, 28.67, 39.24, 43.27, 80.31, 155.00, 157.95. ESI-MS $[C_{16}H_{34}N_5O_4 - I]^{+}$: m/z observed 360.2615, calculated 360.2610.

1,3-bis(2-(tert-butoxycarbonylamino)ethyl)-2-guanidinium iodide (5): Compound **3** (1.00 g, 1.98 mmol) was dissolved in 100 ml of chloroform–and this reaction mixture was brought to 40 ^{o}C. To this mixture, 2 mL 7 N ammonia in methanol was added every hour for the first 4 hours. After 20 h, the reaction mixture was filtered to remove the precipitated impurity, and then the solvent was evaporated *en vacuo* yielding viscous colorless oil. This oil was then dried *en vacuo* to obtain 0.89 g (1.88 mmol, 95%) of compound 5. ^{1}H NMR (400 MHz, $CDCl_3$, TMS): 3.33 (m, 4H, CH_2NHCO), 3.40 (m, 4H, CH_2NHCS), 5.44 (s, 2H, NHCO), 7.02 (s, 2H,

NHCS), 7.68 (s, 2H, $^{+}NH_2$=CS). ^{13}C NMR ($CDCl_3$): δ = 28.36, 39.37, 41.92, 80.21, 156.38, 157.19. ESI-MS $[C_{15}H_{32}N_5O_4 - I]^+$: m/z observed 346.1934, calculated 346.2449.

1,3-bis(2-aminoethyl)-2-methylguanidine trihydrochloride (6): Compound **4** (0.50 g, 1.03 mmol) was dissolved in 10 mL of trifluoroacetic acid (TFA) and stirred at room temperature. After 2 h, the TFA was evaporated under reduced pressure, which resulted in a dark brown oil. This oil was dissolved in 20 mL of ethanol, to which 2 mL of concentrated hydrochloride was added. A white precipitate resulted that was subsequently filtered and washed with cold ethanol. This product was then dried and characterized. Yield (0.16 g, 0.61 mmol, 59%). ^1H NMR (400 MHz, D_2O): δ = 2.82 (s, 3H, CH_3N), 3.19 (CH_2NHC), 3.53 (CH_2NH_2). ^{13}C NMR ($CDCl_3$): δ = 27.81, 38.07, 38.66, 155.52. ESI-MS $[C_6H_{18}N_5 - Cl]^+$: m/z observed 160.1554, calculated 160.1562. Purity from NMR: >99%.

***1,3-bis(2-aminoethyl)-2-guanidine trihydrochloride (7)*:** Compound **5** (0.50 g 1.06 mmol) of was dissolved in 10 mL of trifluoroacetic acid (TFA) and stirred at room temperature. After 2 h, the TFA was evaporated under reduced pressure, which resulted in dark brown oil. This oil was dissolved in 20 mL of ethanol, to which 2 mL of concentrated hydrochloride was added. A white precipitate resulted, that was then isolated via filtration and washed with cold ethanol. The product was then dried and characterized, yield 0.17 g (0.67 mmol, 63%). ^1H NMR (400 MHz, D_2O): δ = 3.19 (CH_2NHC), 3.53 (CH_2NH_2). ^{13}C NMR ($CDCl_3$): δ = 38.06, 38.74, 156.26. ESI-MS $[C_5H_{16}N_5 - Cl]^+$: m/z observed 146.1402, calculated 146.1406. Purity from NMR >95%.

Polymer Synthesis:

Poly(L-tartaramidodiethyleneamine) (T1)[73]: Diethylenetriamine (0.10 g, 0.97 mmol) was weighed out in a round bottom flask and 0.96 mL (2.0 M) of methanol was added to dissolve the diethylenetriamine. Dimethyl-L-tartrate (0.17 g, 0.97 mmol) was added to the round bottom flask. This mixture was then stirred for 24 h at room temperature, after which time 5 mL of water was added to this reaction mixture. This reaction mixture was then dialyzed in 1000 Da molecular weight cut off (MWCO) membrane against ultrapure water for 24 h to purify the polymer material from the residual low molecular weight compounds. This reaction mixture was then lyophilized until dry. The resulting polymer was then characterized via GPC (**Table 2.1**). Yield 0.087 g (41%, Mw = 1.1 kDa, n = 4).

Poly(galactaramidodiethyleneamine) (G1)[19]: Diethylenetriamine (0.3 g, 2.91 mmol) was dissolved in 58.1 mL (0.1 M) of methanol and dimethyl *meso*-galactarate 0.693 g (2.91 mmol) of was added to this reaction mixture. This reaction mixture was stirred for 24 h. Methanol was evaporated under reduced pressure to afford a white solid. This solid, was dissolved in 10 mL of ultrapure and the mixture was transferred in a 1000 Da molecular weight membrane and was exhaustively dialyzed against ultrapure water for 24 h to remove the relatively smaller molecular weight compounds. This mixture was then flash frozen in a scintillation vial and lyophilized to afford a white fluffy solid. The resulting polymer was then characterized via GPC. Yield 0.32 g (38%, Mw = 1.3 kDa, n = 5).

Poly(galactaramidodiethylenemethylguanidine) (Gmeg): Compound **6** (0.15 g, 0.56 mmol) was dissolved in 2 mL of methanol. To this, 400 µL of triethylamine (TEA) was added in 5 x 0.556 mmol aliquots while stirring over the period of 15 min to obtain a homogeneous mixture. Next, dimethyl *meso*-galactarate (0.13 g, 0.56 mmol) was added and the reaction was

stirred at room temperature for 48 h. The reaction mixture was then concentrated under reduced pressure. Ultrapure water (5 mL) was added to the reaction mixture and it was then pipetted into a 1000 Da MWCO membrane and exhaustively dialyzed for 24 h against ultrapure water to remove lower molecular weight impurities. This mixture was then flash frozen in a scintillation vial and was lyophilized to afford a sticky white solid. The resulting polymer was then characterized via GPC. Yield 0.073 g (36%, Mw = 1.3 kDa, n = 4).

Poly(L-tartaramidodiethylenemethylguanidine) (Tmeg): Compound **6** (0.15 g, 0.56 mmol) was dissolved in 1 mL of methanol in a round bottom flask. Triethylamine (400 µL) was added to this mixture in 5 x 0.56 mmol aliquots and stirred for 15 mins to obtain a homogeneous mixture. Next, dimethyl L-tartrate (99.1 mg, 0.56 mmol) was added and stirred for 120 h at room temperature. The methanol was then removed under reduced pressure to afford a white solid and the product was dissolved in 5 mL of ultrapure water, transferred to a 1000 Da MWCO membrane and was exhaustively dialyzed against ultrapure water for 24 hours. This mixture was then flash frozen in a scintillation vial and lyophilized to afford a sticky yellowish solid. The resulting polymer was then characterized via GPC. Yield 0.043 g (23%, Mw = 1.4 kDa, n = 5).

Poly(galactaramidodiethyleneguanidine) (Gg): Compound **7** (0.10 g,0.39 mmol) was added to a round bottom flask and dissolved in 2 mL of methanol. To this mixture, 275 µL of triethylamine (TEA) was added in 5 x 0.393 mmol aliquots while stirring over the period of 15 minutes to obtain homogeneous reaction mixture. Next, dimethyl *meso*-galactarate (0.094 g, 0.39 mmol) was added and the reaction was stirred for 48 h at room temperature. The reaction mixture was concentrated under reduced pressure. Ultrapure water (5 mL) was then added to this reaction mixture and the solution was transferred in a 1000 Da MWCO membrane and was exhaustively dialyzed against ultrapure water for 24 h to remove low molecular weight

impurities. This mixture was then flash frozen in a scintillation vial, after which the remaining water was lyophilized to afford a sticky white solid. The resulting polymer was then characterized via GPC. Yield 0.043 g (31%, Mw = 1.3 kDa, n = 4).

Poly(L-tartaramidodiethyleneguanidine) Tg: Compound 7 (0.15 g, 0.59 mmol) was dissolved in 1 mL of methanol in a 5 mL round bottom flask. Triethylamine (425 µL) was added in 5 x 0.59 mmol aliquots and stirred for 15 mins to obtain a homogeneous mixture. Next, dimethyl L-tartrate (105.5 mg, 0.59 mmol) was added and the reaction mixture was stirred for 120 h. Next, the methanol was removed under reduced pressure to afford an off-white solid. To purify, the solid was dissolved in 5 mL of ultrapure water and transferred into a 1000 Da MWCO membrane and exhaustively dialyzed against ultrapure water for 24 h. This mixture was then flash frozen in a scintillation vial, after which any residue and lyophilized to afford a sticky yellowish solid. The resulting polymer was then characterized via GPC. Yield 0.063 g (36%, Mw = 1.3 kDa, n = 5).

Polymer Characterization:

Molecular weight and polydispersity (PDI) were characterized using a Viscoteck GPCmax with a $GMPW_{XL}$ column coupled to a triple detector (static light scattering, viscometry and refractive index). A solution of 0.5 M sodium acetate in 80:20 water to acetonitrile was used as mobile phase. The pH of the mobile phase was adjusted to pH 7 by adding acetic acid. Sample preparation was done by dissolving 2 mg of polymer sample in 1 mL of mobile phase, and injecting 100 µL this solution onto the column at a flow rate of 0.6 mL/minute.

Polyplex Characterization:

Gel electrophoresis shift assays: The binding between **Gg**, **Gmeg**, **Tg** and **Tmeg** polymers and pDNA was tested via gel electrophoresis under 60 V for 60 minutes. Agarose gel (0.6 % w/v) was created using 1X TAE buffer (IBI Scientific, IA) and ethidium bromide (0.6 μg/mL) was added to the gel contained (Invitrogen, CA). Plasmid DNA (pCMV-*lacZ*) was diluted to create a 0.1 mg/mL stock solution with nuclease-free water (Gibco). Stock solution of every polymer and control were made with nuclease free water at *N/P* 50 (where *N* = number of guanidine groups (for PGAGs) or secondary amines (for PGAAs) on polymer, *P* = number of phosphate groups on DNA) based on 0.1 mg/ml pDNA solution. Polymer stock solutions were further diluted to the desired *N/P* ratios using ultrapure water. Polymer/pDNA complexes (polyplexes) were then formulated at various *N/P* ratios between 0 (pDNA only) to 30. To create the polyplexes at different *N/P* ratios, 10 μr of each polymer solution (diluted from the stock) was added to 10 μL of pDNA solution. The polyplex solutions were then incubated for 60 minutes before 2 μL loading buffer (Blue Juice) was added. A 15 μL aliquot of each polyplex solution was loaded onto the gel for electrophoresis testing. The pDNA migration was visualized by exciting ethidium bromide at 322 nm UV light. The gels were visualized and photographed with a FOTO/FX gel digital imaging system (FOTODYNE, WI).

Dynamic Light Scattering: The hydrodynamic diameter of the polyplexes were measured in triplicate at 25 °C (633 nm and detection angle of 173°) on a Zetasizer (Nano ZS) dynamic light scattering instrument (Malvern Instruments, Malvern, UK). Polyplexes were formed at *N/P* ratios between 2 to 30 by mixing each aqueous polymer solution (150 μL in H_2O) with pCMV-*β* (plasmid factory, Germany) (150 μL, 0.02 μg/μL in H_2O) and allowing the solution to sit for 40

mins. The average size of the polyplexes and standard deviation are reported for each polyplex solution in **Figure 2.2**.

Transmission Electron Microscopy: Polymer-pDNA complexes were prepared at *N/P* = 20 as described above for the dynamic light scattering studies. Samples (5 μL of the polyplex solution in water) were applied in duplicate to 400-mesh carbon-coated grids (EMS, Fort Washington, PA) and incubated for 60 s. Excess liquid was removed by blotting with a kimwipe. Samples were negatively stained with uranyl acetate (2%, w/v) for 90 s and again blotted with a kimwipe. TEM images were recorded with a JEOL JEM-1230 transmission electron microscope operated at 60.

Cell Culture Experiments:

General: HeLa (human cervix adenocarcinoma) cells were purchased from ATCC. Cells were cultured in Dulbecco's Modified Eagle Medium (DMEM) with 10 % fetal bovine serum (FBS), 50 units/mL of penicillin and 50 μg/mL of streptomycin in 5 % CO_2 at 37 ^{o}C. Plasmid DNA including pCMV-*lacZ* and luciferase DNA (pCMV-*luc*) were purchased from PlasmidFactory (Germany). All experiments used an identical passage of cells and the same batch of reagent; all samples were prepared with Gibco nuclease-free water and all materials were autoclaved or treated under UV light for 15 mins to ensure aseptic conditions and reproducible results.

Luciferase and Protein Assays in Serum-free Culture Medium: HeLa cells were cultured in a 24-well plate with a density of $5x10^4$ cells/well and were incubated for 24 h prior to transfection. To form the polyplexes, 150 μL of an aqueous solution of each PGAG (**Gg**, **Gmeg**, **Tg**, **Tmeg**) or positive control polymers (**G1**, **T1**, poly-L-arginine (PLA) and *Glycofect*

Transfection Reagent) were added into 150 μL pCMV-*luc* DNA (0.02 mg/mL) at *N/P* ratios of 5, 10, 15, 20, 25 and 30 at room temperature. The solutions were allowed to incubate for 60-minutes to allow polyplex formation, after which 600 μL of serum-free medium (Opti-MEM) was added to each eppendorf containing the polyplex solutions and mixed gently with a pipette. The HeLa cells were washed with 0.5 mL PBS, after which 300 μL of polyplex solution (containing 1 μg DNA and the designated *N/P* ratios of polymer) was added to the cells in each well. Untranfected cells and cells transfected with pCMV-luc pDNA only were used as the negative controls. Experiments were completed in triplicate. Four hours after initial transfection, 800 μL of DMEM solution containing 10% FBS was added to each well. Twenty four hours after initial transfection, the medium in each well was replaced with 1 mL of fresh DMEM containing 10% FBS . Forty-eight hours after initial transfection, cells were washed with PBS and lysed with 100 μL of 1X cell culture lysis buffer (Promega). A Bio-Rad DC protein assay kit was used to determine the amount of protein in the cell lysates. For luciferase activity, the cell lysates were analyzed by adding luciferase substrate and measuring the relative light units. Luminescence was measured over 10 s with a luminometer (GENios Pro, TECAN US, Research Triangle Park, NC).

Luciferase and Protein Assays in Culture Medium Containing Serum: The luciferase and protein assays in the presence of DMEM containing 10% serum carried out via an identical protocol to the serum-free study with the exception that 600 μL of DMEM containing 10% FBS was added directly to the polyplex solutions and the transfections were completed solely in the presence of this media. Also, only two representative *N/P* ratios (10 and 25) were used for transfection studies with the PGAGs and positive control polymers in the medium containing serum.

MTT Assay: HeLa cells were cultured in a 24-well plate with a density of $5x10^4$ cells/well and incubated for 24 hours prior to transfection. Polyplexes were formed by pipetting 150 μL of the PGAG or positive control polymers (**Gg**, **Gmeg**, **Tg**, **Tmeg**, **G1**, **T1**, PLA or *Glycofect Transfection Reagent*) into 150 μL of pCMV-*lacZ* DNA (0.02 mg/mL) and pipetting up and down to mix the solutions. The polyplexes were formed via this method at *N/P* ratios of 5, 10, 15, 20, 25 and 30 at room temperature. The polyplex solutions were allowed to sit for 60-minutes prior to addition of 600 μL of serum-free medium (Opti-MEM). HeLa cells were washed with 0.5 mL PBS, after which 300 μL of each polyplex solution (containing 1 μg DNA and different *N/P* ratios of each polymer) was added to the cells in each well. Untranfected cells and cells transfected with pCMV-luc pDNA only were used as negative controls. Each experiment was completed in triplicate. Four hours after initial transfection, 800 μL 10% FBS DMEM solution was added to each well. Twenty-four hours after initial transfection, the cells in each well were washed with 0.5 mL PBS. Then 0.5 mL of a 0.5 mg/mL 3-(4,5-Dimethylthiazol-2-yl)-2,5-diphenyltetrazolium bromide (MTT) in 10% FBS DMEM solution was added to each well. After incubation at 37 ^oC for 1 h, the cells in each well were washed with 0.5 mL PBS and lysed with 600 μL DMSO. Cell lysates were shaken for 20 mins in darkness. A 200 μL aliquot of cell lysate was loaded to a 96-well plate for colorimetric measurement. Samples were measured with a spectrophotometer (GENios Pro, TECAN US, Research Triangle Park, NC) with a wavelength of 570 nm. Cell viability profiles were characterized by absorbance results. Cell viability of transfected cells was normalized to that of untransfected cells.

Flow Cytometry: HeLa cells were cultured in a 6-well plate with a density of $2.5x10^5$ cells/well and were incubated for 24 h prior to transfection. Polyplexes were formed by adding 250 μL of each polymer and control (**Gg**, **Gmeg**, **Tg**, **Tmeg**, **G1**, **T1**, PLA and *Glycofect*

Transfection Reagent) into 250 μL *Cy5*-labeled pCMV-*lacZ* DNA (excited at 633 nm) (0.02 mg/mL). Polyplexes were formed at *N/P* ratios of 10 and 25 at room temperature and allowed to sit for 60-minutes at room temperature. After this incubation period, 1 mL of serum-free medium (Opti-MEM) was added. HeLa cells were washed with 1 mL PBS and 1.5 mL polyplex solution (containing 5 μg DNA and each polymer to examine the effect of *N/P* ratios of 10 and 25) was added to cells in each well. Untranfected cells and cells transfected with pDNA only were used as negative controls for the cellular uptake study. Cells treated with PLA and *Glycofect* were used as the positive controls and all of the experiments were completed in duplicate. Two hours after initial transfection, cells were rinsed with PBS several times to remove any polyplexes bound to the cell surface. After, 1 mL of 10% FBS DMEM was then added to allow further endocytosis for 30 mins. Four and a half hours after initial transfection, cells were washed with PBS, trypsinized, pelleted, the supernants were removed, and the cells were resuspended in PBS for flow cytometry analysis. Cells positive for *Cy5* (and the average *Cy5* intensity) were analyzed with a FACSCanto II (Becton Dickenson, San Jose, CA). Approximately 20,000 events were recorded.

2.3 Results and Discussion

Here in, we synthesized and studied a new polymer series we have termed poly(glycoamidoguanidine)s (PGAGs) that have been created as analogues to our previous PGAAs. To examine the biological effects of the charge center, we replaced the amines in our original PGAA structures with guanidine and methylguanidine groups. The guanidine group has a high pKa value of around 12.5 (dependent on the substituent) and is protonated at physiological pH as opposed to the amine groups in the PGAAs; in the case of T1, only about 50% of the

secondary amines are protonated at physiological pH.[22] Because subtle changes in the chemical structure[93,94] of the delivery vehicle can largely impact the resulting biological properties of a polymer, the different charge types in the PGAAs and PGAGs can heavily impact the biological properties such as polyplex formation,[22,54] polyplexes internalization[80] into cells, intracellular trafficking, and possible release from the endosome. Also, according to the proton sponge hypothesis, the presence of PGAGs in a polyplex should not provide buffering capacity in the endosomes, thereby supposedly hindering endosomal release and our study seeks to explore how these structural changes alter the delivery profiles.

Monomer and Polymer Synthesis

Poly(glycoamidoguanidine)s (PGAGs) were designed based on a similar aminolysis chemistry used previously for synthesizing the PGAAs. However, since the diamine with a guanidine moiety in the architecture was not commercially available, we used similar synthetic methods related to those developed by Sambrook et al.[95] As shown in **Scheme 2.1**, mono-*N*-Boc-ethylenediamine (**1**) synthesized from an earlier reported procedure[96] was reacted carefully with thiophosgene at -78 ^{o}C in presence of diisopropylethylamine (DIPEA). The reaction mixture was warmed to room temperature and then refluxed. After purification, the thiourea compound (**2**) was obtained and was subsequently reacted with methyliodide yielding the methyl thiourea species (**3**). The methyl thiourea was then treated with either ammonia or methylamine, which afforded the desired methyl guanidine (**4**) and guanidine (**5**) compounds respectively. Both compounds (**4** and **5**) were then treated with trifluoroacetic acid (TFA) to remove the Boc groups and liberate the amine salts. The final methyl guanidine-containing (**6**) and guanidine (**7**)

monomers were obtained by dissolving the materials in ethanol and precipitating out the structures by treating each respective solution with concentrated HCl.

The PGAG oligomers were synthesized by reacting the guanidine (**g, 7**) or methylguanidine (**meg, 6**) moieties with dimethyl *meso*-galactarate (**G**) or dimethyl-L-tartrate (**T**) to yield four structures (**Scheme 2.2**). To synthesize the galactarate polymers, monomers **6** or **7** were each dissolved in methanol separately in the presence of TEA and then reacted with dimethyl *meso*-galactarate for 48 h.

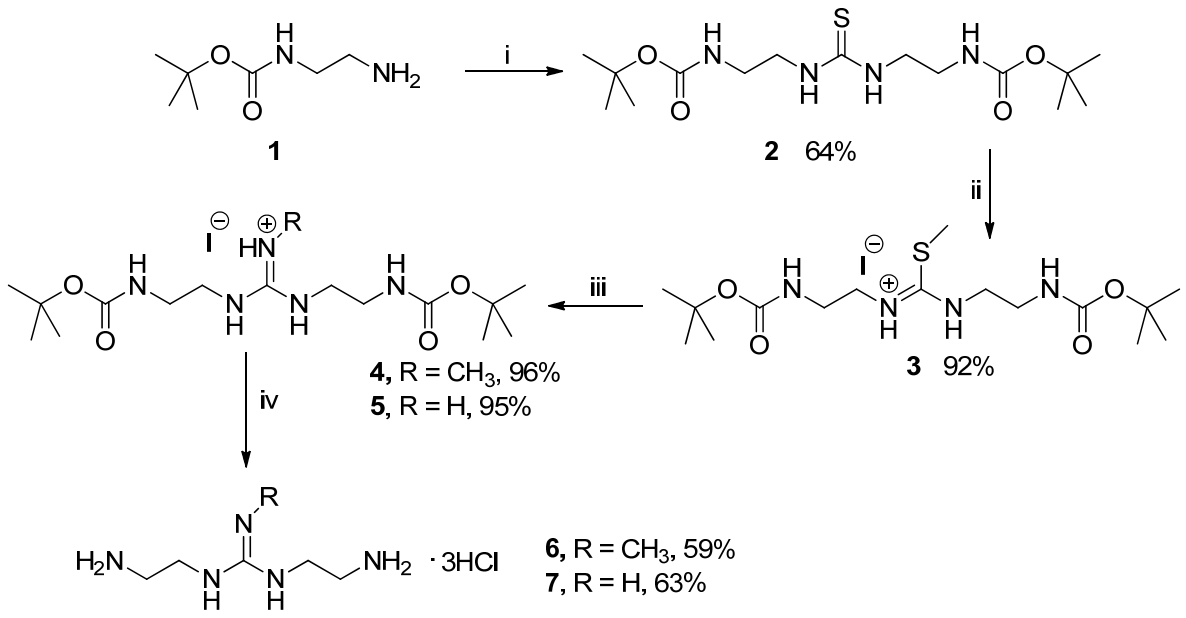

Scheme 2.1, Synthetic scheme for the synthesis of the guanidine containing monomers. i) Thiophosgene, DIPEA, -78 ^{o}C reflux, $CHCl_3$; ii) methyl iodide, 50 ^{o}C, acetonitrile; iii) 4.0 N methylamine in THF for and 6.0 N ammonia in methanol for (**5**); iv) TFA, and wash with 0.5% HCl in EtOH.

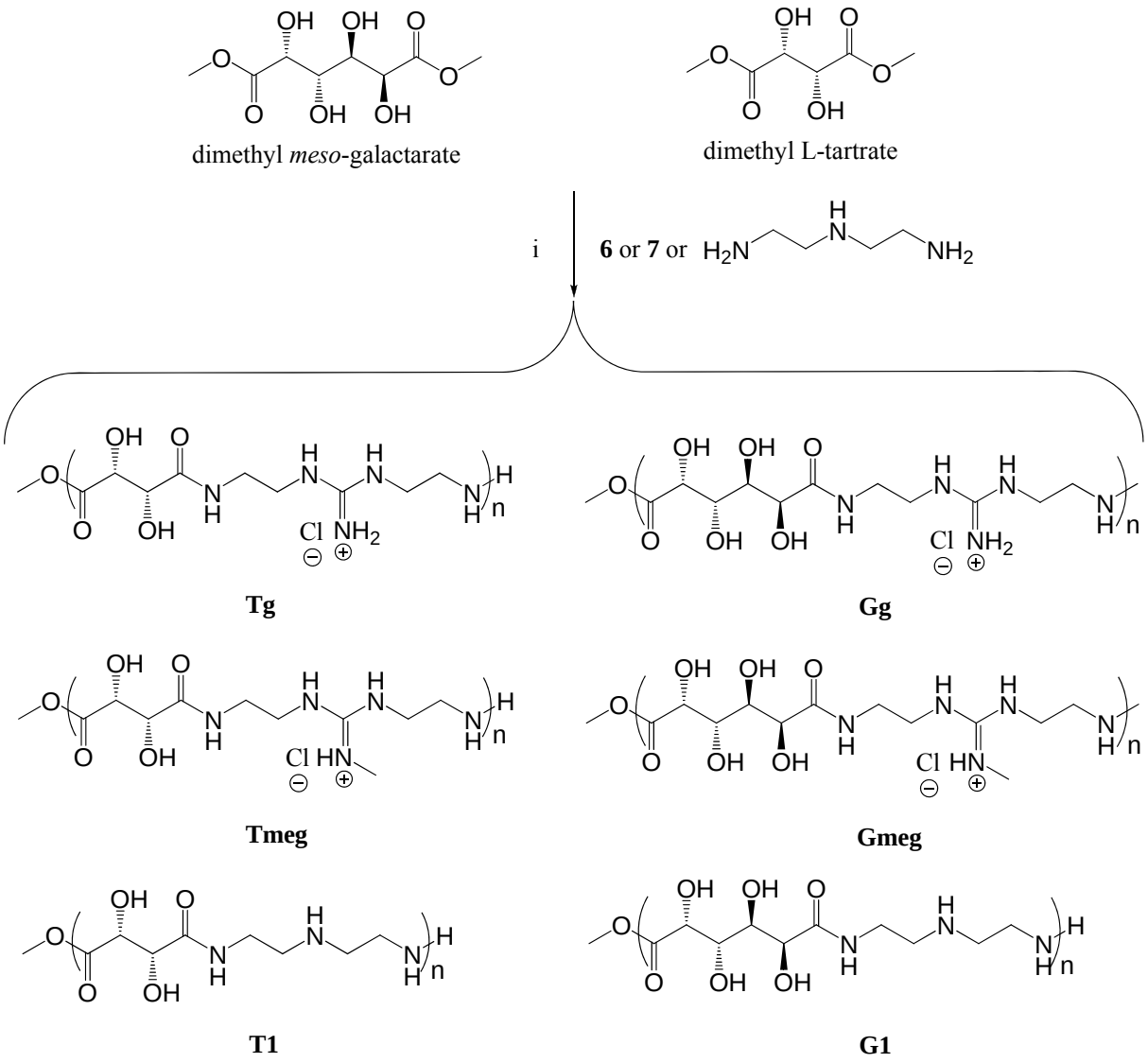

Scheme 2.2, Synthetic scheme for polymerization of the diamine monomers such as **6**, **7**, or diethylenetriamine with dimethyl-*meso*-galactarate or dimethyl-L-tartrate in TEA, MeOH.

The tartrate series was synthesized by reacting monomers **6** and **7** with dimethyl-L-tartrate under similar conditions for 120 h. After polymerization of each mixture, the reaction mixtures were each dialyzed with a 1000 MWCO membrane against ultrapure water for 24 hours

to purify the polymers from unreacted monomer and each product was characterized via GPC. The PGAAs with one secondary amine created with galactarate or tartrate monomers (**G1** and **T1**) were also synthesized to obtain similar short oligomers to more accurately compare the effects of the charge center on the biological properties and to assure that the differences observed in the biological activity are related to the charge center alterations. **Table 2.1** reveals the characterization data for each of the polymers created for this study.

Table 2.1, The weight average molecular weight (Mw), polydispersity index (Mw/Mn) and degree of polymerization (n) for the guanidine and amine containing oligomers.

Polymer	Mw (kDa)	Mw/Mn	n
Gg	1.3	1.2	4
Gmeg	1.3	1.3	4
Tg	1.3	1.2	5
Tmeg	1.4	1.2	5
G1	1.3	1.3	5
T1	1.1	1.3	4

Polyplex Characterization

Gel Electrophoresis Shift Assay: The ability of each PGAG polymer to bind with the pDNA was examined using a gel electrophoresis shift assay to observe the inhibition of pDNA migration with increasing the polymer concentration (*N/P* ratio). Polyplexes were prepared at a variety of *N/P* ratios from zero (pDNA only) to 30 and loaded onto the gel. As shown in **Figure**

2.1, at *N/P* zero (pDNA only) pDNA migrates towards the positive electrode and all four of the guanidine polymers were shown to bind with pDNA and inhibit gel migration at low *N/P* ratios of 2.5 or lower. While, gel electrophoresis shift assay conducted with guanidine monomers (compound **6** and **7**) revealed no binding with pDNA. Therefore, no biological studies were applied to these two compounds.

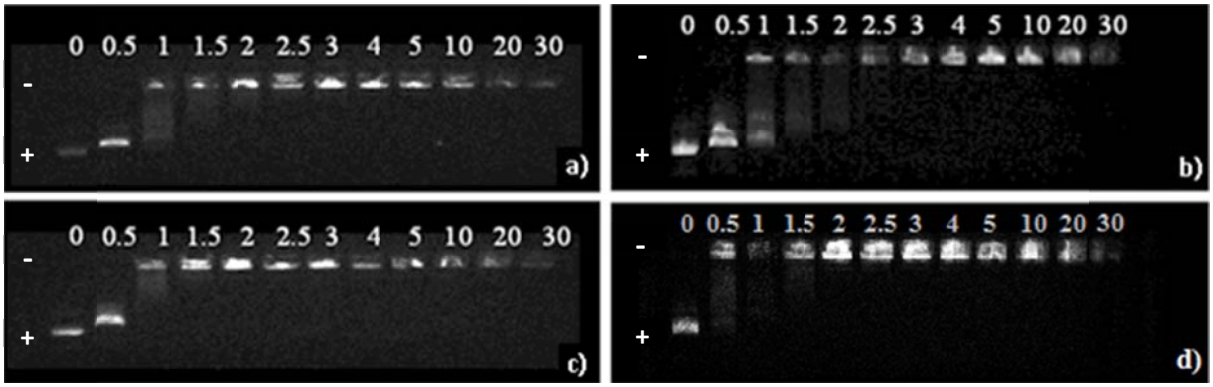

Figure 2.1, Gel electrophoresis shift assay for the PGAGs. Each polymer was complexed with pDNA in different *N/P* ratios between 0 (pDNA only, migrates with the electrophoretic field) and 30. These data show that: a) **Gmeg** binds with pDNA at *N/P* = 2, b) **Tmeg** binds with pDNA at *N/P* = 2.5, c) **Gg** binds with pDNA at *N/P* = 1.5, and d) **Tg** binds pDNA at *N/P* = 2.

The analogous PGAA polymers, **T1** and **G1** showed pDNA migration inhibition at *N/P* of 10 or higher. Thus, at similar degrees of polymerization, the guanidine-containing oligomers (PGAGs) exhibited a higher affinity for pDNA binding compared to the amine-containing polymers (PGAAs). The galactarate-based, guanidine-containing polymers (**Gg** *N/P* = 1.5, **Gmeg** *N/P* = 2) were shown to bind pDNA at a lower *N/P* ratio as compared to the tartrate-based polymers (**Tg** *N/P* = 2, **Tmeg** *N/P* = 2.5). This supports our previous data showing that the galactarate moiety appears to play a role at enhancing the polymer binding affinity to pDNA. In addition, the PGAGs with a methyl guanidine group (**Tmeg** and **Gmeg**) bound pDNA at a higher

N/P ratio when compared to the PGAGs with a guanidine group, indicating that the methyl group may slightly weaken the binding affinity due to a lower electrostatic interaction. Interestingly, the Zeta potential data supports this hypothesis.

***Polyplex Size*:** Polyplex size was characterized via dynamic light scattering (DLS) at various *N/P* ratios between 2 and 20. **Figure 2.3** shows the data for polyplexes formed with each of the new PGAGs at *N/P* = 5 and 20. The average size of the polyplexes at a low *N/P* ratio of 2 was approximately 600 nm likely due to the incomplete plasmid compaction (and negative Zeta potential, *vide infra*). However, at an *N/P* ratio of 5, the polyplex size significantly decreased to between 78-124 nm and remained consistent at this size, with the exception of polyplexes formed with **Gmeg**, which revealed larger sizes of around 200 nm. The polyplex size of Gmeg at *N/P* 20 was also determined using TEM and it was found that, these polyplexes might be forming dimers which could be the reason for the observed DLS measurements. Interestingly, **G1** and **T1** polyplexes revealed large particle sizes of between 400-700nm even at higher *N/P* ratios, revealing that these materials may not fully compact pDNA into polyplexes effectively. However, the positive controls, PLA and Glycofect were both very effective at compacting pDNA into polyplexes. The disparity in polyplex size when comparing the small PGAG polyplexes to the complexes formed with the PGAAs is likely due to differences in the electrostatic interaction of these short oligomers with pDNA (PGAGs are more cationic and appear to promote a higher binding affinity at lower *N/P* ratio).

***Zeta Potential*:** As shown in **Figure 2.2**, the Zeta potential of the PGAG polyplexes in an aqueous solution was depended on the *N/P* ratio of formulation. At low *N/P* ratio of 2, the polyplex Zeta potential values were all neutral or slightly positive (0 to +2 mV), with the exception of **Gmeg** complexes (-7 mV). At polyplex formulations greater than 2, the polyplexes

all resulted in a moderately positive surface charge on the polyplexes (4-12). Polyplexes formed with **Tmeg** yielded the lowest Zeta potential values, which were near neutral (+5 mV), even at *N/P* = 20; this result supports the gel shift assays that had the highest *N/P* ratio of complexation. Interestingly, with the controls, the **T1** exhibited lower Zeta potential values at *N/P* ratios of both 10 and 25 (Supporting Information).

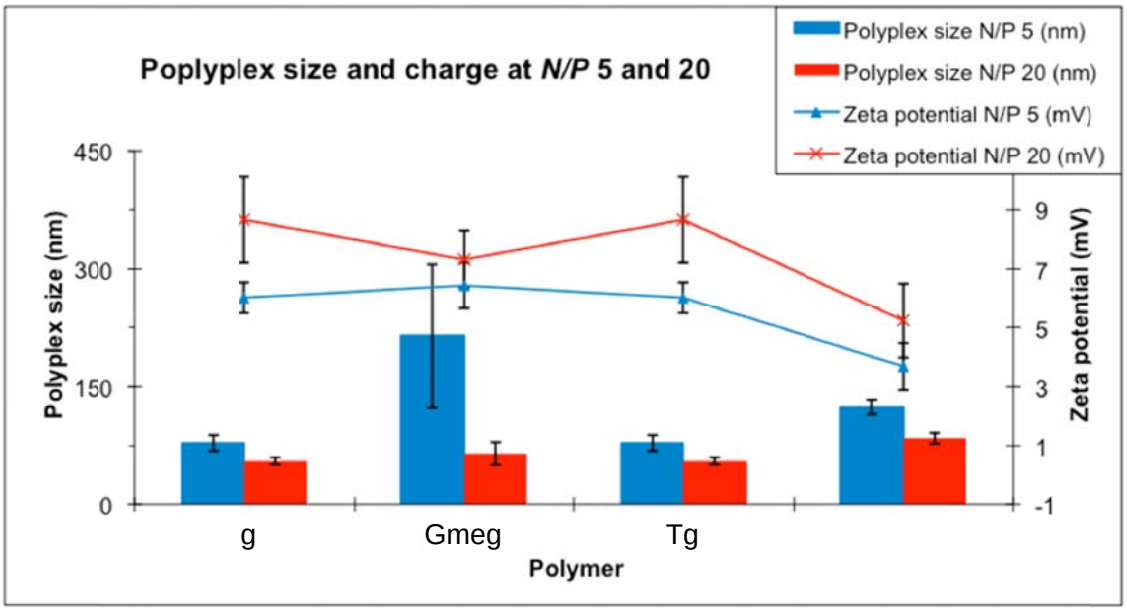

Figure 2.2, The PGAG polyplex size and Zeta potential. The PGAG polymers were dissolved in water and complexed with pDNA at *N/P* = 5 and 20.

Cell Culture Experiments

Cellular Uptake and Transgene Expression Studies: To examine the cellular uptake of the PGAG-based polyplexes (**Gg**, **Gmeg**, **Tg**, **Tmeg**) and compare the results to the controls cells, pDNA, poly-L-Lysine (PLA, *N/P* = 5), *Glycofect Transfection Reagent* (*N/P* = 25), **G1** and **T1** (*N/P*s = 10 and 25), a flow cytometry assay was carried out to ascertain both the number of cells positive for *Cy5*-labeled pDNA and the average intensity of *Cy5* florescence in the cells.

PGAG polyplexes were formed at *N/P* 10 and 25 and HeLa cells were incubated with each polyplex solution and control for 2 hours, after which, the cells were washed multiple times with PBS, trypsanized, pelleted, washed with PBS, and pelleted and repeated several times to remove surface bound polyplexes for accurate flow cytometry characterization. Results are shown in **Figure 2.3** for the percentage of cells positive for *Cy5* fluorescence, as well as for mean fluorescence intensity. Specifically, only 20% of the cells were positive for *Cy5* fluorescence with pDNA only. All of the polymers (PGAGs, PGAAs, and positive controls) facilitated an increase in the uptake of pDNA in HeLa cells over the negative controls. It is also interesting to note that the PGAGs promoted similar cellular uptake of pDNA as the positive controls, *Glycofect,* a glycopolymer that consists of repeated galatarate residues along with four ethyleneamines and poly-L-arginine (PLA) a polypeptide consisting of repeated pendant guanidine charge centers, and also revealed higher cellular uptake than the other PGAAs analogues (**G1** and **T1**). Polyplexes formed with **G1** and **T1** were internalized by about 70% of cells while the PGAGs promoted higher cellular internalization, where on average, 90% of the cells were positive for *Cy5*-pDNA (with the exception of **Tg** polyplexes at *N/P* = 10). While the uptake of the **Tg** polyplexes at *N/P* = 10 is low, we currently do not understand this result. When comparing the mean *Cy5* intensity per cells, surprisingly the **Tg** (*N/P* = 10) and the control PLA polyplex samples revealed the lowest intensity values, indicating that these formulations do not facilitate effective nucleic acid transfer into cells. On the high end, both of the methylated guanidine analogs, **Gmeg** (*N/P* = 25) and **Tmeg** (*N/P* 10 and 25) yielded high *Cy5* internalization, similar or higher than *Glycofect*. This result was very interesting and prompted our comparison of the gene expression profile for these systems.

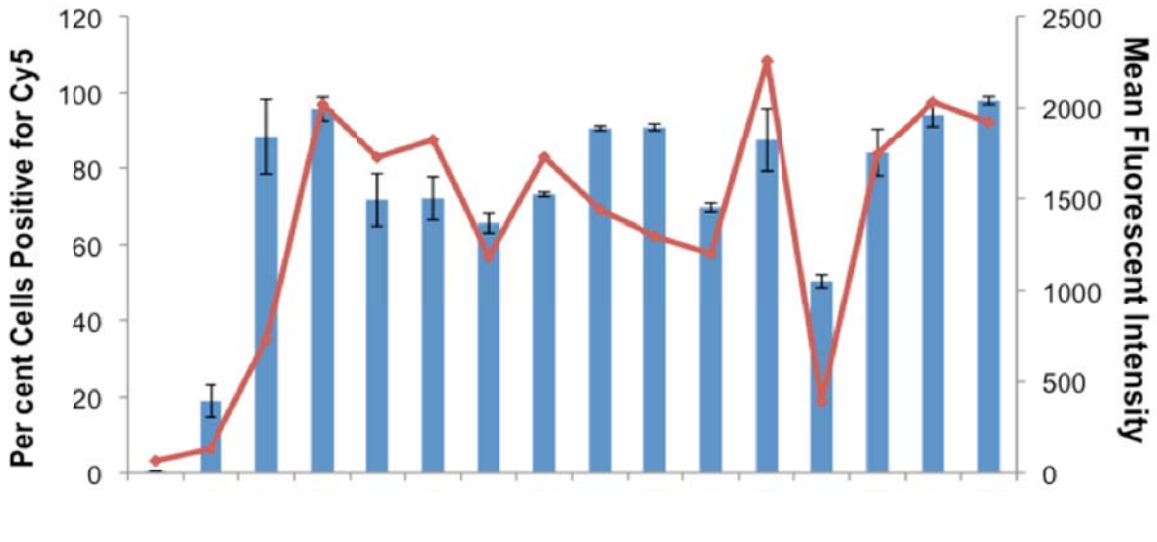

Figure 2.3, HeLa cell uptake of *Cy5*-pDNA delivered with the PGAG and PGAA polymers complexed with pDNA at *N/P* ratio 10 and 25. Cells only and DNA only are used as negative controls and *Glycofect Transfection Reagent* (*N/P* 25) and poly-L-arginine (PLA) were used as the positive controls. The bars represent the percentage of cells positive for *Cy5* fluorescence; the line represents the mean fluorescence intensity of the cells.

Luciferase Assays in Serum and Serum-free Media: Luciferase reporter gene expression assays were carried out in order to characterize how efficiently the guanidine-containing oligomers can deliver pDNA to HeLa cells and promote transgene expression. Similar to the flow cytometry studies, two positive controls were used: *Glycofect Transfection Reagent* and poly-L-arginine. The luciferase reporter gene delivery experiments were carried out both in the absence and presence of serum (**Figures 2.4** and **2.5**, respectively) for each polyplex type and control and the data revealed some interesting trends. In the absence of serum (Opti-MEM), it was found that transgene expression with the PGAG polyplexes, increased with an increase in

the *N/P* ratios from 5 to 30. Overall, of the new polymers examined, **Gg** was found to yield the highest transgene expression within this series. Also, at lower *N/P* ratios, the galactarate polymers **Gg** and **G1** revealed the highest gene expression (similar to PLA), which correlates to our findings that the galactarate units in the polymer appear to enhance interactions with pDNA and promote stable polyplex formation.[22] As the *N/P* ratio is increased, transgene expression with the tartrate polymers (in particular, Tmeg) increases. Over all, the controls, *Glycofect* revealed the highest gene expression in serum-free media. PLA revealed a similar gene expression profile to the PGAGs and PGAAs (**G1** and **T1**), however, above an *N/P* ratio of 15, total cell death was observed and expression values were not able to be recorded.

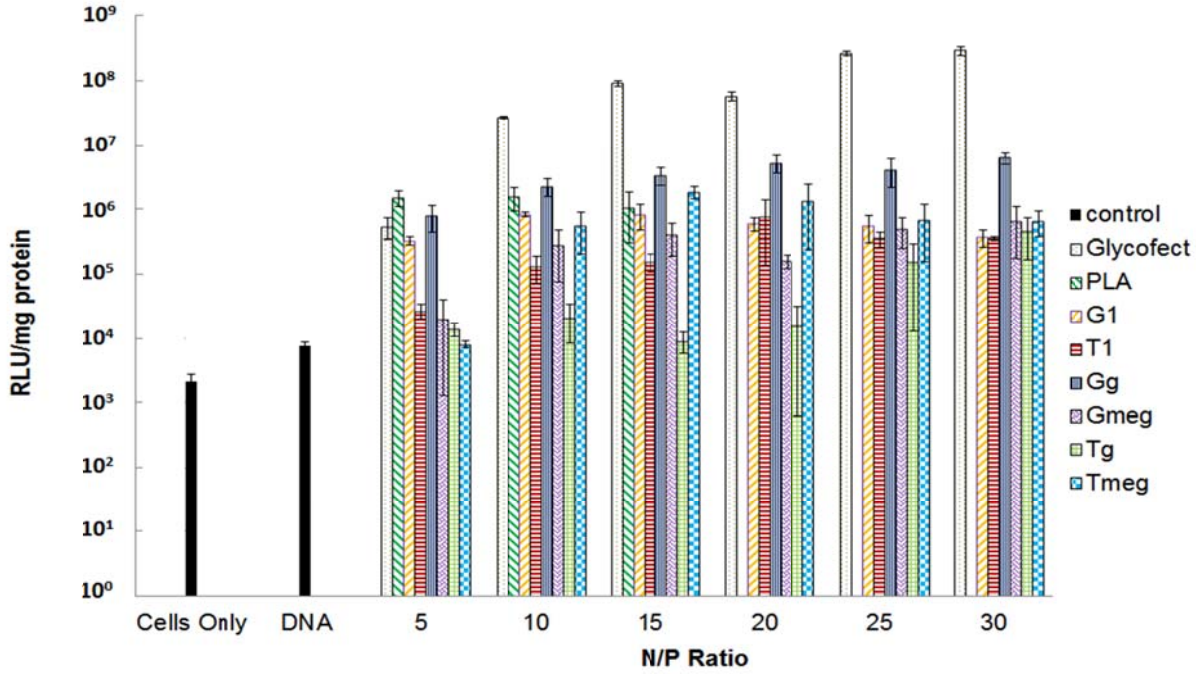

Figure 2.4, Luciferase gene expression observed with polyplexes formed with the PGAGs, PGAAs, and the positive controls, *Glycofect Transfection Reagent*, and poly-L-arginine Opti-MEM (reduced serum culture medium). The polyplexes are formed at different *N/P* ratios from 5 to 30. The gene expression values are shown as relative light units (RLU/mg of protein). The data is reported as the mean and standard of deviation of three replicates.

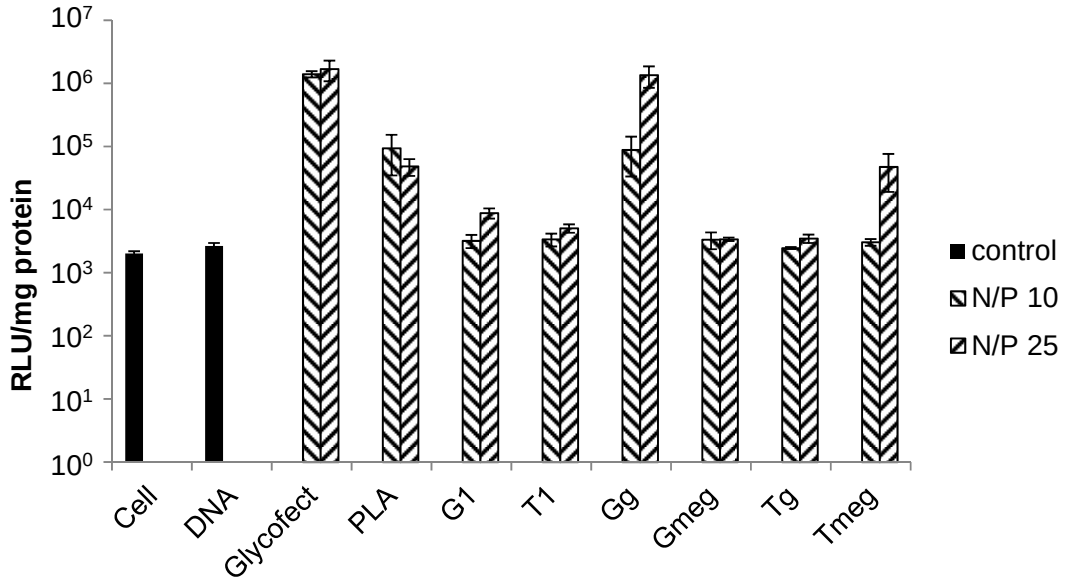

Figure 2.5, Luciferase gene expression observed with polyplexes formed with the PGAGs, PGAAs and the positive controls *Glycofect Transfection Reagent* and poly-L-arginine in DMEM containing 10% serum. The polyplexes are formed at *N/P* ratio 10 and 25. The gene expression values are shown as relative light units per milligram of protein (RLU/mg). The data is reported as the mean and standard of deviation of three replicates.

Figure 2.5 shows the transgene expression data for the PGAG and control polyplexes formed at *N/P* ratios of 10 and 25 in the presence of serum. At both *N/P* ratios, compounds **G1**, **T1**, **Gmeg**, **Tg**, and **Tmeg** (*N/P* 10 only) revealed minimal luciferase expression (similar to the negative controls). However, polyplexes formed with **Gg**, particularly at *N/P* = 25, revealed high gene expression similar to *Glycofect* and higher than PLA. This result is intriguing because the guanidine oligomers are completely protonated at physiological pH and therefore do not have a buffering capacity, however, **Gg** revealed gene expression values similar to *Glycofect*, which has secondary amines in the polymer backbone. These results do not agree with the proton sponge

hypothesis and suggest that the galactarate residues may play a role in the transfection. Interestingly, when comparing the positive controls, PLA revealed lower gene expression than *Glycofect* with Hela cells, and this result is likely related to its high toxicity (polyplexes formulated at *N/P* ratios higher than 15 caused complete cell death in the experiment, which is why the gene expression data is not available in **Figure 2.4** for these *N/P* ratios). Overall, polyplexes formed with **Gg** appeared to be the most effective pDNA delivery vehicles of the PGAG oligomer series. This agent promoted binding at the lowest *N/P* ratio (1.5), the smallest polyplex sizes, and the highest number of cells positive for *Cy5*-pDNA of all the PGAG created and studies here. It is also interesting to note that **Gg** had a higher gene expression level than **Gmeg**, while a reverse trend was observed for the tartrate-based, guanidine-containing polymers; interestingly **Tmeg** promoted luciferase expression at *N/P* = 25, where **Tg** polyplexes were complexly inactive. These data indicate that both the charge center and the carbohydrate type play a large role in the delivery of pDNA to the cellular nucleus for transgene expression.

MTT Assay: The cell viability was characterized via an MTT assay using HeLa cells. As shown in **Figure 2.6**, all of the PGAG and PGAA polyplexes exhibited low toxicity, as more than 90% of the cells were viable at *N/P* ratios ranging from 5 to 30 over the 48 hour experimental time course. The positive control, *Glycofect*, showed similar low toxicity. PLA, however, revealed a very high cytotoxic response. Even though it displayed 80% cell viability at an *N/P* ratio of 5, cell viability drastically decreased to about 16% as the *N/P* ratio increased to 20 and above. The large difference in cytoxic response when comparing the PGAGs to PLA is likely two-fold: i) the low molecular weight of the PGAG oligomers likely plays a major role in their low cytotoxic profile, and ii) the presence of a carbohydrate group could also be a factor in promoting a biocompatible response.

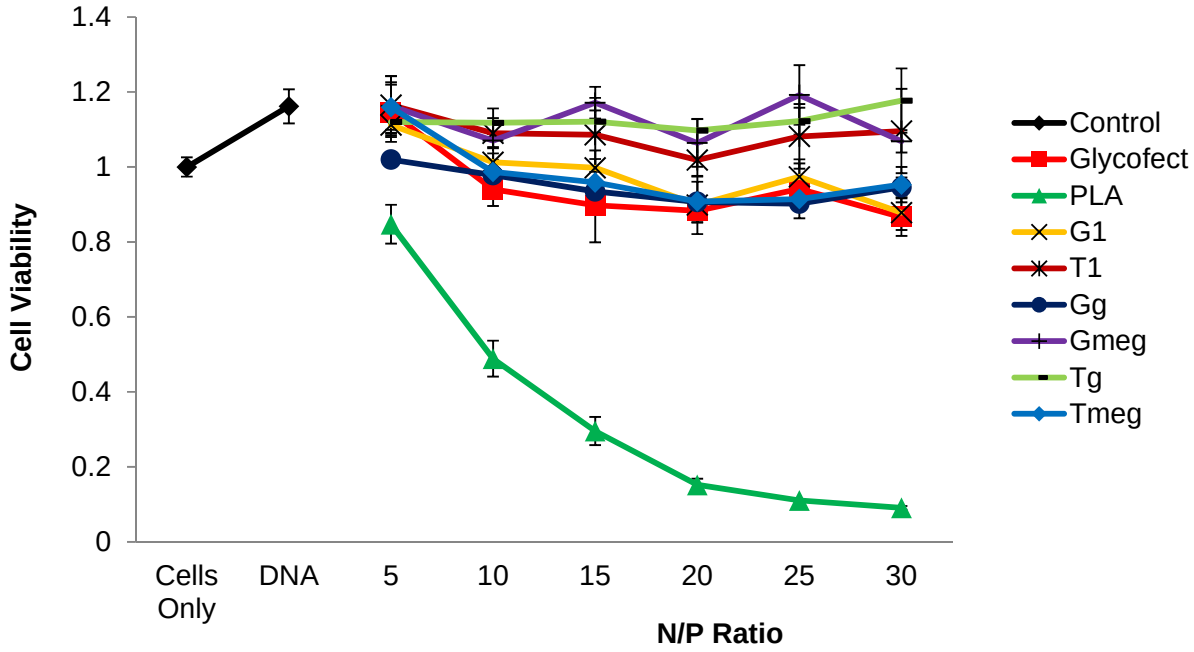

Figure 2.6, HeLa cell viability following a 24 hour exposure to polyplexes formed with pDNA and each PGAG, PGAAs, *Glycofect Transfection Reagent* and poly-L-arginine at different *N/P* ratios from 5 to 30 in reduced serum culture medium. The fraction cell survival is normalized to the untransfected cells and pDNAonly was also used as an experimental control.

2.4 Conclusions

Herein, a new series of carbohydrate-containing nucleic acid carriers [poly(glycoamidoguanidine)s or PGAGs] has been synthesized by copolymerizing either dimethylgalatarate or dimethyl-L-tartrate with monomers containing either a guanidine or methyl-guanidine charge center. These polymers have been created as analogs to the extensively studied previous systems that contain oligoethyleneamine charge centers (PGAAs) to compare the effect of charge center type on the biological properties of these glycopolymers. The PGAG vehicles bound pDNA at lower *N/P* ratios when compared to their PGAA analogs (**T1** and **G1**)

and readily formed polyplexes with pDNA at sizes approximately around 100 nm, as characterized from gel electrophoresis shift assay and DLS studies, respectively. Interestingly, the PGAG oligomers were not cytotoxic and all analogs revealed high cellular uptake and transgene expression in HeLa cells as compared to their amine-containing analogs (**G1** and **T1**). It is interesting to note that others have reported that guanidine groups within the backbone of polymer vehicles can possibly assist in the cellular entry of nanoparticles.[97,98] This study also revealed that while the PGAGs do not provide any buffering capacity in the endosomal pH range, two of the derivatives, **Gg** and **Tmeg**, promoted higher transgene expression values than their amine-containing analogs **T1** and **G1**. While we still do not fully understand these intriguing results, we have found that a number of our polymer systems do not strictly obey the proton sponge hypothesis, as analogous PGAA polymers (with a higher buffering capacity in the cellular pH range) do not necessarily lead to higher transgene expression.[53] To this end, extensive studies in our lab are currently focused on understanding how the polymer structure affects the routes of polyplex intracellular trafficking and results of these studies will be reported in due course.

Chapter 3

Fast Amide Hydrolysis: Potential to Increase Transfection Efficiency with Novel Self-degrading Structures

Key words: amide hydrolysis, non-enzymatic fast hydrolysis, asymmetric amide hydrolysis, mild pH condition, neighboring group participation, hydrogen bond

3.1 Introduction

Since biodegradable polymers can facilitate stable release of drugs and avoid accumulation in body,[6] these types of polymers gained significant attention for nucleic acid delivery due to low cytotoxicity and low requirement for drug dosage.[99] Previous studies showed that PGAAs with oligo secondary amines degraded at physiological pH.[21] This property could potentially contribute to high transfection efficiency and low toxicity observed with these polymers. Also, PGAAs degrade slower than esters and could provide for a new motif that has a longer and tunable degradation lifetime for drug release. Moreover, PGAAs degrade at physiological pH rather than the low pH (around 4) required for acetals.[100] The proposed mechanism for PGAA degradation is via hydrolysis of amide linkages, but further studies are needed to understand this.[21] Generally, amide groups except sp^3-hybridized nitrogen are recognized to be very stable under mild pH conditions due to their resonance stabilization.[101] The normal conditions to promote amide hydrolysis involves hot and concentrated base or acid environment. Fast amide hydrolysis usually involves enzymatic hydrolysis under physiological pH.[102,103] The half-life of non-enzymatic amide hydrolysis at physiological pH is over 7 years.[104,105] Recent studies showed that neighboring group participation involving distorting the amide bond and lowering the resonance with carbonyl group could also contribute to fast amide hydrolysis.[105-108]

PGAAs with different hydroxyl stereochemistry have similar degradation rates, even though they showed different binding properties with pDNA. Interestingly, PGAAs degrade faster at higher pH (7.4) than at lower pH (5). These results suggest that the degree of protonation of secondary amines could be potential to affect degradation properties.[21]

In order to study the mechanism of the fast amide hydrolysis of PGAAs, Dr. Vijay P. Taori synthesized several small molecule modeling systems to mimic the structure of **T4**. (**Figure 3.1**) All degradation studies were done in PBS under 37 ^{o}C to mimic physiological pH conditions.

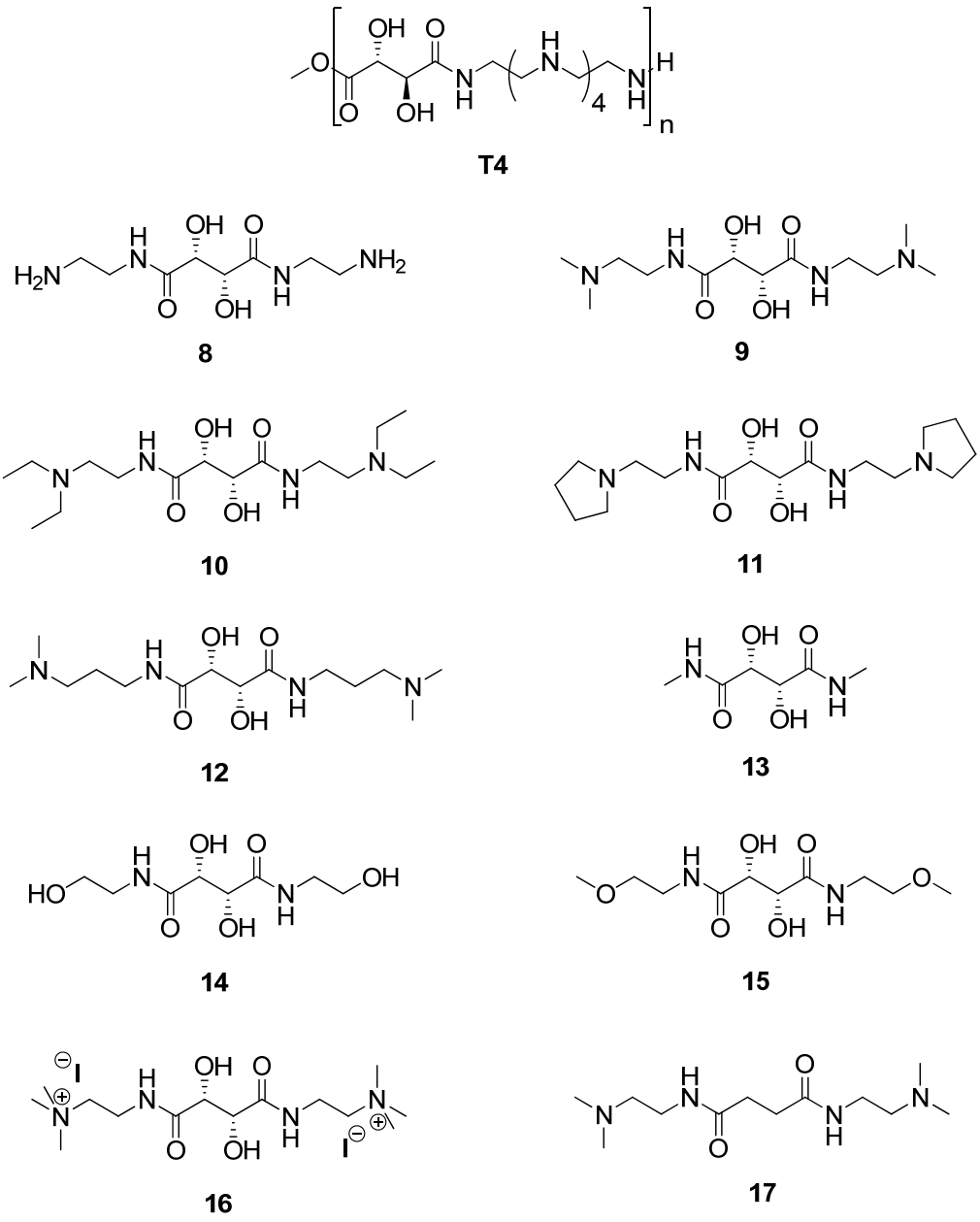

Figure 3.1, L-tartrate or succinate based small molecule models.

Compound **8, 9, 10, 11** have the same L-tartrate center with different types of amine end groups in order to examine the effects of end amines on hydrolysis; compound **8** and compound **12** have two or three methylene groups between end tertiary amines and amide nitrogen to examine the effects of distance on hydrolysis; compound **13** did not have end amines and end groups of compound **14** and **15** were replaced by hydroxyl or methoxy groups to examine the effects of disappearance of end amines on hydrolysis; end tertiary amines of compound **16** were methylated to examine the effects of the loss of amine free electrons on hydrolysis; compound **17** was succinate based model, which does not have hydroxyl groups at the center to examine the effect of hydroxyls on hydrolysis. All degradation studies were characterized by nuclear magnetic resonance (NMR).

Table 3.1, Hydrolysis of one-side amide hydrolysis for different models. ("+" means hydrolysis happened, "-" means no hydrolysis happened)

Model	Degradability	Model	Degradability
8	+	**13**	-
9	+	**14**	-
10	+	**15**	-
11	+	**16**	-
12	+	**17**	+

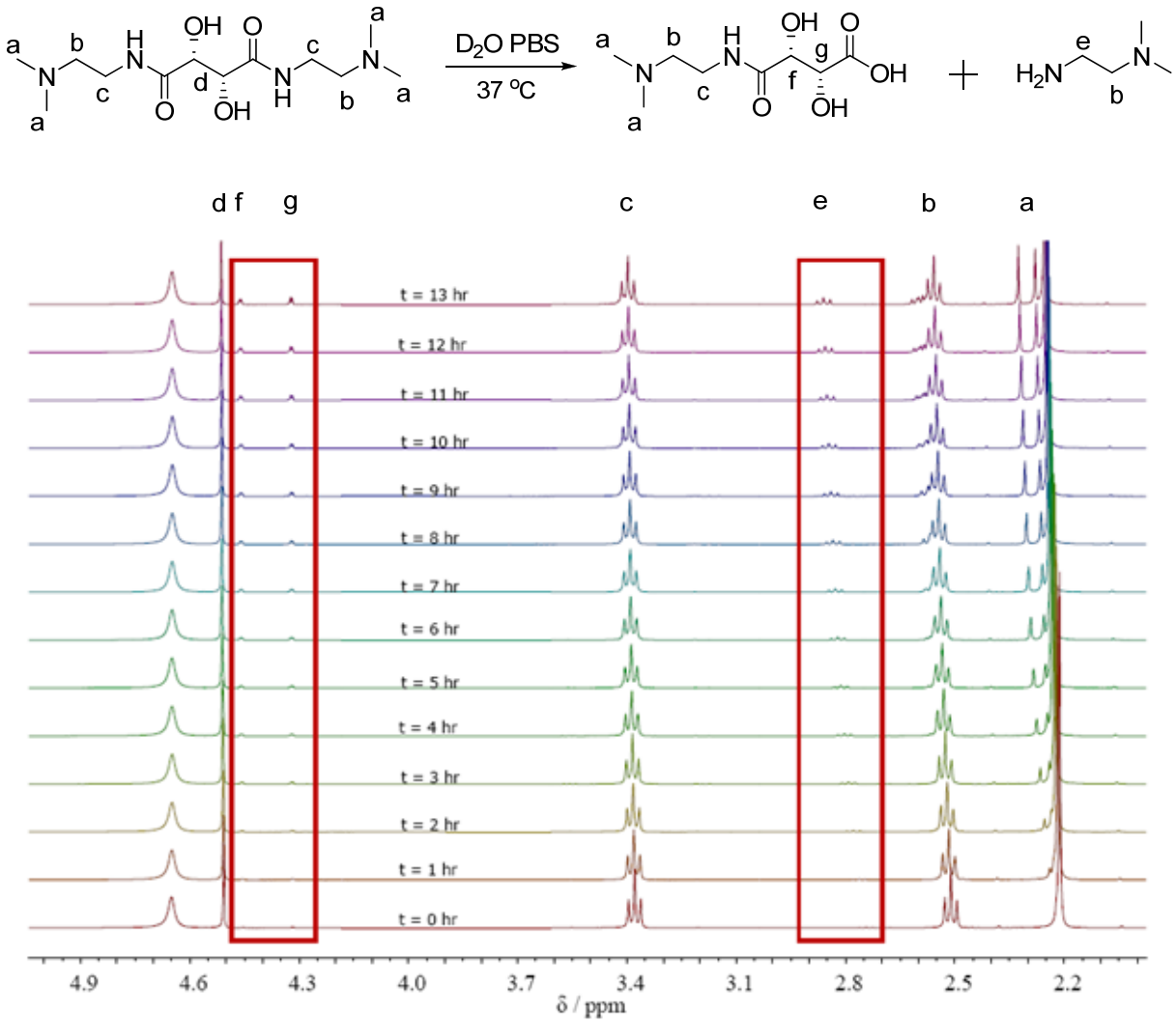

Figure 3.2, ^{1}H NMR of compound **9** during hydrolysis at different times. Figure adapted from Dr. Vijay P. Taori's dissertation.

Because NMR of compound **9** and the resulting degraded molecule was easy to be elucidated, compound **9** was studied first. **Figure 3.2** was the assay NMR degradation experiment of compound **9** under physiological condition for 13 hours. Two regions (highlighted by red rectangles) of newly formed peaks were discovered: 1. Peak **e** near 2.8-2.9 ppm were from newly formed free amine groups representing 3.4 ppm (peak **c**) of same groups in compound **b)**; 2. Peak **f** and **g** near 3.3 and 3.45 ppm were from newly formed asymmetric

protons next to hydroxyls on carbohydrate groups representing 4.5 ppm (peak **d**) of same but symmetric protons next to hydroxyls in compound **9**. Also, peak **b** showed a small chemical shift during degradation. These data showed rapid amide hydrolysis. More interestingly, this compound degraded on one side, which means only one amide group of these molecules degrades, leaving the other amide group intact on the structure. Also, it was found that the hydrolysis reaction was first order to model concentration. Compound **8**, **10**, **11**, **12** and **17** showed similar amide hydrolysis pattern, which indicates all compounds with free end amine groups facilitated hydrolysis, even though the degradation rates were not same. (**Table 3.1**) Compound **9**, **10** and **11** degraded faster than compound **8** indicating that the compounds with end tertiary amines degrade faster than that with primary amines. Compound **17** degraded slower indicating the hydroxyl groups on carbohydrates are important to facilitate hydrolysis. Compound **13**, **14**, **15** and **16**, the models without end amine groups, with hydroxyl end groups, with methoxyl end groups, or with quaternary end ammonium showed no degradation over long periods of time, indicating that the end amine groups are essential to facilitate fast hydrolysis.

However, it still remains uncertain why hydrolysis occurs rapidly and why hydrolysis always occurs only on one side of the molecules. My work was to further study different models to understand the mechanism of hydrolysis.

3.2 Experimental Procedures

Materials Synthesis:

General: Unless specified, all chemicals were purchased from Sigma Aldrich Chemical Co. and were used without further purification. NMR spectra were collected on a Varian Inova

MR-400MHz spectrometer and mass spectra of final compounds were obtained on an IonSpec HiResESI mass spectrometer.

(2R,3R)-2,3-dihydroxy-N^1,N^4-bis(2-(methylamino)ethyl)succinamide (20, Scheme 3.1): 3.00 g (0.041 mol) N-methylethylenediamine was dissolved in 30 ml dry MeOH. 6.40 g (0.045 mol) ethyl trifluoroacetate (CF_3COOEt) was dissolved in 20 ml dry MeOH and was dropwise added to N-methylethylenediamine solution at 0 ^oC. Reaction mixture was further stirred at room temperature for 24 hours followed by the addition of 10.00 g (0.046 mol) Boc anhydride. After 6 hours, solvent was rotary evaporated and the *tert*-butyl 2-aminoethyl(methyl)carbamate (**18**) was recrystallized from 30 ml 1:1 (v/v) DCM/hexane twice to give a white powder. **18** was further dissolved in 9:1 (v/v) MeOH/H_2O mixture. 15 g anhydrous K_2CO_3 was added to solution. The reaction mixture was stirred for 24 hours under room temperature and evaporated to stop the reaction. The residue oil was redissolved in DCM and washed twice with H_2O. The oil layer was kept and solvent was again removed via rotary evaporation to give a yellowish oil. The product (**19**) was further dried *en vacuo* overnight. (Yield: 4.11 g, 0.024 mol, 58%) 0.50 g (2.8 mmol) of dimethyl L-tartrate was dissolved in 20 ml MeOH followed by the addition of 1.10 g (6.3 mmol) of compound (**19**). Reaction mixture was stirred under room temperature for 48 hours after which the solvent was removed via rotary evaporation. Crude compound was purified with a silica gel column with 10:1 (v/v) $CHCl_3$/190 proof EtOH solvent system. Tert-butyl group of this compound was further deprotected by reacting with 4 M HCl in dioxane for 1 hour to obtain compound (**20**) (Yield: 0.47 g, 1.8 mmol, 64%). ^1H NMR (400 MHz, D_2O) δ = 2.68 (s, 6H), 3.16 (t, 4H), 3.57 (t, 4H), 4.57 (s, 2H), ^{13}C NMR (400 MHz, D_2O), 32.93, 35.59, 48.45, 72.30, 174.61, m/z = 263.1692 $(M+H)^+$

N^1,N^4-bis(2-(dimethylamino)ethyl)-N^1,N^4-dimethylsuccinamide (21, Scheme 3.1): All glassware was pre dried overnight before reaction. 1.00 g (9.8 mmol) of *N,N,N'*-trimethylethylenediamine and 5.00 g (0.050 mol) of triethylamine (TEA) was dissolved in 20 ml dry DCM in a 200-ml round bottom flask. 0.70 g (4.6 mmol) of succinyl chloride was dissolved in 10 ml dry DCM and dropwise added to the round bottom flask from additional funnel. The reaction was stirred in ice bath during addition followed by at room temperature for 2 hours. TEA•HCl salt precipitated out and was filtered. Solvent was rotary evaporated, and excessive amine was removed *en vacuo* overnight. Crude product was dissolved in 1 ml MeOH again followed by precipitation and washed with THF to give a slightly yellow powder (**21**) (Yield: 1.10 g, 3.8 mmol, 83%). ^{1}H NMR (400 MHz, D_2O) δ = 2.79 (s, 6H), 3.18 (s, 12H), 3.41 (t, 4H), 3.83 (t, 2H), ^{13}C NMR (400 MHz, D_2O), 27.86, 35.16, 42.95, 43.18, 54.98, 175.84, m/z = 287.2429 $(M+H)^+$

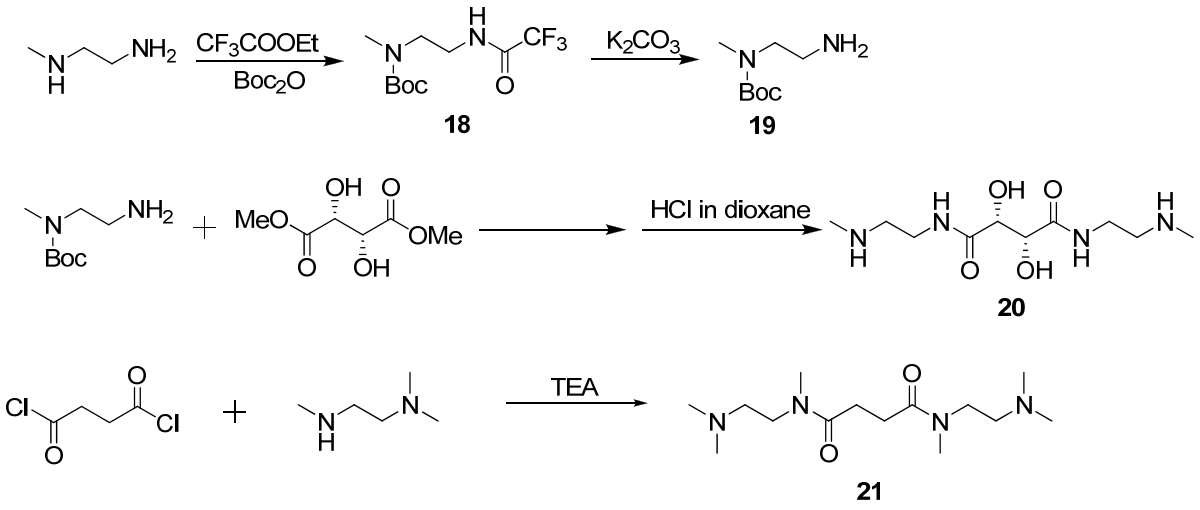

Scheme 3.1, Synthesis of compound **20** and **21**

(2R,3R)-N^1-(2-(dimethylamino)ethyl)-2,3-dihydroxysuccinamide (23, Scheme 3.2): 0.50 g (2.3 mmol) of degraded compound from compound **9** and 20 ml MeOH was added to a 50-ml round bottom flask. Concentrated HCl solution was added dropwise until all solid was dissolved. Solution was brought up to boil to remove excessive HCl. 0.005 g (0.03 mmol) p-toluenesulfonic acid monohydrate was added to solution after cooled down. Reaction mixture was refluxed for 48 hours. Most of solvent was rotary evaporated, and ethyl acetate (EA) was added to precipitate out compound (**22**). **22** was dried *en vacuo* overnight. 0.20 g (0.85 mmol) **22** was dissolved in 1 ml MeOH with 5 ml 4 M NH_3 in MeOH in a 50-ml round bottom flask. Reaction was stirred for 48 hours. MeOH and excessive NH_3 were rotary evaporated. Crude product was dissolved in small amount of MeOH and precipitate against EA twice. Product was dried *en vacuo* overnight to give a white powder (**23**) (Yield: 0.17 g, 0.78 mmol, 91%). ^{1}H NMR (400 MHz, D_2O) δ = 3.11 (s, 6H), 3.52 (t, 2H), 3.86 (t, 2H), 4.75 (s, 2H), ^{13}C NMR (400 MHz, D_2O), δ = 34.39, 43.04, 56.47, 72.17, 72.26, 174.62, 176.73, m/z = 220.1553 $(M+H)^+$

(2R,3R)-N^1-(3-(dimethylamino)propyl)-2,3-dihydroxysuccinamide (25, Scheme 3.2): 0.50 g (2.1 mmol) of degraded compound from compound **12** and 20 ml MeOH was added to a 50-ml round bottom flask. Concentrated HCl solution was added dropwise until all solid was dissolved. Solution was brought up to boil to remove excessive HCl. 0.005 g (0.03 mmol) p-toluenesulfonic acid monohydrate was added to solution after cooled down. Reaction mixture was refluxed for 48 hours. Most of solvent was rotary evaporated, and ethyl acetate (EA) was added to precipitate out compound (**24**). **24** was dried *en vacuo* overnight. 0.20 g (8.1 mmol) **24** was dissolved in 1 ml MeOH with 5 ml 4 M NH_3 in MeOH in a 50-ml round bottom flask. Reaction was stirred for 48 hours. MeOH and excessive NH_3 were rotary evaporated. Crude product was dissolved in small amount of MeOH and precipitate against EA twice. Product was

dried *en vacuo* overnight to give a white powder (**25**) (Yield: 1.67 g, 7.2 mmol, 89%). ^{1}H NMR (400 MHz, D_2O) δ = 2.10 (m, 2H), 3.00 (s, 6H), 3.27 (t, 2H), 3.50 (m, 2H) 4.67 (s, 2H), ^{13}C NMR (400 MHz, D_2O), 24.10, 35.74, 42.74, 55.19, 72.15, 72.23, 174.07, 176.86, m/z = 234.1720 $(M+H)^+$

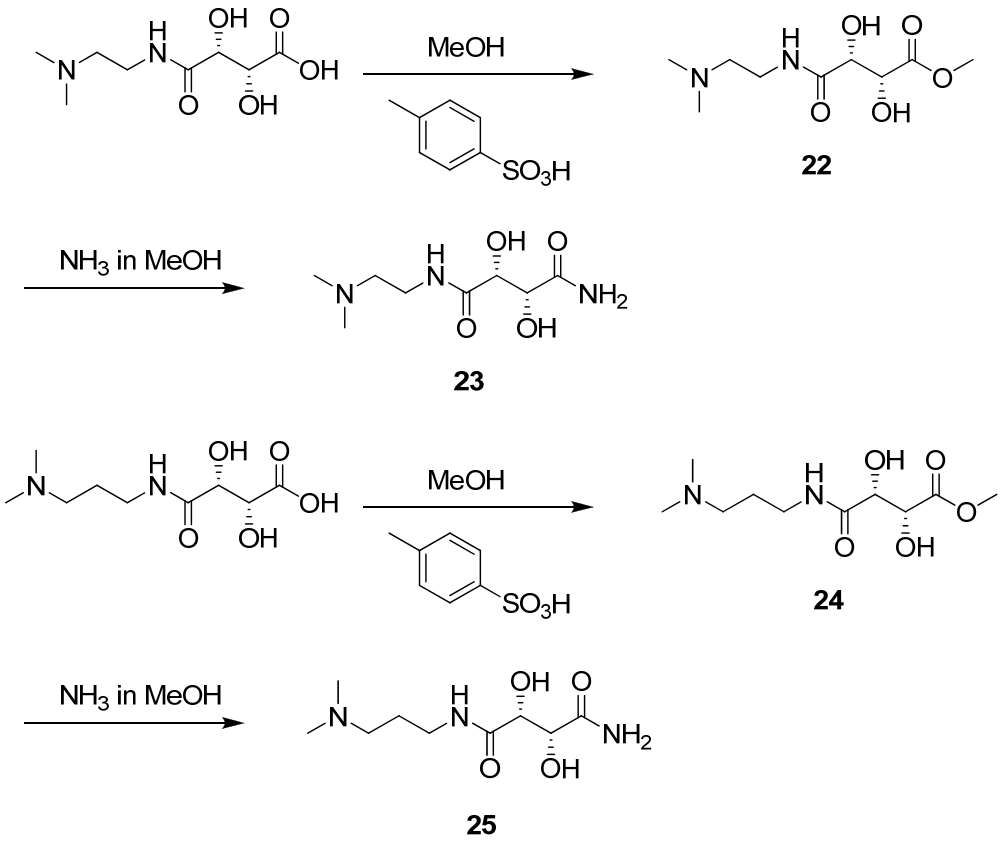

Scheme 3.2, Synthesis of compound **23** and **25**

(4S,5R)-N^4,N^5-bis(2-(dimethylamino)ethyl)-2,2-dimethyl-1,3-dioxolane-4,5-dicarboxamide (27, Scheme 3.3): The synthesis of compound **26** was completed in a similar manner to the method of dimethyl 2,3-O-isopropylidene-L-tartrate.[109] 4.00 g (0.024 mol) *meso*-tartaric acid monohydrate, 20 ml 2,2-dimethoxypropane, and 0.05 g (0.3 mmol) p-toluenesulfonic acid monohydrate were mixed in a 100 ml round bottom flask and refluxed under

N_2 (g) for 5 hours to form a dark red solution, after which an additional 5 ml 2,2-dimethoxypropane and 25 ml cyclohexane were added into solution. The flask was fitted with a Vigreux column and a variable reflux distilling head. The mixture was distilled to remove the MeOH-cyclohexane and acetone-cyclohexane azeotropes. 1 g of anhydrous K_2CO_3 was added to the solution and the mixture was stirred for another 3 hours. The K_2CO_3 was filtered out and the volatile residue was evaporated. The mixture was recrystallized under low temperature (-80 ^oC) with hexane twice to give a slightly yellow oil dimethyl 2,3-O-isopropylidene-*meso*-tartrate (**26**) at room temperature. (Yield: 4.52 g, 0.020 mol, 84%) 2.00 g (9.2 mmol) of **26** and 1.90 g (0.022 mol) of N,N-dimethylethylenediamine were dissolved in 10 ml MeOH in a 50-ml round bottom flask. The reaction mixture was stirred for 24 hours. The solvent was evaporated and the remaining yellow oil was dried *en vacuo* overnight to remove excessive amines. Product was recrystallized with 15 ml hexane twice to form a light yellow powder. The product (**27**) was filtered and dried *en vacuo* overnight. (Yield: 2.58 g, 7.9 mmol, 86%) ^1H NMR (400 MHz, $CDCl_3$) δ = 1.40 (s, 3H), 1.67 (s, 3H) 2.22 (s, 12H), 2.39 (t, 4H), 3.31 (t, 4H), 4.75 (s, 2H), 6.77 (s, 2H), ^{13}C NMR (400 MHz, $CDCl_3$), δ = 25.22, 26.58, 36.59, 45.23, 57.66, 77.84, 111.27, 167.43, m/z = 331.2626 $(M+H)^+$

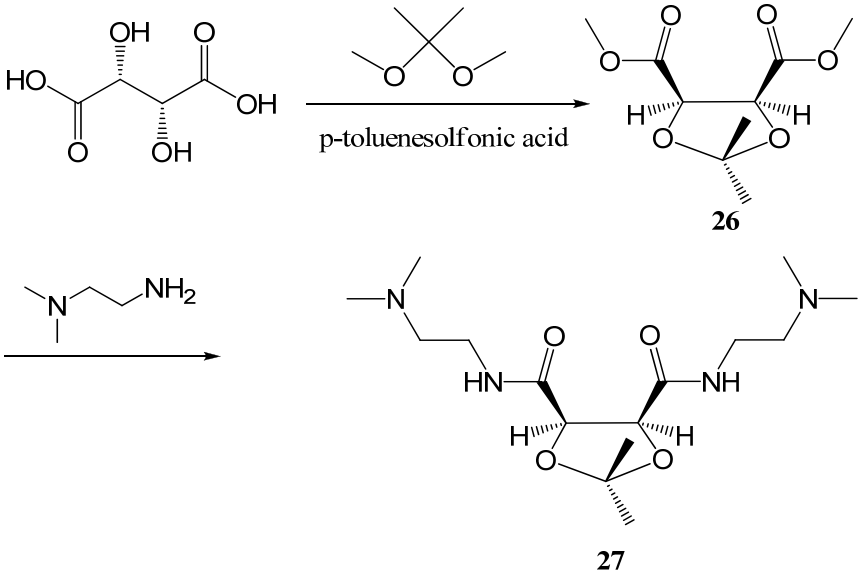

Scheme 3.3, Synthesis of compound **27**

(4R,5R)-N^4,N^5-bis(2-(dimethylamino)ethyl)-2,2-dimethyl-1,3-dioxolane-4,5-dicarboxamide (28): 2.00 g (9.2 mmol) of dimethyl 2,3-O-isopropylidene-L-tartrate, 1.90 g (0.022 mol) N,N-dimethylethylenediamine were dissolved in 10 ml MeOH in a 50-ml round bottom flask. The reaction mixture was stirred for 24 hours. The solvent was removed via rotary evaporation and the remaining yellow oil was dried *en vacuo* overnight to remove excessive amines. The mixture was recrystallized under low temperature (-80 ^{o}C) with hexane two times to yield a slightly yellow oil at room temperature. The product was dried *en vacuo* overnight to yield **28**. (Yield 2.83 g, 8.5 mmol, 93%) ^{1}H NMR (400 MHz, D_2O) δ = 1.51 (s, 6H), 2.26 (s, 12H), 2.55 (t, 4H), 3.42 (t, 4H), 4.65 (s, 2H), ^{13}C NMR (400 MHz, D_2O), δ = 25.16, 36.58, 43.94, 56.68, 77.16, 113.65, 171.12, m/z = 331.2637 $(M+H)^+$

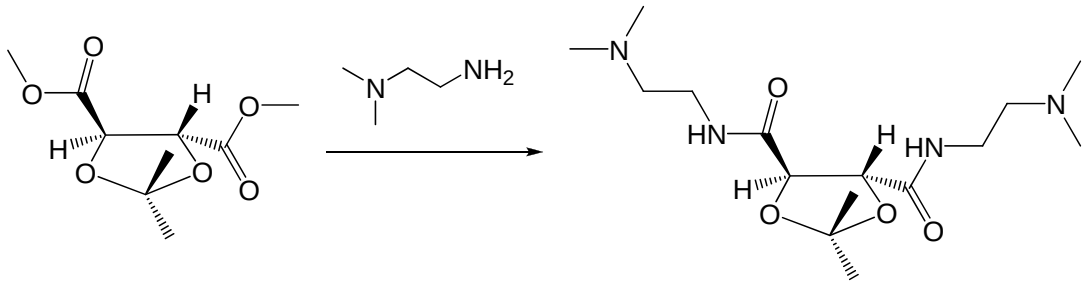

28

Scheme 3.4, Synthesis of compound **28**

(2R,3S)-N^1,N^4-bis(2-(dimethylamino)ethyl)-2,3-dihydroxysuccinamide (29, Scheme 3.5): 0.50 g (1.5 mmol) of **27** was mixed with 3 ml 4 M HCl in dioxane. The mixture was stirred at room temperature for 2 hours. The solvent and excess HCl was then removed via rotary evaporation. The remaining powder was further dried *en vacuo* overnight to give a white powder (**29**) Yield: (0.38 g, 1.3 mmol, 87%). ^{1}H NMR (400 MHz, D_2O) δ = 2.95 (s, 12H), 3.35 (t, 4H), 3.70 (m, 4H), 4.62 (s, 2H), ^{13}C NMR (400 MHz, D_2O), 34.07, 43.09, 56.60, 73.20, 173.82, m/z = 291.2269 $(M+H)^+$

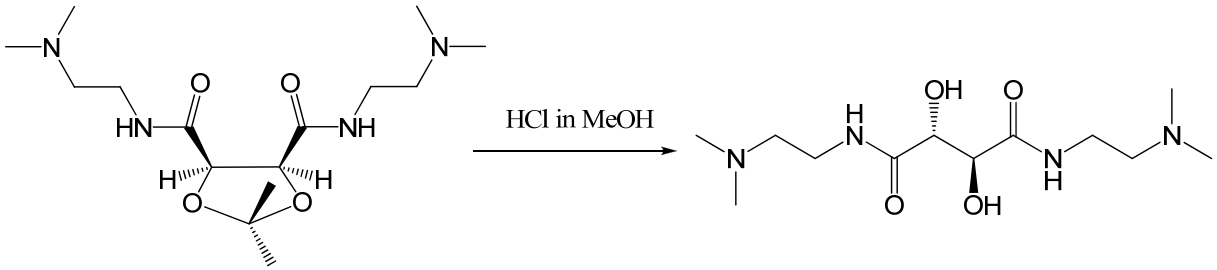

27 **29**

Scheme 3.5, Synthesis of compound **29**

Hydrolysis Kinetics Studies:

General: All kinetics studies were done at pD 7.5 in D_2O-PBS (pH for H_2O-PBS = 7.4) or at pD 11.2 in D_2O-K_2CO_3 (pH for H_2O-K_2CO_3 = 11.0) unless specified under 37 ^oC. Phosphate buffered saline (PBS) was purchased from Invitrogen (Carlsbad, CA). Deuterated phosphate buffered saline (D_2O-PBS) was prepared by freeze drying certain amount of PBS followed by adding of D_2O to re-dissolve the buffer salt to its initial volume. D_2O-K_2CO_3 was prepared by dissolving K_2CO_3 in D_2O for desired pD. The concentration of different model molecules was maintained at 0.05 mole/L. Each hydrolysis was measured in duplicate with two same samples in two NMR tubes.

Hydrolysis at different pD: All kinetics models were done at pD 7.5 and pD 11.2. Compound **9** and **12** was further studied at pD 2.0 and 5.0.

Hydrolysis under D_2O/CD_3OD mixture: In order to understand the effect of water concentration on amide cleavage, hydrolysis was done in solution with D_2O/CD_3OD mixture at different ratios: 75% D_2O/25% CD_3OD, 50% D_2O/50% CD_3OD, 25% D_2O/ 75% CD_3OD and 100% CD_3OD.

pH Titration Studies:

Most of the symmetric compounds have two amines at the terminal position of the molecules. Therefore, there exist different combinations of three statuses at different pH: 1. both amines protonated; 2. only one amine is protonated; 3.both amines deprotonated. Because of the ease to measure the NMR of the compounds both pre- and post-hydrolysis of **9** and **12**, these two compounds were used for study.

Solutions of compound **9** and **12** were made to have a concentration of 0.035 mole/L in ultrapure water. The pH was adjusted to around 1 with 1 mole/L HCl to avoid hydrolysis at high pH. The solution was titrated with standardized NaOH and pH was recorded with a Fisher accumet BASIC AB 15 pH meter (Pittsburgh, PA). NaOH was standardized with a known mass of primary standard potassium hydrogen phthalate. Potassium hydrogen phthalate was dried overnight and was kept dry to be cooled down before standardization.

3.3 Results and Discussion

All compounds were made based on different parameters that could potentially affect hydrolysis profiles including the terminal amine type, hydroxyl stereochemistry, secondary or tertiary amide, and asymmetry of two terminal groups. (**Figure 3.3**)

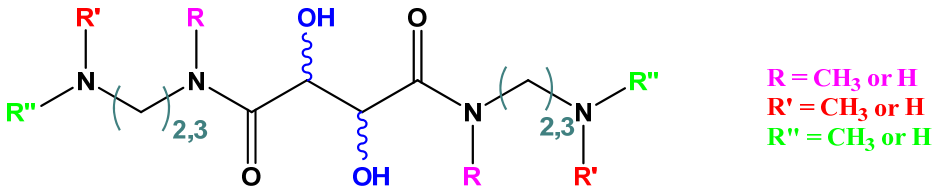

Figure 3.3, Possible changeable parameters for hydrolysis models.

To compare all different hydrolysis effects of each structure characteristic with that of compound **9**, different models mimicking compound **9** but with different functionalities were synthesized. Compound **20** was synthesized with terminal secondary amines to examine whether the difference in pKa or amine types will affect hydrolysis rate. Compound **21** was synthesized with tertiary amides ($R = CH_3$) instead of secondary amide. Compound **23** and **25** were asymmetric compounds to see whether only one terminal amine can facilitate hydrolysis and on which side amide hydrolysis occurs. Also, the spacers between amine nitrogen and amide

nitrogen can be altered: 2 methylene groups for **23** and 3 methylene groups for **25**. Also, it should be noted that compound **27** and compound **28** are two diastereomers. The hydroxyl groups of these two models were protected, and therefore, the conformation of the hydroxyl groups are locked resulting in a smaller distance between two amide groups for **27** and a larger distance between two amide groups for **28**. The difference in the distance and conformation of the amides and amines could affect the interaction of the two end chains and possibly the hydrolysis rate. Compound **29** is a diastereomer to compound **9**. Studying the hydrolysis kinetic difference between compound **29** and **9** could confirm whether the different hydrolysis rates of compound **27** and **28** resulted from the distance between the amide groups and terminal amines. The possible hydrolysis mechanism will be discussed after the hydrolysis kinetics studies.

Hydrolysis Kinetics Studies at pD 7.5 and 11.2:

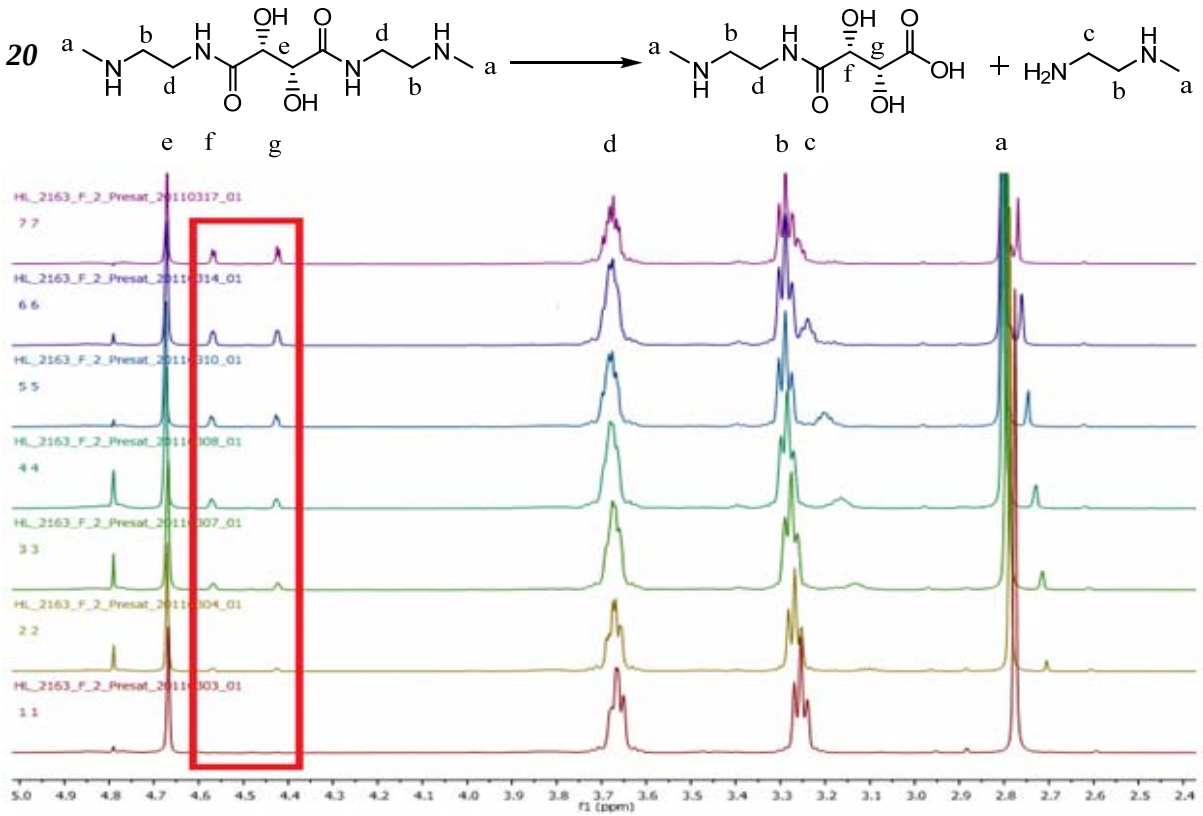

Figure 3.4, ^{1}H NMR of compound **20** during hydrolysis.

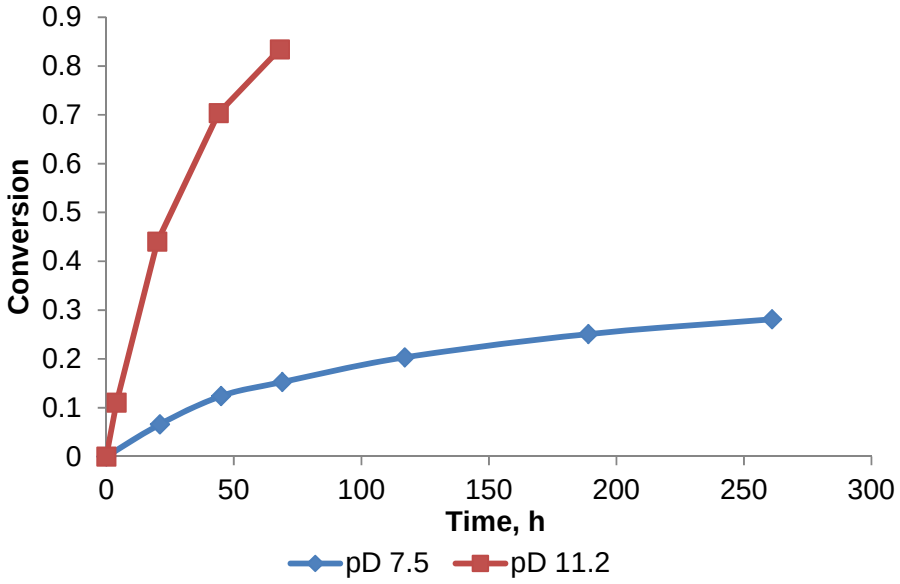

Figure 3.5, Hydrolysis kinetics of compound **20**.

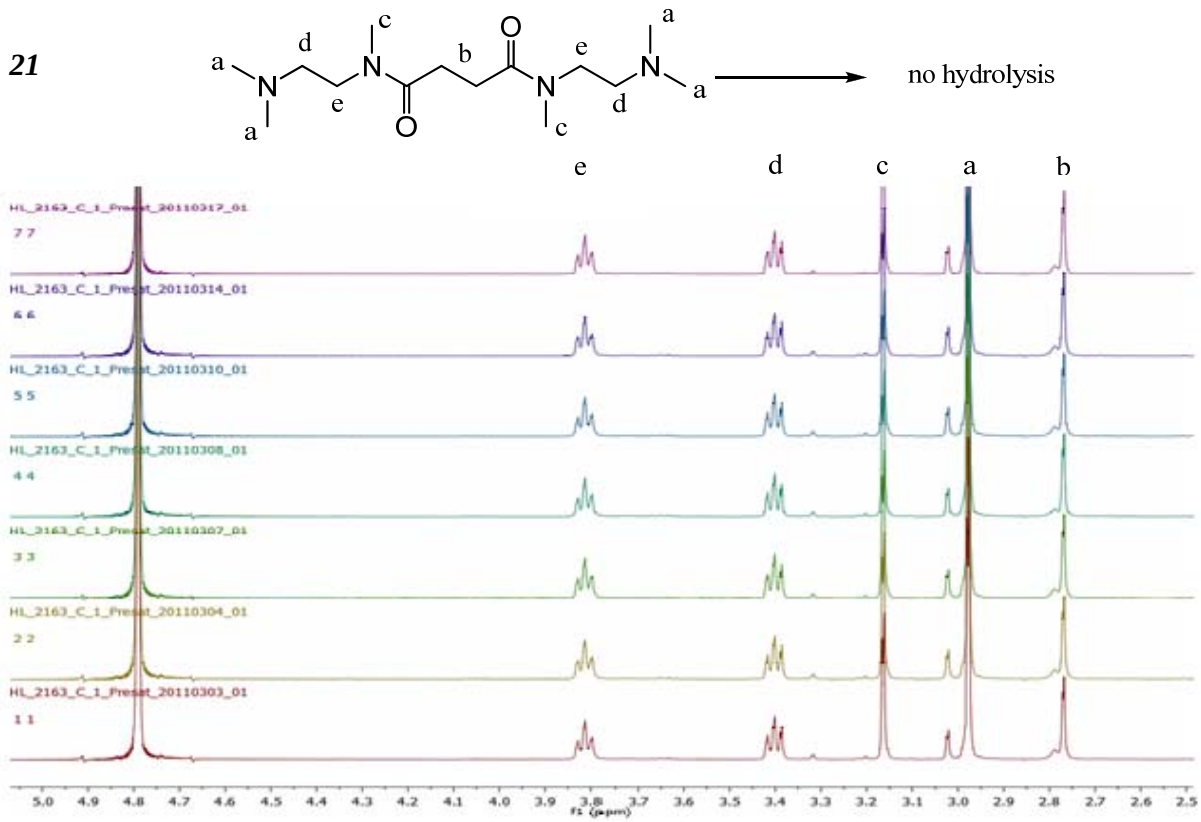

Figure 3.6, ^{1}H NMR of compound **21** during hydrolysis.

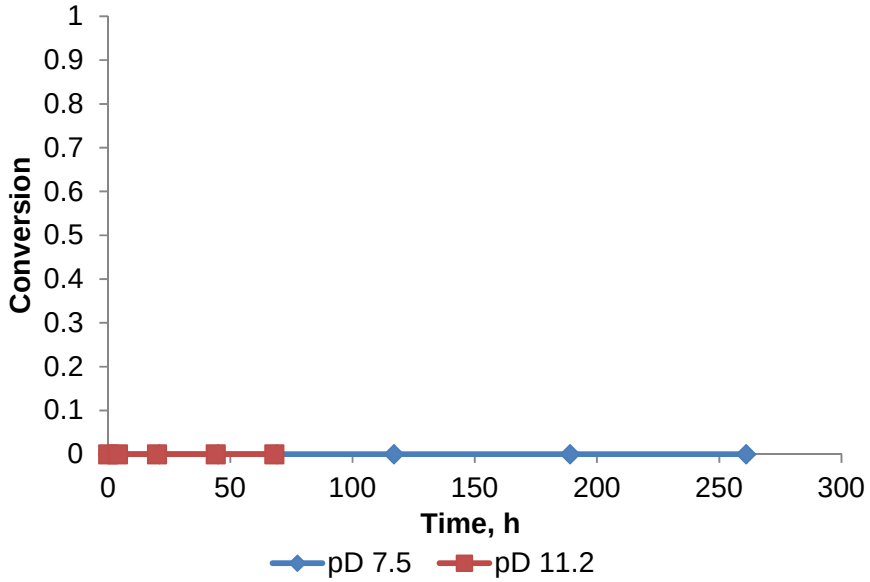

Figure 3.7, Hydrolysis kinetics of compound **21**.

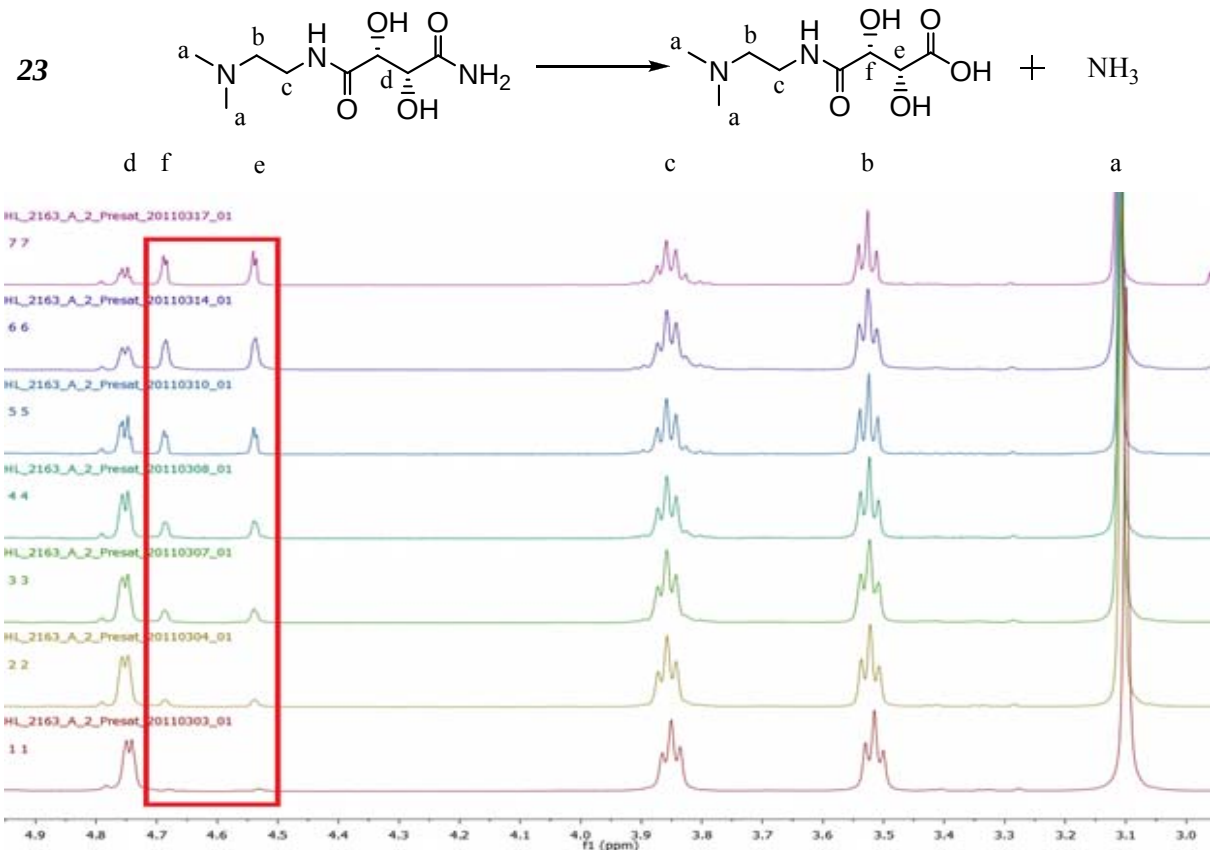

Figure 3.8, ^{1}H NMR of compound **23** during hydrolysis.

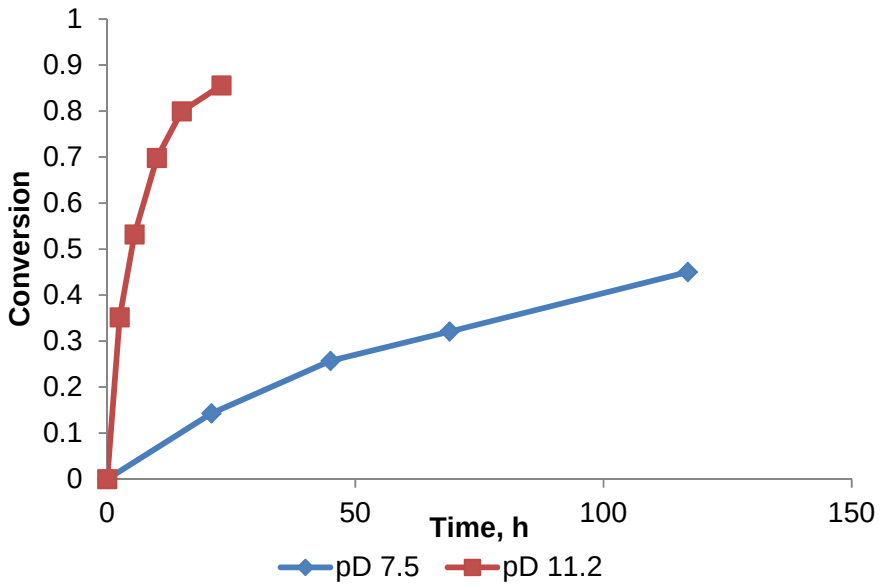

Figure 3.9, Hydrolysis kinetics of compound **23**.

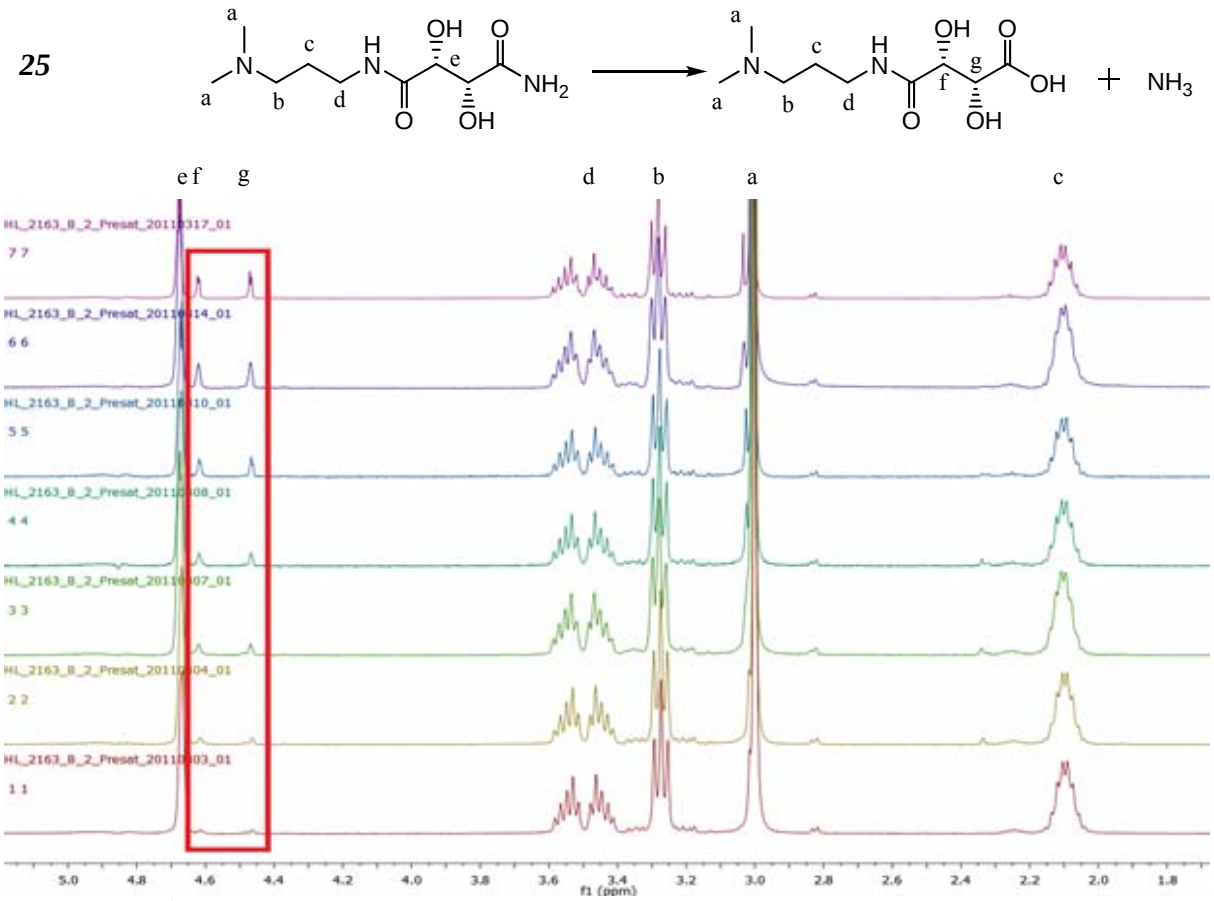

Figure 3.10, ^{1}H NMR of compound **25** during hydrolysis.

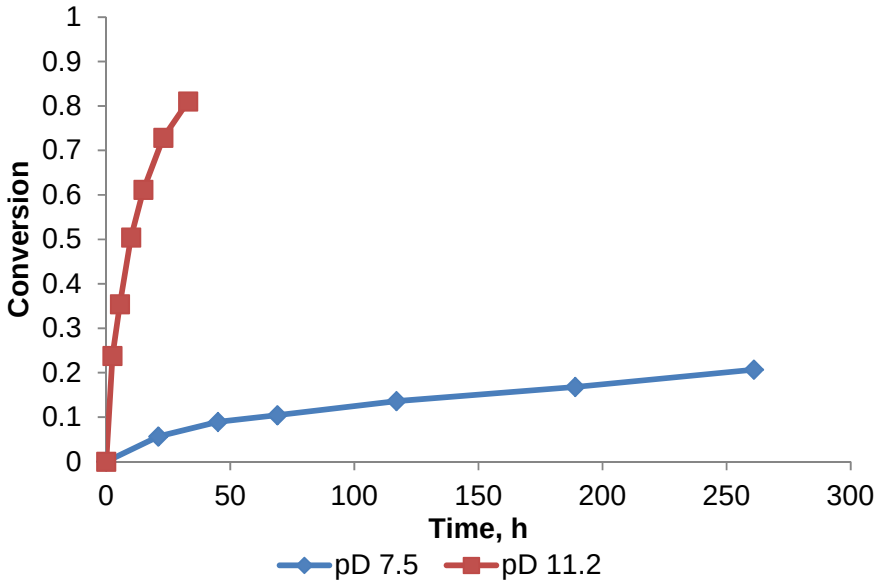

Figure 3.11, Hydrolysis kinetics of compound **25**.

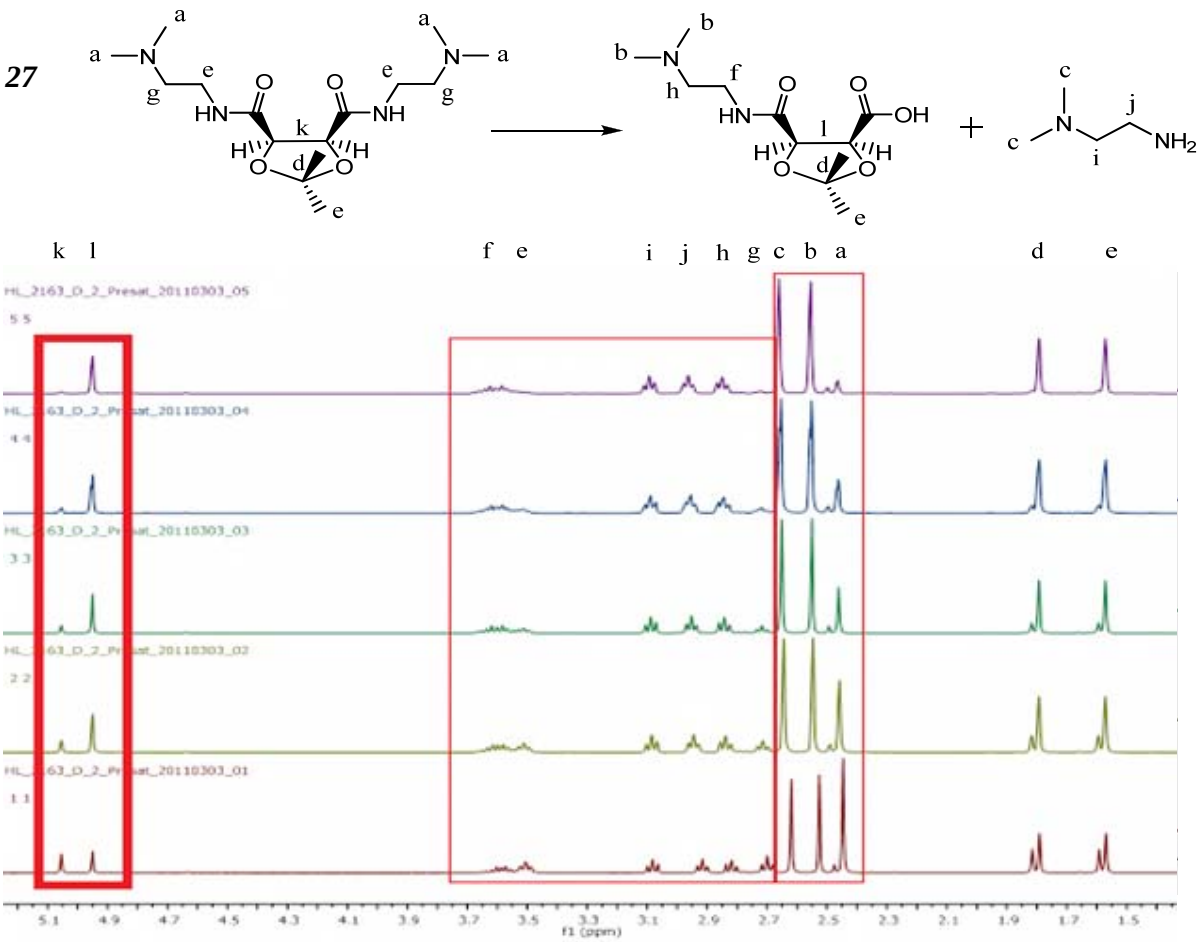

Figure 3.12, ^{1}H NMR of compound **27** during hydrolysis.

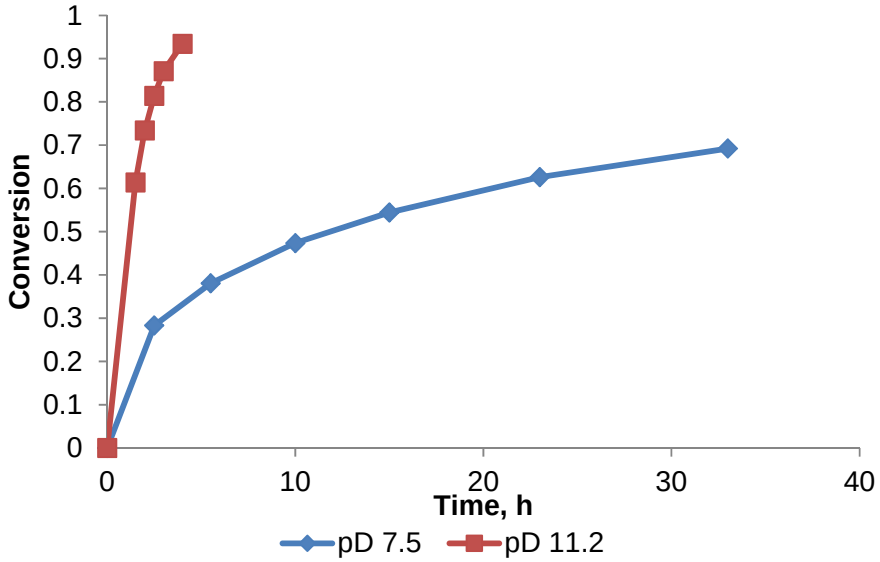

Figure 3.13, Hydrolysis kinetics of compound **27**.

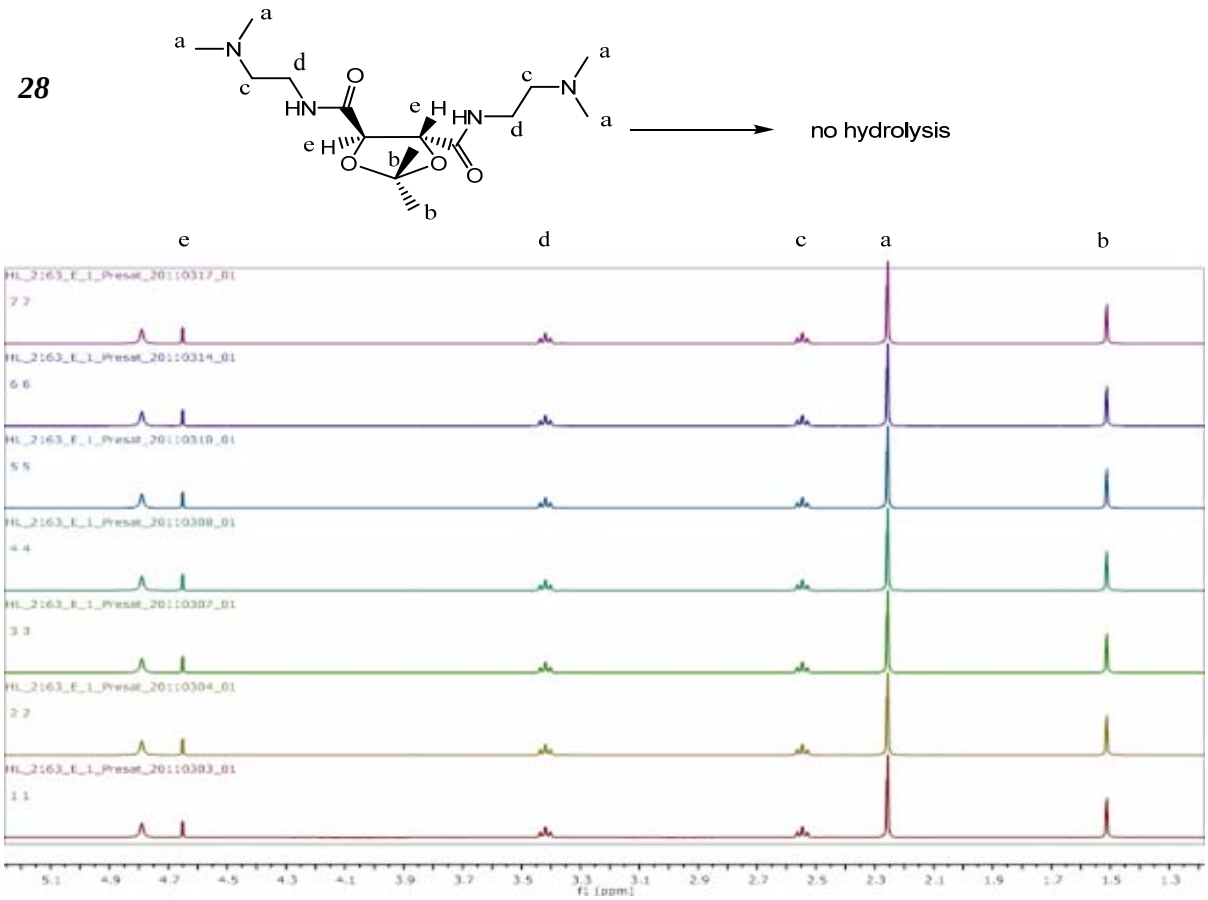

Figure 3.14, ^{1}H NMR of compound **28** during hydrolysis.

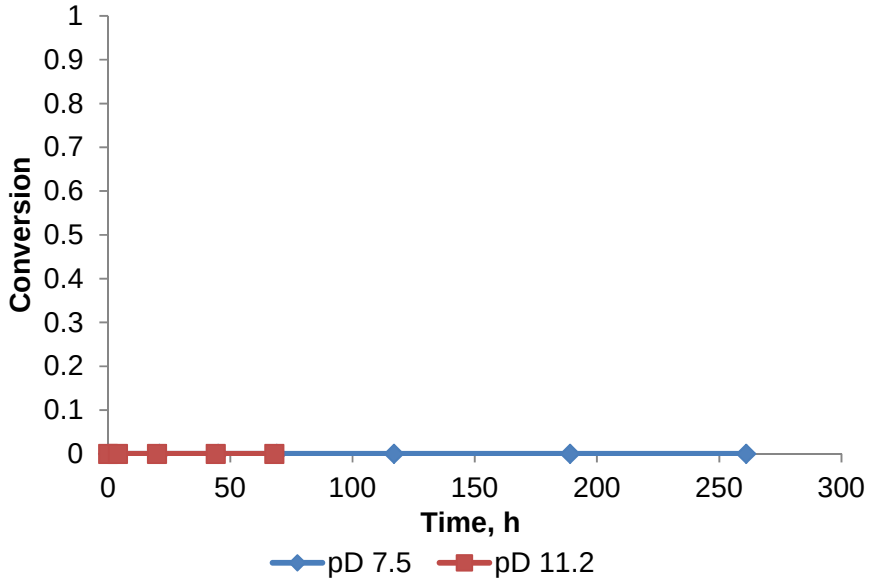

Figure 3.15, Hydrolysis kinetics of compound **28**.

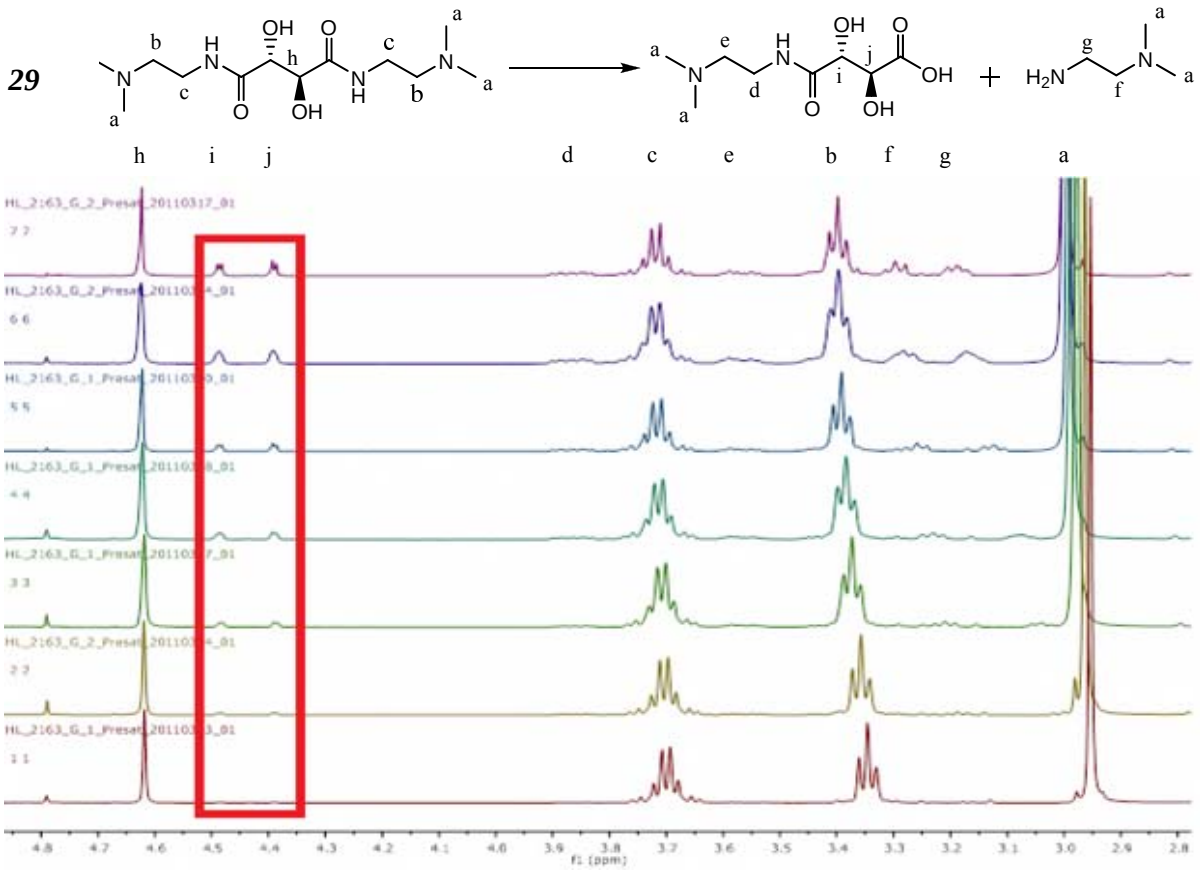

Figure 3.16, ^{1}H NMR of compound **29** during hydrolysis.

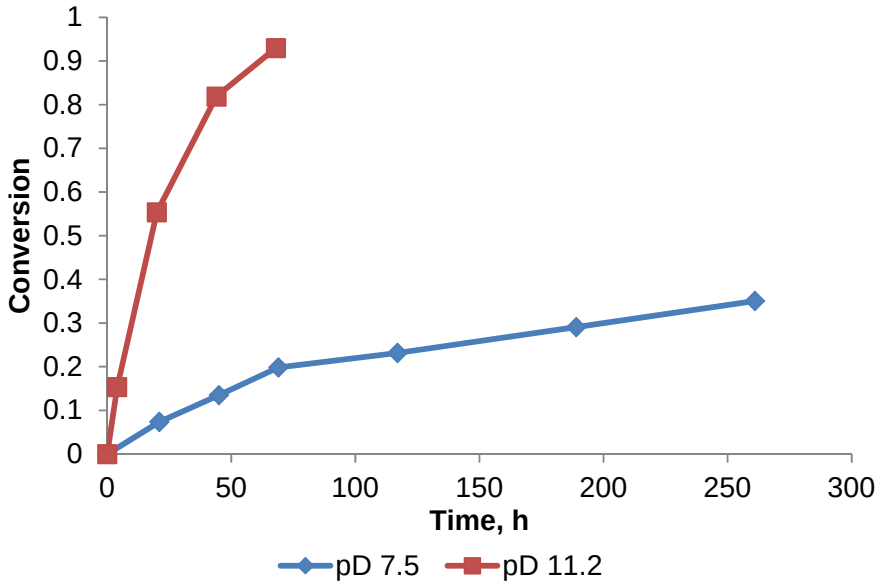

Figure 3.17, Hydrolysis kinetics of compound **29**.

Table 3.2, Hydrolysis kinetics of different models. ("-" means that model did not hydrolyze.)

Models	K (pD 7.5), h^{-1}	Half-life (pD 7.5), h	K (pD 11.2), h^{-1}	Half-life (pD 11.2), h
8	0.0007	971	0.0088	79
9	0.0020	347	0.030	23
12	0.0006	1155	0.0043	161
20	0.0015	462	0.027	26
21	-	-	-	-
23	0.0054	128	0.114	6
25	0.0014	495	0.055	13
27	0.048	14	0.675	1
28	-	-	-	-
29	0.0019	364	0.039	18

Generally, all hydrolysis kinetics were calculated based on the integration of new formed peaks highlighted in the red rectangles from ^{1}H NMR. All hydrolysis reactions behave first-order to modeling compound concentration. Interestingly, it has been found that hydrolysis only occurs on one side of the model molecules due to the nonequivalence of asymmetric hydrolysis products that appeared in the ^{1}H NMR trace. A bigger K value or a smaller half-life in **Table 3.2** represents a faster hydrolysis rate and *vice versa*.

Compound **20** hydrolyzed slower than compound **21** but faster than compound **20** at both pH. Also, previous studies showed that compound **23** and compound **25** hydrolyzed faster than compound **9**. There results stated higher basicity of terminal amine resulted in faster hydrolysis.

Compound **21** which had tertiary amides showed no hydrolysis at both pDs for a long time, indicating that the hydrogen on the amide nitrogen is important to facilitate hydrolysis. Also, this behavior is not due to the lack of hydroxyl groups because compound **17** (the secondary amide analog) exhibits hydrolysis at same pD.

Compound **23** and **25** were two asymmetric compounds with tertiary amines on one end chain. These two compounds showed amide hydrolysis on the side without the terminal amine. (m/z for **23** hydrolysis product = 221.1139 $(M+H)^+$) These results showed that terminal amines were important to hydrolysis. Also, compound **25** hydrolyzed slower than compound **23** indicating a longer spacer between amide nitrogen and amine nitrogen slows down hydrolysis. This result matches the slower hydrolysis of compound **12** compared to compound **9**.

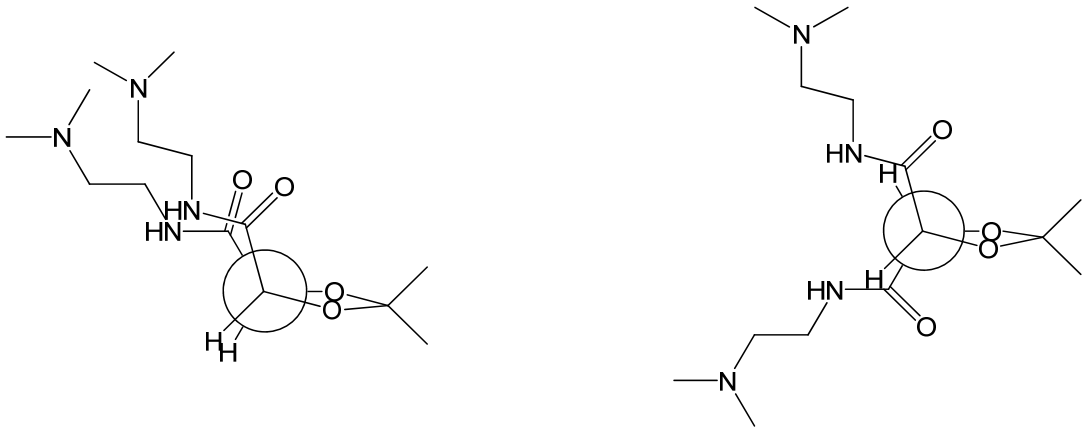

1e 1f

Figure 3.18, Conformations of compound **27** and **28**.

Figure 3.18 shows the Newman Projections of the diastereomers **27** and **28** by viewing through the two central carbons of *meso*-tartrate or the L-tartrate moiety. Newman projections showed that the distance of the two end chains of compound **27** is much closer than that of **28**. Compound **27** hydrolyzed significantly faster than any other models studied at both pDs, while **28** showed a complete lack of hydrolysis. Final product (m/z = 260.1372 $(M+H)^+$) indicated that hydrolysis still occurred only on one end chain for compound **27**. These data suggest the interaction of two end chains or the close proximity of the amide carbonyls could facilitate neighboring group participation mechanism and be the cause to increase the rate of hydrolysis.

Compound **29** and **9** are diastereomers like **27** and **28** except the two center carbons of *meso*-tartrate or L-tartrate moiety can rotate freely for terminal groups to move close to each other. The two model compounds were synthesized as controls for compound **27** and **28**. Interestingly, the kinetics results showed almost no difference between the hydrolysis kinetics of these two compounds at both pDs. The similarity of the kinetics could support that the intramolecular interaction of end chains is important to hydrolysis suggested by absolutely different hydrolysis kinetics of compound **27** and **28**.

All these hydrolysable compounds facilitated unexpected rapid hydrolysis even at pD 7.5. A small difference in structure resulted in very different hydrolysis profiles.

Hydrolysis at different pD:

Early studies showed that normal amide hydrolysis can be facilitated in strong acidic or basic conditions. Compound **9** and **12** were further studied at acidic pD: 2.0 and 5.0. However, no hydrolysis was observed for these two compounds even at pD 2.0. (**Figure 3.19** and **Figure 3.20**) This suggests that the hydrolysis does not follow normal amide hydrolysis which should

functionalize at low pH also, and supports that the free terminal amines are important to hydrolysis. Therefore, a pH titration was completed to determine the pKa of the terminal amines and relate the hydrolysis phenomena with the degree of prononation of the terminal amines.

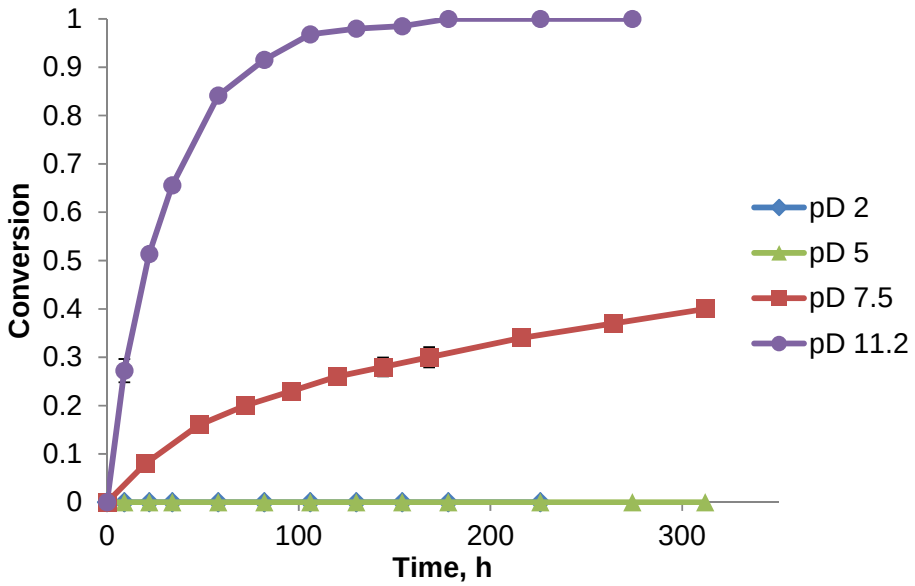

Figure 3.19, Hydrolysis of compound **9** at various pD.

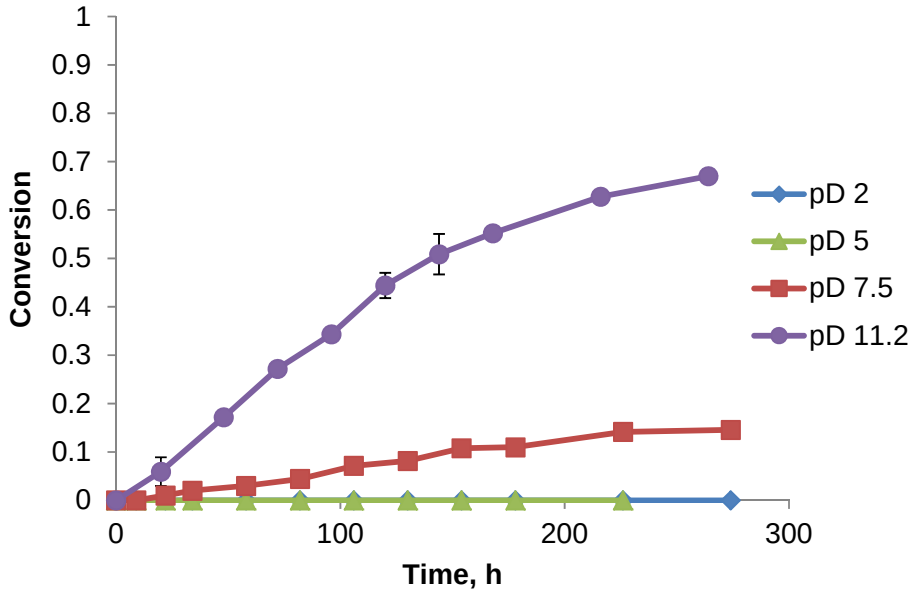

Figure 3.20, Hydrolysis of compound **12** at various pD.

pKa Measurement and pH Titration Studies:

pH titration experiments were completed to determine pKa for the diamine model **9** and **12** conjugate di-acids. The pKa can tell how many terminal amines were protonated at a certain pH. pKa was measured by pH titration: pH at middle point of two pH jump point given by the secondary derivative of pH vs. volume. (**Figure 3.21**)

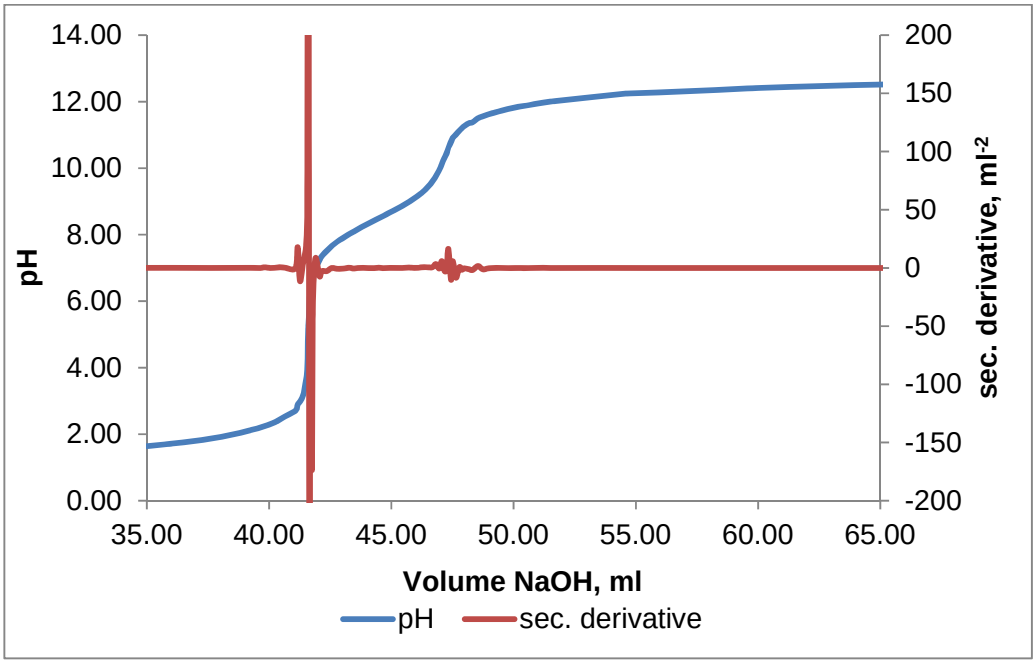

Figure 3.21, pH titration curve for compound **9**

Table 3.3, pKa values of conjugate acids of compound **9** and **12**

Models	pKa
9	8.75
12	9.25

Calculated from the pKa of compound **9** and **12**, at pH 11, both terminal amines are deprotonated, while at pH 7.4, more than 80% terminal amines are protonated. Therefore, the free amine can still facilitate hydrolysis at both pDs, except that hydrolysis rate was slower at a pD 7.5. However, at lower pD such as 2.0 and 5.0, two effects could dramatically slow down or terminate hydrolysis: 1. concentration of OH^- or OD^- significantly decreases; 2. terminal amines tend to be protonated.

Hydrolysis under D_2O/CD_3OD mixture:

All the reactions are first order to concentration of model. However, the concentration of D_2O or OD^- never was changed during the hydrolysis experiments. Therefore, PBS-D_2O/CD_3OD mixtures at different ratios: 75% D_2O/25% CD_3OD, 50% D_2O/50% CD_3OD, 25% D_2O/ 75% CD_3OD and 100% CD_3OD were used as solvent. The pD was adjusted to 9 for a moderate hydrolysis rate.

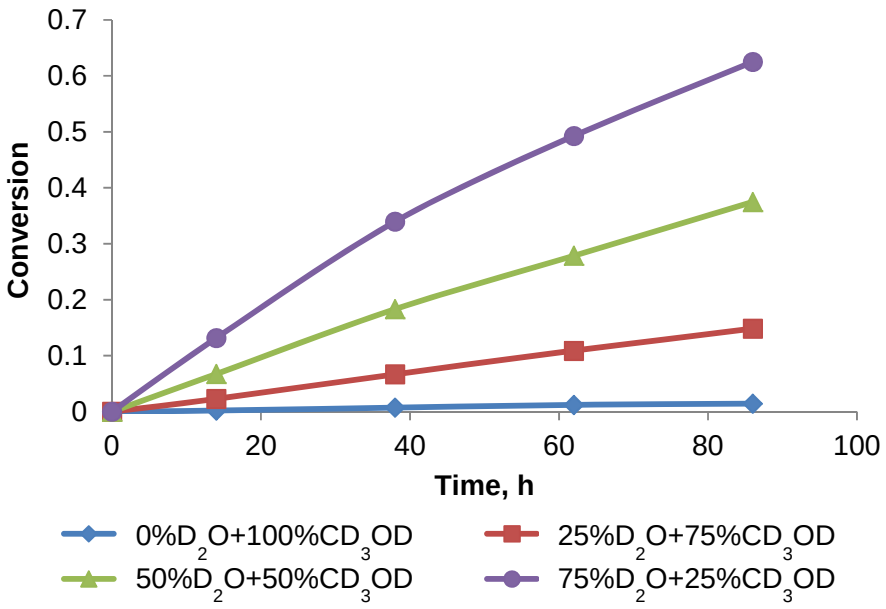

Figure 3.22, Hydrolysis of compound **9** in D_2O CD_3OD mixture

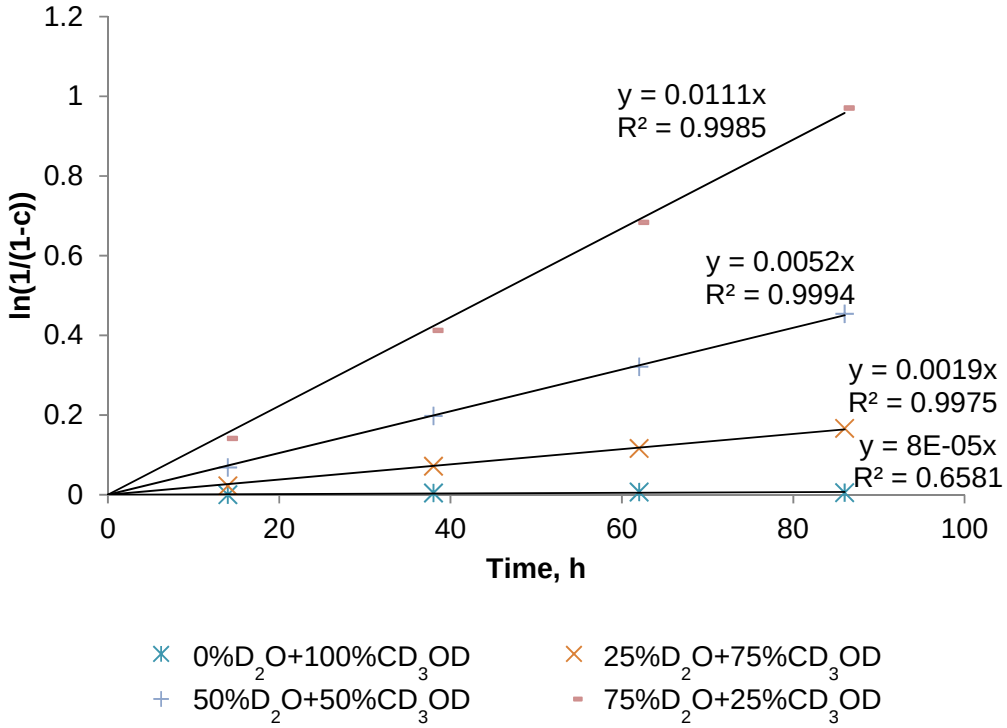

Figure 3.23, Kinetics of ln(1/(1-c)) = Kt

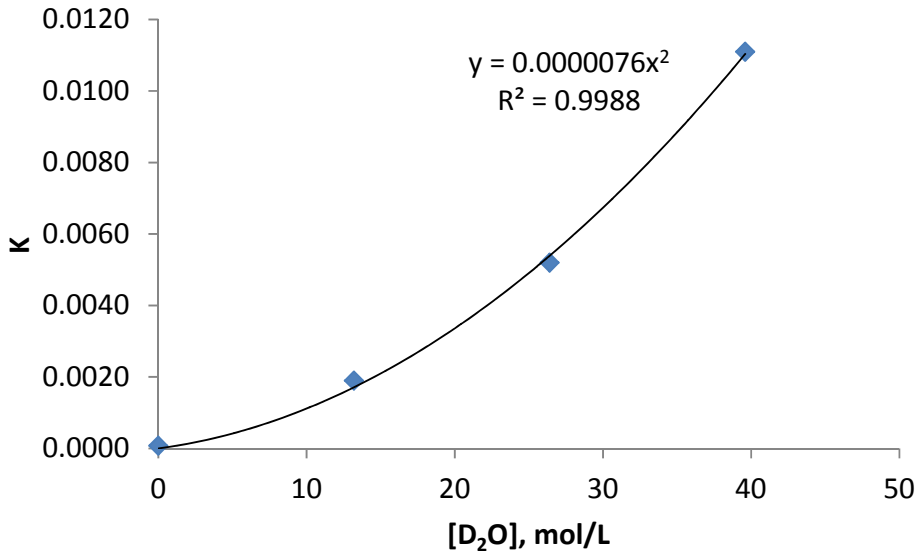

Figure 3.24, Kinetics of $K = k[D_2O]^2$

It was previously determined that the hydrolysis kinetics rate follows first order to model compound concentration, or r = K*[Model]. Hydrolysis kinetics showed that K is also directly proportional to $[D_2O]^2$. Furthermore, faster hydrolysis rates were observed in a basic environment. Therefore, the functional group could be both OD^- and D_2O. Reaction rate could be expressed by $r = k[Model]*[D_2O]^2$ at a certain pD or $r = k[Model]*[H_2O]^2$ at a certain pH.

Possible Mechanisms:

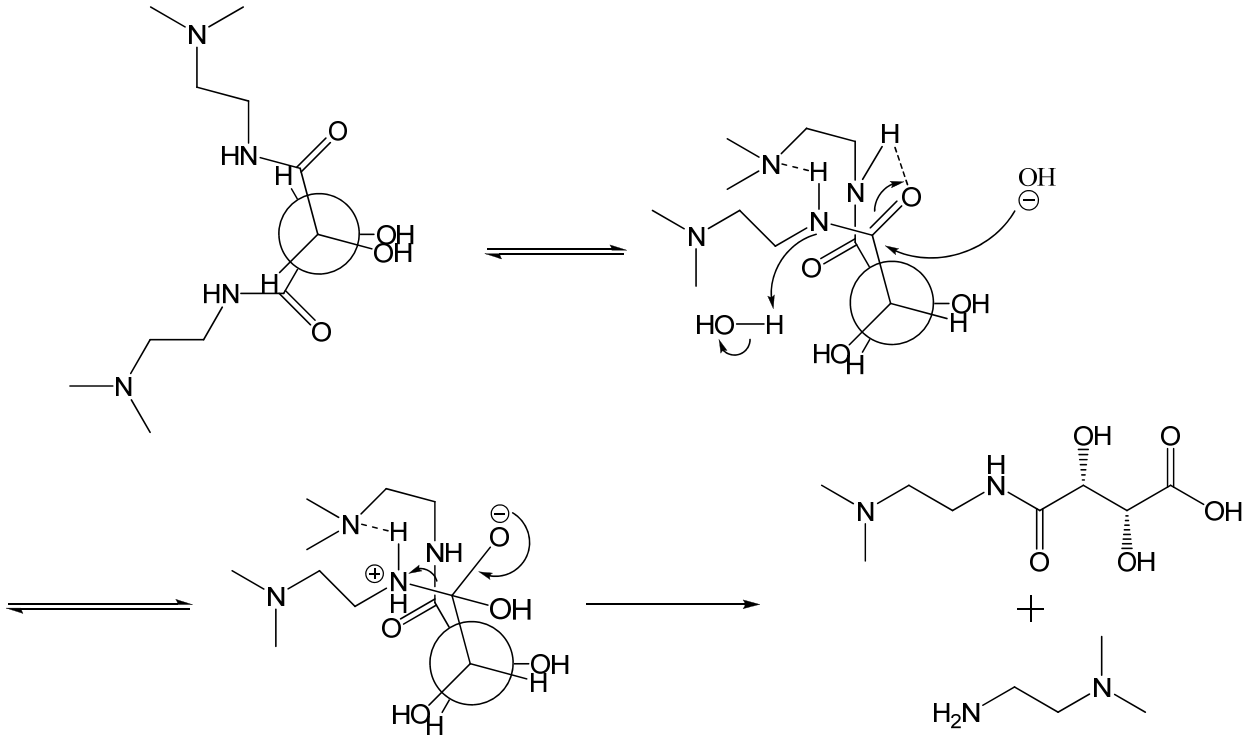

Figure 3.25, Possible mechanism **1**

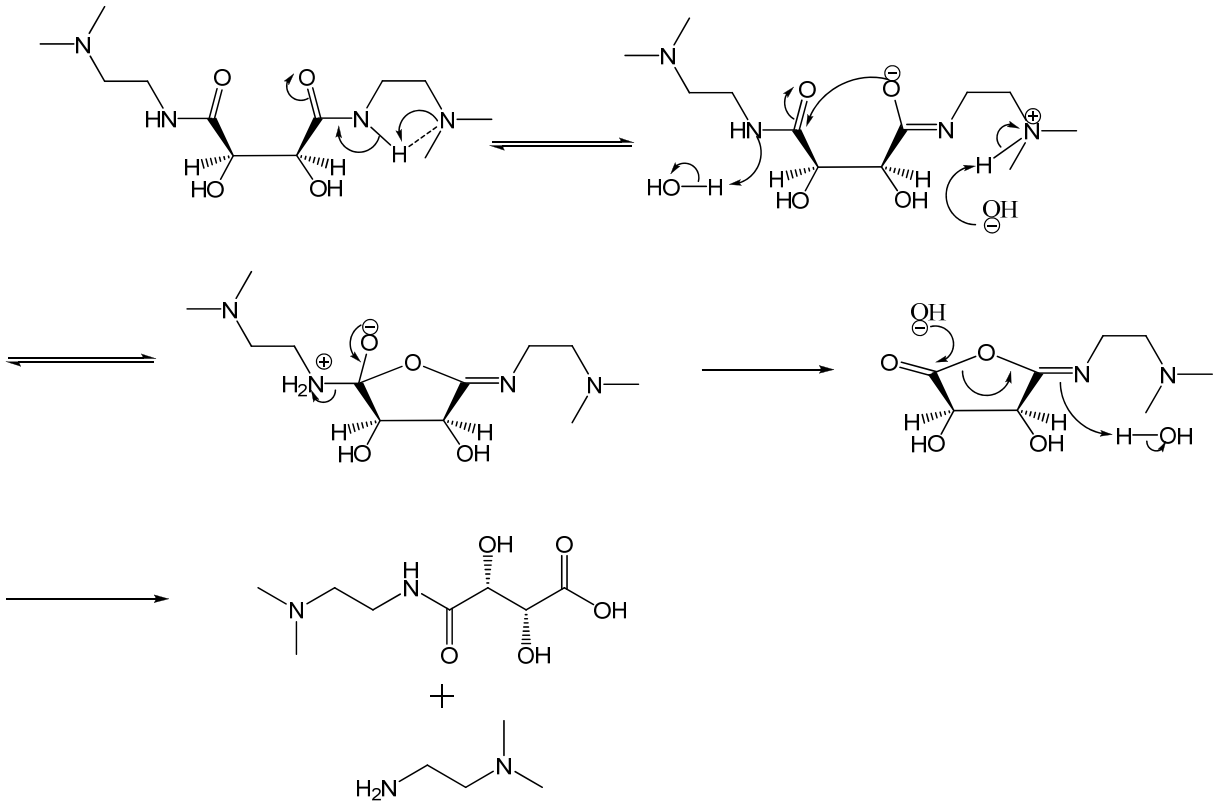

Figure 3.26, Possible mechanism **2**

Two different possible mechanisms were proposed to explain the fast amide hydrolysis.

Possible mechanism **1** (**Figure 3.25**) states that the amide hydrogen on end chain 1 will form a hydrogen bond with the terminal amine on the end chain 2 and the amide hydrogen on end chain 2 will form hydrogen bond with carbonyl oxygen on end chain 1. The resulting effect is to pull the electron cloud away from the carbonyl carbon and to make it more positively charged. This effect could make the OH^- attack the carbonyl carbon and facilitate hydrolysis more easily.

Possible mechanism **2** (**Figure 3.26**) states that the end amine on end chain 1 will attack the amide hydrogen on its own side. The enol group will attack the carbonyl carbon on end chain

2, forming a 5-membered ring. Amide bond breakage is followed by the ring opening of the lactone.

Both of the possible mechanisms are able to state why all hydrolysis reactions happened only on one side chain, why free deprotonated terminal amines were important to facilitate hydrolysis, why hydrolysis occurs on the chain without terminal amines for asymmetric compounds, why the compounds hydrolyzed much faster in basic solution while no hydrolysis was observe in acidic environment, and why the small end chain distance is required for hydrolysis. However, the only difference between these two mechanisms is that mechanism 1 requires both amides are primary or secondary amides for formation of two hydrogen bonds, while mechanism 2 only requires primary or secondary amide on the end chain with terminal amines for formation of one hydrogen bond.

Hydrolysis studies at pD 7.5 with compound **22** and dimethyl L-tartrate were compared. Esters were used here instead of amides due to the easy synthesis. Further, high pH studies were avoided due to the ease of hydrolysis of ester. If possible mechanism **1** is correct, neither of these two compounds should hydrolyze due to the lack of one hydrogen bond. However, if mechanism **2** is correct, **22** should hydrolyze and dimethyl L-tartrate should not.

Results showed that only compound **22** hydrolyzed at pD 7.5 while dimethyl L-tartrate did not. (**Figure 3.27**, **3.28**, **3.29**) Therefore, mechanism **2** could be the possible correct mechanism.

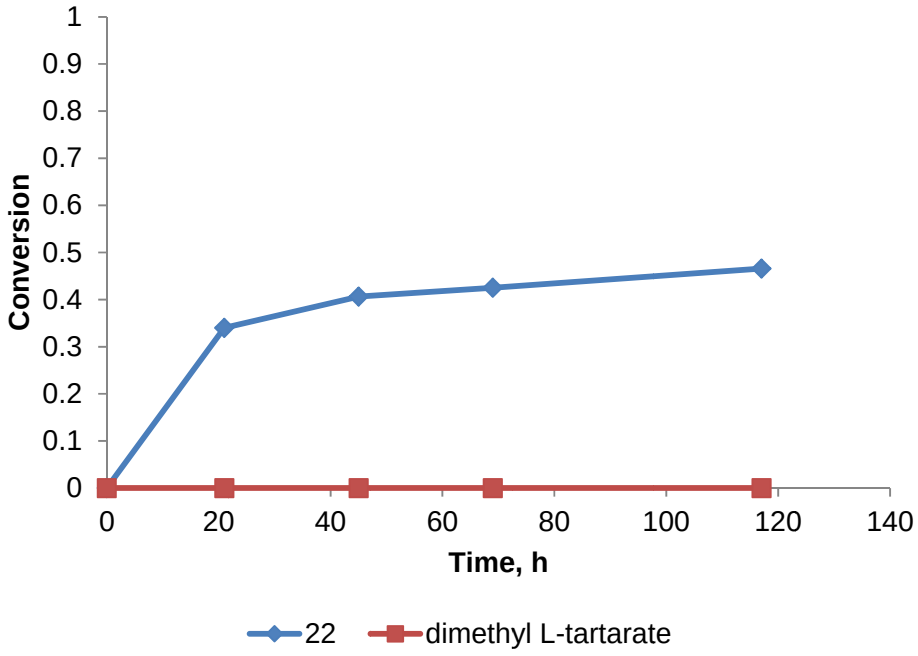

Figure 3.27, Hydrolysis studies with **22** and dimethyl L-tartrate at pD 7.5

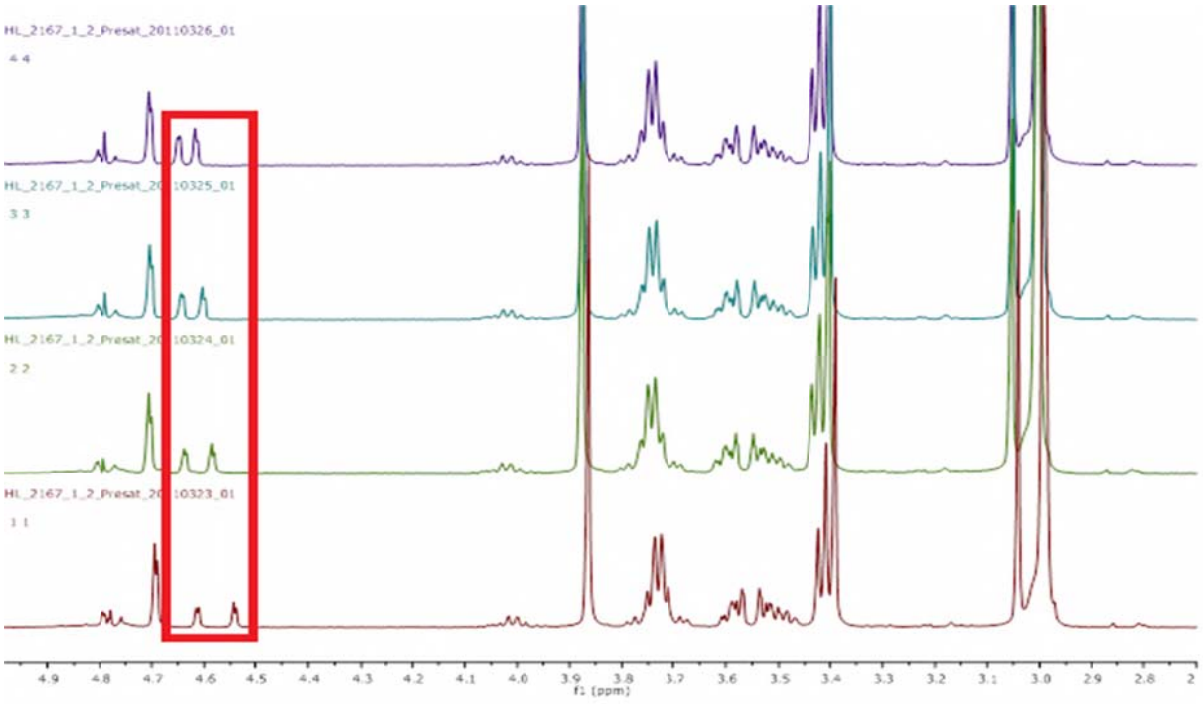

Figure 3.28, Hydrolysis kinetics of compound **22**

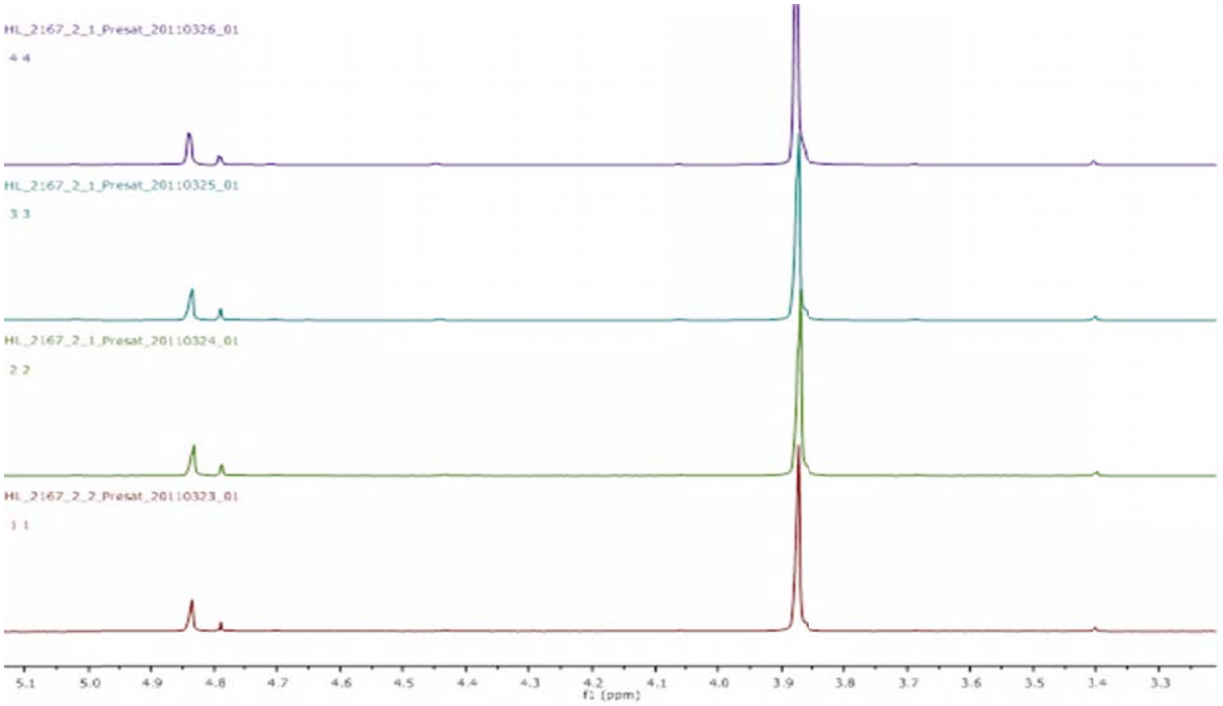

Figure 3.29, Hydrolysis kinetics of dimethyl L-tartrate

3.4 Conclusions

Different models mimicking **T1** delivery vehicles were synthesized to study which functional groups could affect and increase the amide degradation rate. All these models showed hydrolysis reactions happened only on one end chain; free deprotonated terminal amines were important to facilitate hydrolysis; amides on the side of free terminal amines cannot not be tertiary amides to facilitate hydrolysis; hydrolysis occurs on the chain without terminal amines for asymmetric compounds; compounds hydrolyzed much faster in basic solution while no hydrolysis was observed in acidic environment; and a small end chain distance is required for hydrolysis. Hydrolysis rate followed first order to compound concentration and first order to OH^- or OD^- concentration. The proposed mechanism suggests that neighboring group participation between two end chains could increase the hydrolysis rate.

Chapter 4

Future Directions

4.1 Introduction

Since studies showed that the degradation of nucleic acid delivery vehicles could release drugs and help increase transfection efficiency,[14,56-59] novel polymers with different degradation properties could be synthesized with the model monomers synthesized above. These polymers could potentially increase the transfection efficiency and be used to tune the degradation rate.

4.2 New Fast Degrading PGAAs for Nucleic Acid Delivery

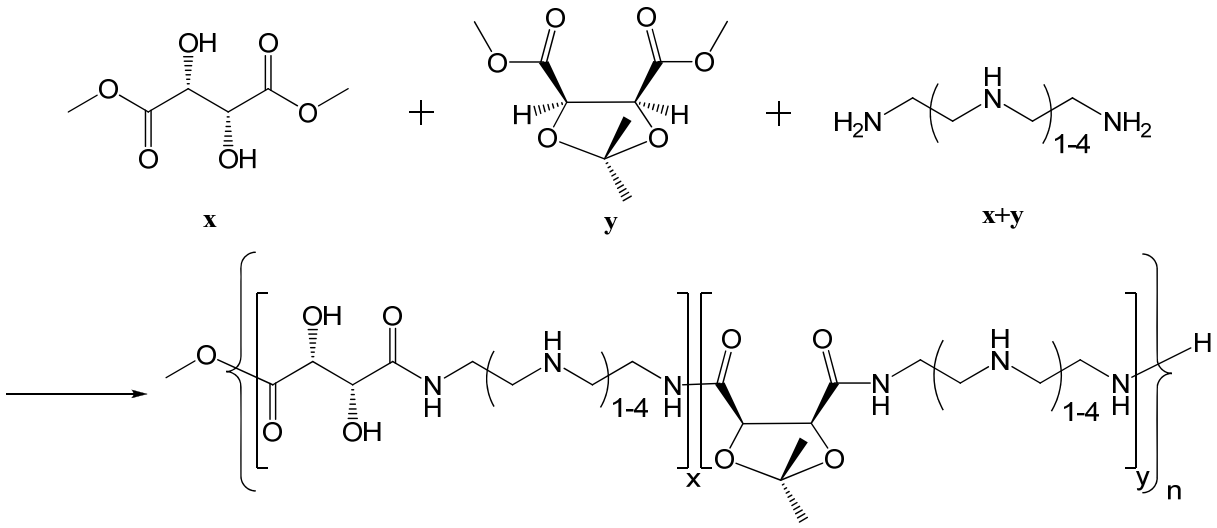

Scheme 4.1, Synthesis of fast degrading PGAAs

The new PGAAs random copolymers will be synthesized by copolymerization of dimethyl L-tartrate, 2,3-O-isopropylidene-*meso*-tartrate and oligoamines. (**Scheme 4.1**) Discussed in Chapter 3, L-tartrate based models degraded much slower than 2,3-O-isopropylidene-*meso*-tartrate based models, therefore, different ratios of these two models will be

applied. The polymers are assumed to degrade faster with higher percentage of 2,3-O-isopropylidene-*meso*-tartrate moiety and degrade slower with higher L-tartrate moiety.

Experiments:

Degradation studies: Gel permeation chromatography (GPC) will be used to measure polymer molecular weight. Polymers will be dissolved in PBS or pH 5 buffers and incubated at 37 ^{o}C for degradation studies. Sample at different time points will be measured by GPC to tell how fast different polymers degrade.

Gel binding assay: Gel binding assay will be used to measure the ability of polymers to bind nucleic acids. Polymer pDNA complexes (polyplexes) will be made at different *N/P* ratios. Gel electrophoresis will measure from what *N/P* ratio polyplexes will be formed. Furthermore, the stable polyplexes can be incubated at 37 ^{o}C for longer time. Gel binding assay of the polyplexes after different incubation time points could tell from what time points polyplexes will not be stable and nucleic acids will be released.

Cell culture experiments: Toxicity, cellular uptake and transfection efficiency assays will be conducted with HeLa cells to measure how bio-active different polymers behave while maintaining low cytotoxicity. Moreover, bio-activities of polymers on different cell lines are different. Potentially, more cell types will be transfected with polyplexes.

Degradation and biological data will be correlated and show how the degradation rate will affect nucleic acid delivery.

References

(1) Yang, Z. R.; Wang, H. F.; Zhao, J.; Peng, Y. Y.; Wang, J.; Guinn, B.-A.; Huang, L. Q. *Cancer Gene Therapy* **2007**, *14*, 599.

(2) Niven, R.; Pearlman, R.; Wedeking, T.; Mackeigan, J.; Noker, P.; Simpson-Herren, L.; Smith, J. G. *J. Pharm. Sci.* **1998**, *87*, 1292.

(3) Kunisawaa, J.; Masudaa, T.; Katayamaa, K.; Yoshikawaa, T.; Tsutsumia, Y.; Akashib, M.; Mayumia, T.; Nakagawa, S. *Journal of Controlled Release* **2005**, *105*, 344.

(4) Verma, I. M.; Somia, N. *NATURE* **1997**, *389*, 239.

(5) Mintzer, M. A.; Simanek, E. E. *Chem. Rev.* **2009**, *109*, 259.

(6) Luten, J.; Nostrum, C. F. v.; Smedt, S. C. D.; Hennink, W. E. *Journal of Controlled Release* **2008**, *126*, 97.

(7) Ghosn, B.; Haselton, F. R.; Gee, K. R.; Monroe, W. T. *Photochemistry and Photobiology* **2005**, *81*, 953.

(8) Handwerger, R. G.; Diamond, S. L. *Bioconjugate Chem.* **2007**, *18*, 717.

(9) Wang, C. Y.; Huang, L. *Biochemistry* **1989**, *28*, 9508.

(10) Xu, R.; Wang, X.-L.; Lu, Z.-R. *Langmuir* **2010**, *26*, 13874.

(11) Lin, Y.-L.; Jiang, G.; Birrell, L. K.; El-Sayed, M. E. H. *Biomaterials* **2010**, *31*, 7150.

(12) Bachelder, E. M.; Beaudette, T. T.; Broaders, K. E.; Dashe, J.; Frechet, J. M. J. *J. AM. CHEM. SOC.* **2008**, *130*, 10494.

(13) Wang, X.; Xie, X.; Cai, C.; Rytting, E.; Steele, T.; Kissel, T. *Macromolecules* **2008**, *41*, 2791.

(14) Lim, Y.-B.; Han, S.-O.; Kong, H.-U.; Lee, Y.; Park, J.-S.; Jeong, B.; Kim, S. W. *Pharm. Res.* **2000**, *17*, 811.

(15) Hwang, S. J.; Davis, M. E. *Current Opinion in Molecular Therapeutics* **2001**, *3*, 183.

(16) Koh, J. J.; Ko, K. S.; Lee, M.; Han, S.; Park, J. S.; Kim, S. W. *Gene Therapy* **2000**, *7*, 2099.

(17) Erickson, H. K.; Widdison, W. C.; Mayo, M. F.; Whiteman, K.; Audette, C.; Wilhelm, S. D.; Singh, R. *Bioconjugate Chem.* **2010**, *21*, 84.

(18) Liu, Y.; Wenning, L.; Lynch, M.; Reineke, T. M. *J. AM. CHEM. SOC.* **2004**, *126*, 7422.

(19) Liu, Y.; Reineke, T. M. *J. Am. Chem. Soc.* **2005**, *127*, 3004.

(20) Lee, C.-C.; Liu, Y.; Reineke, T. M. *Bioconjugate Chem.* **2008**, *19*, 428.

(21) Liu, Y.; Reineke, T. M. *Biomacromolecules* **2010**, *11*, 316.

(22) Prevette, L. E.; Kodger, T. E.; Reineke, T. M.; Lynch, M. L. *Langmuir* **2007**, *23*, 9773.

(23) Gabrielson, N. P.; Pack, D. W. *Journal of Controlled Release* **2008**, *136*, 54.

(24) Liu, W. G.; Yao, K. D. *Journal of Controlled Release* **2002**, *83*, 1.

(25) Coué, G.; Engbersen, J. F. J. *Journal of Controlled Release* **2011**, *xxx*, xxx.

(26) Griffiths, P. C.; Paul, A.; Khayat, Z.; Wan, K.-W.; King, S. M.; Grillo, I.; Schweins, R.; Ferruti, P.; Franchini, J.; Duncan, R. *Biomacromolecules* **2004**, *5*, 1422.

(27) Strand, S. P.; Lelu, S.; Reitan, N. K.; Davies, C. d. L.; Artursson, P.; Vårum, K. M. *Biomaterials* **2010**, *31*, 975.

(28) MacLaughlin, F. C.; Mumper, R. J.; Wang, J.; Tagliaferri, J. M.; Gill, I.; Hinchcliffe, M.; Rollanda, A. P. *Journal of Controlled Release* **1998**, *56*, 259.

(29) Germershaus, O.; Mao, S.; Sitterberg, J.; Bakowsky, U.; Kissel, T. *Journal of Controlled Release* **2008**, *125*, 145.

(30) Mao, H.-Q.; Roy, K.; Troung-Le, V. L.; Janes, K. A.; Lin, K. Y.; Wang, Y.; August, J. T.; Leong, K. W. *Journal of Controlled Release* **2001**, *70*, 399.

(31) Brissault, B.; Kichler, A.; Guis, C.; Leborgne, C.; Danos, O.; Cheradame, H. *Bioconjugate Chem.* **2003**, *14*, 581.

(32) Neu, M.; Fischer, D.; Kissel, T. *J. Gene Med.* **2005**, *7*, 992.

(33) Mecke, A.; Lee, D.-K.; Ramamoorthy, A.; Orr, B. G.; Holl, M. M. B. *Langmuir* **2005**, *21*, 8588.

(34) Allende, D.; Simon, S. A.; McIntosh, T. J. *Biophysical Journal* **2005**, *88*, 1828.

(35) Yang, L.; Harroun, T. A.; Weiss, T. M.; Ding, L.; Huang, H. W. *Biophysical Journal* **2001**, *81*, 1475.

(36) Xu, Y.; Francis C. Szoka, J. *Biochemistry* **1996**, *35*, 5616.

(37) Fattal, E.; Nir, S.; Parente, R. A.; Francis C. Szoka, J. *Biochemistry* **1994**, *33*, 6721.

(38) Akinc, A.; Thomas, M.; Klibanov, A. M.; Langer, R. *J. Gene Med.* **2005**, *7*, 657.

(39) BOUSSIF, O.; LEZOUALC'H, F.; ZANTA, M. A.; MERGNY, M. D.; SCHERMAN, D.; DEMENEIX, B.; BEHR, J.-P. *Proc. Natl. Acad. Sci.* **1995**, *92*, 7297.

(40) KHALIL, I. A.; KOGURE, K.; AKITA, H.; HARASHIMA, H. *Pharmacol. Rev.* **2006**, *58*, 32.

(41) Wen, Y.; Pan, S.; Luo, X.; Zhang, X.; Zhang, W.; Feng, M. *Bioconjugate Chem.* **2009**, *20*, 322.

(42) Pathak, A.; Patnaik, S.; Gupta, K. C. *Nucleic Acids Symposium Series* **2009**, *53*, 57.

(43) Pun, S. H.; Bellocq, N. C.; Liu, A.; Jensen, G.; Machemer, T.; Quijano, E.; Schluep, T.; Wen, S.; Engler, H.; Heidel, J.; Davis, M. E. *Bioconjugate Chem.* **2004**, *15*, 831.

(44) Wang, C.-H.; Hsiue, G.-H. *Bioconjugate Chem.* **2005**, *16*, 391.

(45) Kircheis, R.; Wightman, L.; Schreiber, A.; Robitza, B.; Rossler, V.; Kursa, M.; Wagner, E. *Gene Therapy* **2001**, *8*, 28.

(46) Ferruti, P.; Marchisio, M. A.; Barbucci, R. *Polymer Preprints* **1985**, *26*, 1336.

(47) Barbucci, R.; Casolaro, M.; Ferruti, P.; Barone, V.; Leli, F.; Oliva, L. *Macromolecules* **1981**, *14*, 1203.

(48) Ferruti, P.; Manzoni, S.; Richardson, S. C. W.; Duncan, R.; Pattrick, N. G.; Mendichi, R.; Casolaro, M. *Macromolecules* **2000**, *33*, 7793.

(49) Richardson, S.; Ferruti, P.; Duncan, R. *Journal of Drug Targeting* **1999**, *6*, 391.

(50) Tomalia, D. A.; Baker, H.; Dewald, J.; Hall, M.; Kallos, G.; Martin, S.; Roeck, J.; Ryder, J.; Smith, P. *Polym. J.* **1985**, *17*, 117.

(51) Ottaviani, M. F.; Furini, F.; Casini, A.; Turro, N. J.; Jockusch, S.; Tomalia, D. A.; Messori, L. *Macromolecules* **2000**, *33*, 7842.

(52) Sonawane, N. D.; Szoka, F. C. J.; Verkman, A. S. *The Journal of biological chemistry* **2003**, *278*, 44826.

(53) Liu, Y.; Reineke, T. M. *Bioconjugate Chem.* **2007**, *18*, 19.

(54) Prevette, L. E.; Lynch, M. L.; Reineke, T. M. *Biomacromolecules* **2010**, *11*, 326.

(55) Reineke, T. M. *Journal of Polymer Science: Part A: Polymer Chemistry* **2006**, *44*, 6895.
(56) Anderson, D. G.; Lynn, D. M.; Langer, R. *Bioconjugate Chem.* **2003**, *42*, 3153.
(57) Kakizawa, Y.; Harada, A.; Kataoka, K. *J. Am. Chem. Soc.* **1999**, *121*, 11247.
(58) Lackey, C. A.; Press, O. W.; Hoffman, A. S.; Stayton, P. S. *Bioconjugate Chem.* **2002**, *13*, 996.
(59) Oster, C. G.; Wittmar, M.; Unger, F.; Lucian, B.-T.; Schaper, A. K.; Kissel, T. *Pharm. Res.* **2004**, *21*, 927.
(60) Lackey, C. A.; Press, O. W.; Hoffman, A. S.; Stayton, P. S. *Bioconjugate Chem.* **2002**, *13*, 996.
(61) Saito, G.; Swanson, J. A.; Lee, K.-D. *Adv. Drug. Delivery Rev.* **2003**, *55*, 199.
(62) Lim, Y. B.; Kim, C. H.; Kim, K.; Kim, S. W.; Park, J. S. *J. AM. CHEM. SOC.* **2000**, *122*, 6524.
(63) Kim, T. I.; Seo, H. J.; Choi, J. S.; Yoon, J. K.; Baek, J. U.; Kim, K.; J.S. Park *Bioconjugate Chem.* **2005**, *16*, 1140.
(64) Wu, D.; Liu, Y.; Jiang, X.; Chen, L.; He, C.; Goh, S. H.; Leong, K. W. *Biomacromolecules* **2005**, *6*, 3166.
(65) Li, X.; Su, Y.; Chen, Q.; Lin, Y.; Tong, Y.; Li, Y. *Biomacromolecules* **2005**, *6*, 3181.
(66) Gillies, E. R.; Goodwin, A. P.; Frechet, J. M. J. *Bioconjugate Chem.* **2004**, *15*, 1254.
(67) McKenzie, D. L.; Smiley, E.; Kwok, K. Y.; Rice, K. G. *Bioconjugate Chem.* **2000**, *11*, 901.
(68) Davis, M. E.; Zuckerman, J. E.; Choi, C. H. J.; Seligson, D.; Tolcher, A.; Alabi, C. A.; Yen, Y.; Heidel, J. D.; Ribas, A. *NATURE* **2010**, *464*, 1067.
(69) Davis, M. E. *Current Opinion in Biotechnology* **2002**, *13*, 128.
(70) Putnam, D.; Gentry, C. A.; Pack, D. W.; Langer, R. *Proc. Natl. Acad. Sci.* **2001**, *98*, 1200.
(71) Guo, X.; Szoka Jr, F. C. *Acc. Chem. Res.* **2003**, *36*, 335.
(72) Davis, M. E. *Mol. Pharmaceutics* **2009**, *6*, 659.
(73) Liu, Y.; Wenning, L.; Lynch, M.; Reineke, T. M. *In Polymeric Drug Delivery I: Particulate Drug Carriers* **2006**, *923*, 217.
(74) Gopin, A.; Pessah, N.; Shamis, M.; Rader, C. *Angewandte Chemie* **2003**, *115*, 341.
(75) Srinivasachari, S.; Liu, Y.; Zhang, G. D.; Prevette, L.; Reineke, T. M. *J. AM. CHEM. SOC.* **2006**, *128*, 8176.
(76) Lee, C.-C.; Liu, Y.; Reineke, T. M. *Bioconjugate Chem.* **2008**, *19*, 428.
(77) Liu, Y.; Reineke, T. M. *Bioconjugate Chem.* **2006**, *17*, 101.
(78) Bryson, J. M.; Fichter, K. M.; Chu, W. J.; Lee, J. H.; Li, J.; Madsen, L. A.; McLendon, P. M.; Reineke, T. M. *Proc. Natl. Acad. Sci.* **2009**, *106*, 16913.
(79) Taori, V. P.; Liu, Y.; Reineke, T. M. *Acta biomaterialia* **2009**, *5*, 925.
(80) McLendon, P. M.; Buckwalter, D. J.; Davis, E. M.; Reineke, T. M. *Mol. Pharmaceutics* **2010**, *7*, 1757.
(81) Mislick, K. A.; Baldeschwieler, J. D. *Proc. Natl. Acad. Sci. U.S.A.* **1996**, *93*, 12349.
(82) McLendon, P. M.; Fichter, K.; Reineke, T. M. *Molecular Pharmaceutics* **2010**, *7*, 738.

(83) Fattal, E.; Nir, S.; Parente, R. A.; Szoka Jr, F. C. *Biochemistry* **1994**, *33*, 6721.
(84) Medina-Kauwe, L. K.; Xie, J.; Hamm-Alvarez, S. *Gene Therapy* **2005**, *12*, 1734.
(85) Gabrielson, N. P.; Pack, D. W. *Biomacromolecules* **2006**, *7*, 2427.
(86) Behr, J. P. *CHIMIA International Journal for Chemistry* **1997**, *1*, 34.
(87) Boussif, O.; Lezoualc'h, F.; Zanta, M. A.; Mergny, M. D.; Scherman, D.; Demeneix, B.; Behr, J. P. *Proc. Natl. Acad. Sci.* **1995**, *92*, 7297.
(88) Pang, S. W.; Park, H. Y.; Jang, Y. S.; Kim, W. S.; Kim, J. H. *Colloids and Surfaces B: Biointerfaces* **2002**, *26*, 213.
(89) Dubruela, P.; Christiaensb, B.; Vanloob, B.; Brackea, K.; Rosseneub, M.; Vandekerckhoveb, J.; E., S. *European Journal of Pharmaceutical Sciences* **2003**, *18*, 211.
(90) Funhoff, A. M.; Nostrum, C. F.; Lok, M. C.; Fretz, M. M.; Crommelin, D. J. A.; E., H. W. *Bioconjugate Chem.* **2004**, *15*, 1212.
(91) Nimesh, S.; Chandra, R. *European Journal of Pharmaceutics and Biopharmaceutics* **2008**, *68*, 647.
(92) Bromberg, L.; Raduyk, S.; Hatton, T. A.; Concheiro, A.; Rodriguez-Valencia, C.; Silva, M.; Alvarez-Lorenzo, C. *Bioconjugate Chem.* **2009**, *20*, 1044.
(93) Reineke, T. M.; Davis, M. E. *Bioconjugate Chem.* **2003**, *14*, 247.
(94) Reineke, T. M.; Davis, M. E. *Bioconjugate Chem.* **2003**, *14*, 255.
(95) Sambrook, M. R.; Beer, P. D.; Wisner, J. A.; Paul, R. L.; Cowley, A. R.; Szemes, F.; Drew, M. G. B. *J. AM. CHEM. SOC.* **2005**, *127*, 2292.
(96) Lucas, R. L.; Benjamin, M.; Reineke, T. M. *Bioconjugate Chem.* **2008**, *19*, 24.
(97) Funhoff, A. M.; van Nostrum, C. F.; Lok, M. C.; Fretz, M. M.; Crommelin, D. J. A.; Hennink, W. E. *Bioconjugate Chem.* **2004**, *15*, 1212.
(98) Kim, T.; Lee, M.; Kim, S. W. *Biomaterials* **2010**, *31*, 1798.
(99) Kanczler, J. A.; Ginty, P. J.; Barry, J. J. A.; Clarke, N. M. P.; Howdle, S. M.; Shakesheff, K. M.; Oreffo, R. O. C. *Biomaterials* **2008**, *29*, 1892.
(100) Tomlinson, R.; Klee, M.; Garrett, S.; Heller, J.; Duncan, R.; Brocchini, S. *Macromolecules* **2002**, *35*, 473.
(101) Somayaji, V.; Keillor, J.; Brown, R. S. *J. AM. CHEM. SOC.* **1988**, *110*, 2625.
(102) Mukherjee, T.; Zhang, Y.; Abdelwahed, S.; Ealick, S. E.; Begley, T. P. *J. AM. CHEM. SOC.* **2010**, *132*, 5550.
(103) Bisogno, T.; Petrocellis, L. D.; Marzo, V. D. *Current Pharmaceutical Design* **2002**, *8*, 125.
(104) Kahne, D.; Still, W. C. *J. Am. Chem. Soc.* **1988**, *110*, 7529.
(105) Gltisenkamp, K.-H.; Mengede, C.; Drosdziok, W.; Jahde, E.; Rajewsky, M. F. *Bioorg. Med. Chem. Lett.* **1998**, *8*, 285.
(106) Kogan, R. L.; Fife, T. H. *J. Org. Chem.* **1984**, *49*, 5229.
(107) Hegarty, A. F.; Frost, L. N.; Coy, J. H. *J. Org. Chem.* **1974**, *39*, 1089.
(108) Kirby, A. J.; McDonald, R. S.; Smith, C. R. *J. Chem. Soc., Perkin Trans. 2* **1974**, 1495.
(109) Feit, P. W. *J. Med. Chem.* **1964**, *7*, 14.